

# **Applied Nonlinear Dynamics 322**

**Hermann Riecke**

**Engineering Sciences and Applied Mathematics**

**Northwestern University**

**h-riecke@northwestern.edu**

# Contents

<b>References</b>	<b>4</b>
<b>1 Introduction<sup>1</sup></b>	<b>6</b>
<b>2 1-d Flow</b>	<b>11</b>
2.1 Flow on the Line <sup>2</sup> . . . . .	11
2.1.1 Impossibility of Oscillations . . . . .	16
2.2 Existence and Uniqueness . . . . .	17
2.3 Bifurcations in 1 Dimension <sup>3</sup> . . . . .	21
2.3.1 Implicit Function Theorem . . . . .	21
2.3.2 Some Simple Examples: Normal Forms . . . . .	23
2.3.3 General Functions $f(x, \mu)$ : Saddle-Node Bifurcation . . . . .	24
2.3.4 Transcritical Bifurcation . . . . .	31
2.3.5 Pitchfork Bifurcation . . . . .	34
2.3.6 Subcritical Pitchfork Bifurcation: . . . . .	41
2.3.7 Imperfect Bifurcations . . . . .	42
2.4 Flow on a Circle <sup>4</sup> . . . . .	48
2.4.1 Examples for SNIC Bifurcations . . . . .	51
<b>3 Two-dimensional Systems</b>	<b>56</b>
3.1 Classification of Linear Systems <sup>5</sup> . . . . .	56
3.2 Stability <sup>6</sup> . . . . .	61
3.3 General Properties of the Phase Plane . . . . .	64
3.3.1 Hartman-Grobman theorem <sup>7</sup> . . . . .	64
3.3.2 Phase Portraits <sup>8</sup> . . . . .	66
3.3.3 Ruling out Persistent Dynamics <sup>9</sup> . . . . .	68

<sup>1</sup>Strogatz Book Ch.1 & Lectures Video 1 ([https://www.youtube.com/watch?v=ycJEoqmQvwg&list=PLbN57C5Zdl6j\\_qJA-pARJnKsmROzPnO9V&index=1](https://www.youtube.com/watch?v=ycJEoqmQvwg&list=PLbN57C5Zdl6j_qJA-pARJnKsmROzPnO9V&index=1))

<sup>2</sup>cf. Strogatz Ch.2 and Lecture 2

<sup>3</sup>cf. Strogatz Ch.3 Lecture 2

<sup>4</sup>cf. Strogatz Ch.4

<sup>5</sup>cf. Strogatz Ch.5 and Lecture 5

<sup>6</sup>Strogatz 6.3

<sup>7</sup>Strogatz Ch. 6.3

<sup>8</sup>Strogatz Ch. 6.1

<sup>9</sup>Strogatz Ch. 7.2 and Lecture 9

3.3.4 Poincaré-Bendixson Theorem: No Chaos in 2 Dimensions <sup>10</sup> . . . . .	71
3.4 Relaxation Oscillations <sup>11</sup> . . . . .	77
3.5 Weakly Nonlinear Oscillators <sup>12</sup> . . . . .	79
3.5.1 Failure of Regular Perturbation Theory . . . . .	80
3.5.2 Multiple Scales . . . . .	83
3.5.3 Hopf Bifurcation <sup>13</sup> . . . . .	87
3.6 1d-Bifurcations in 2d: Reduction of Dynamics . . . . .	94
3.6.1 Center-Manifold Theorem . . . . .	95
3.6.2 Reduction to Dynamics on the Center Manifold . . . . .	98
3.6.3 Reduction to Center Manifold without Multiple Scales . . . . .	103
<b>4 Chaos</b>	<b>106</b>
4.1 Lorenz Model <sup>14</sup> . . . . .	106
4.1.1 Simple Properties of the Lorenz Model . . . . .	109
4.1.2 Lyapunov Exponents . . . . .	112
4.2 One-Dimensional Maps <sup>15</sup> . . . . .	115
4.3 Self-Similarity: Renormalization <sup>16</sup> . . . . .	129
4.4 Strange Attractors and Fractal Dimensions <sup>17</sup> . . . . .	133
4.4.1 Dimensions . . . . .	137
4.5 Experimental Data: Attractor Reconstruction and Poincaré Section . . . . .	142

---

<sup>10</sup>cf. Strogatz Ch.7.3

<sup>11</sup>Strogatz Ch. 7.5

<sup>12</sup>Strogatz Ch. 7.6

<sup>13</sup>Strogatz Ch. 8.2

<sup>14</sup>Strogatz Ch. 9.2, 9.3, 9.4

<sup>15</sup>Strogatz Ch. 10

<sup>16</sup>Strogatz Ch 10.7

<sup>17</sup>Strogatz Ch. 11, 12

## References

- Ainsworth M., Lee S., Cunningham M.O., Traub R.D., Kopell N.J., and Whittington M.A. (2012). Rates and rhythms: a synergistic view of frequency and temporal coding in neuronal networks. *Neuron* *75*, 572–583.
- Aitta A., Ahlers G., and Cannell D.S. (1985). Tricritical phenomena in rotating Couette-Taylor flow. *Phys. Rev. Lett.* *54*, 673.
- Aoi S., Katayama D., Fujiki S., Tomita N., Funato T., Yamashita T., Senda K., and Tsuchiya K. (2013). A stability-based mechanism for hysteresis in the walk-trot transition in quadruped locomotion. *Journal of the Royal Society Interface* *10*, 20120908.
- Bagyan S., Mair T., Suchorski Y., Hauser M., and Straube R. (2008). Spatial desynchronization of glycolytic waves as revealed by Karhunen-Loeve analysis. *J. Phys. Chem. B* *112*, 14334–14341.
- Bodenschatz E., deBruyn J.R., Ahlers G., and Cannell D.S. (1991). Transitions between patterns in thermal convection. *Phys. Rev. Lett.* *67*, 3078.
- Buonviso N., Amat C., Litaudon P., Roux S., Royet J., Farget V., and Sicard G. (2003). Rhythm sequence through the olfactory bulb layers during the time window of a respiratory cycle. *Eur J Neurosci* *17*, 1811–1819.
- Edelstein-Kesher L. (2005). Mathematical models in biology (SIAM).
- Ermentrout G.B., and Kopell N. (1986). Parabolic bursting in an excitable system coupled with a slow oscillation. *SIAM J. Appl. Math.* *46*, 233–253.
- Fauve S., and Libchaber A. (1983). Two-parameter study of the routes to chaos. *Ann. New York Acad. Sci.* *404*, 34.
- Fraser A.M., and Swinney H.L. (1986). Independent coordinates for strange attractors from mutual information. *Phys. Rev. A* *33*, 1134–1140.
- Grassberger P., and Procaccia I. (1983). Characterization of strange attractors. *Phys. Rev. Lett.* *50*, 346–349.
- Libchaber A., Fauve S., and Laroche C. (1983). Two-parameter study of the routes to chaos. *Physica D* *7*, 73.
- Liu J., and Ahlers G. (1997). Rayleigh-Bénard convection in binary-gas mixtures: Thermophysical properties and the onset of convection. *Phys. Rev. E* *55*, 6950–6968.
- Lücke M., Mihelcic M., Wingerath K., and Pfister G. (1984). Flow in a small annulus between concentric cylinders. *J. Fluid Mech.* *140*, 343–353.
- Müller S., Mair T., and Steinbock O. (1998). Traveling waves in yeast extract and in cultures of *Dictyostelium discoideum*. *Biophys Chem* *72*, 37–47.
- Roux J.C., Simoyi R.H., and Swinney H.L. (1983). Observation of a strange attractor. *Physica D* *8*, 257–266.

Scherer M.A., Ahlers G., Hörner F., and Rehberg I. (2000). Deviations from linear theory for fluctuations below the supercritical primary bifurcation to electroconvection. *Phys. Rev. Lett.* *85*, 3754–3757.

Selkov E. (1968). Self-oscillations in glycolysis .1. a simple kinetic model. *Eur. J. Biochem.* *4*, 79.

# 1 Introduction<sup>18</sup>

Dynamical systems: predict temporal evolution

Characterize the state of the system by a set of quantities:  $\mathbf{x}(t)$

To predict future states it is sufficient to know the rate of change of the system at any given time, which in very many systems depends only on the current states of the system<sup>19</sup>,

$$\frac{d\mathbf{x}(t)}{dt} = \mathbf{f}(\mathbf{x}(t)).$$

Thus, we want to understand the behavior of systems of differential equations. What is the key issue in this class?

Consider, e.g., the linear 2nd-order differential equation

$$\frac{d^2x}{dt^2} + x = 0,$$

which we can write as a first-order system by introducing  $v(t) = \frac{dx}{dt}$ ,

$$\begin{aligned}\frac{dx}{dt} &= v \\ \frac{dv}{dt} &= -x.\end{aligned}$$

It has the two linearly independent solutions

$$x_1(t) = \cos t \quad x_2(t) = \sin t.$$

The linear superposition

$$x_g(t) = Ax_1(t) + Bx_2(t)$$

provides the solution for any *initial* condition

$$x(0) = x_0 \quad \left. \frac{dx}{dt} \right|_{t=0} = v_0.$$

Thus, **any** solution of this system for **any** initial condition is a simple ‘mixture’ of two basic solutions. We know essentially everything about the system and all of its solutions, if we have  $x_{1,2}(t)$ : we ‘understand’ the system.

The same principle holds for linear systems with more components; we just have a larger set of basic solutions.

So, what is the problem?

---

<sup>18</sup>Strogatz Book Ch.1 & Lectures Video 1 ([https://www.youtube.com/watch?v=ycJEoqmQvwg&list=PLbN57C5Zdl6j\\_qJA-pARJnKsmROzPnO9V&index=1](https://www.youtube.com/watch?v=ycJEoqmQvwg&list=PLbN57C5Zdl6j_qJA-pARJnKsmROzPnO9V&index=1))

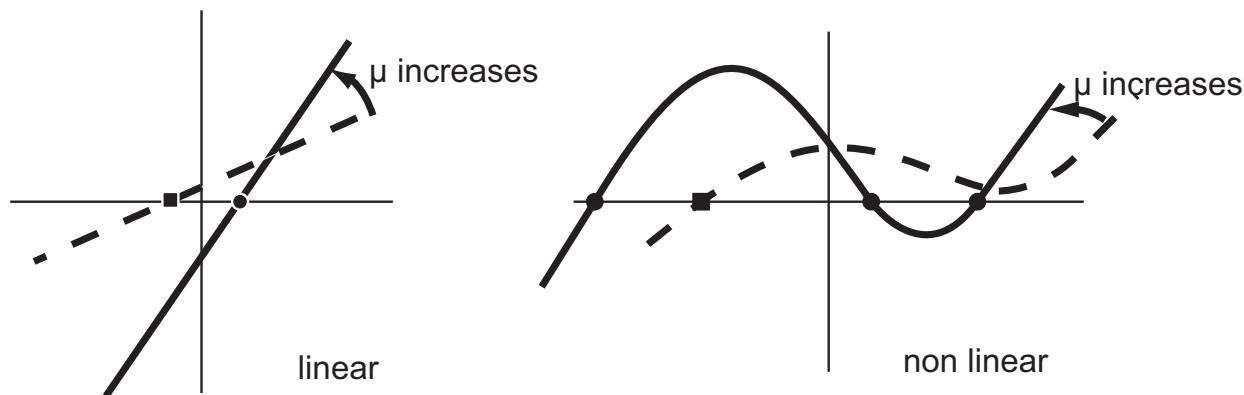
<sup>19</sup>It can also depend on earlier times, in which case one gets delay equations which are much harder to solve,  $\frac{d\mathbf{x}(t)}{dt} = \mathbf{f}(\mathbf{x}(t)) + \mathbf{g}(\mathbf{x}(t - \tau)) + \dots$ .

- Superposition is possible only for linear equations
- For nonlinear systems the solution cannot simply be built from a few basic solutions
  - for different initial conditions the solutions can be qualitatively different
  - the set of solutions can be extremely rich
  - the set of solutions can change **qualitatively** as a system parameter is changed

Simple illustration: steady states in a linear vs. a nonlinear system

Consider zeros  $x_0$  of a function  $f$  that depends on a parameter  $\mu$

$$f(x, \mu) = 0$$



### Linear Systems:

- change in parameter leads to **quantitative** change of solution
- **unique** solution for any given value of the parameter

### Nonlinear Systems:

- solutions can **appear** or **disappear** as parameters are changed
  - interacting oscillators with different natural frequencies
    - \* linear: for any coupling strength one gets beating, i.e. over time the two oscillators keep going in and out of phase
    - \* nonlinear (pendula):
      - weak coupling: asynchronous behavior similar to beating
      - strong coupling: synchronous oscillations.
      - these solutions disappear/appear as the coupling strength is changed
- **multiple** solutions possible for a given parameter value: hysteresis
- the physically observed **stable** solution

- can depend on parameters in a **non-smooth** fashion (cf. Rayleigh-Benard convection Fig.1)
- can undergo **qualitative changes** at such transition points (cf. Figs.2,3)
- chaotic dynamics
  - complex, non-repeating dynamics characterized by broad Fourier spectra, co-existing (unstable) periodic solutions (e.g. Belousov-Zhabotinsky reaction)

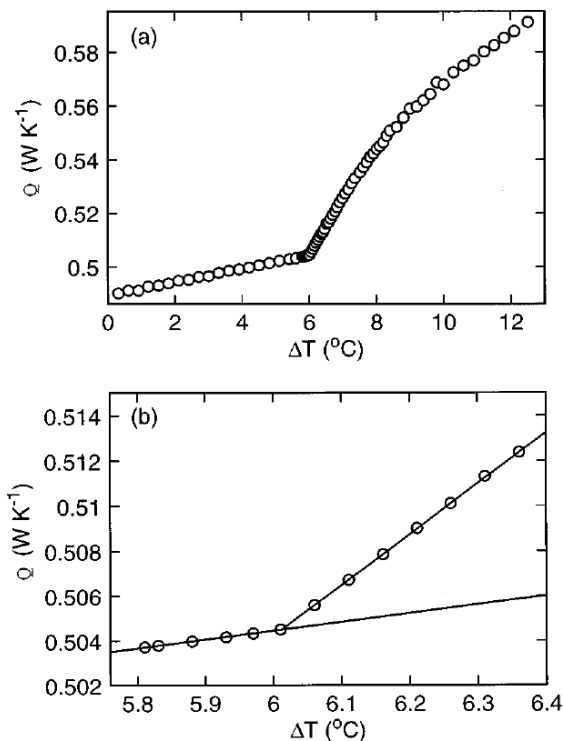


Figure 1: Heat flux in Rayleigh-Benard convection in a fluid layer heated from below. At the onset of convection the slope is discontinuous. Lower figure is an enlargement of the upper one near the onset temperature (Liu and Ahlers, 1997).

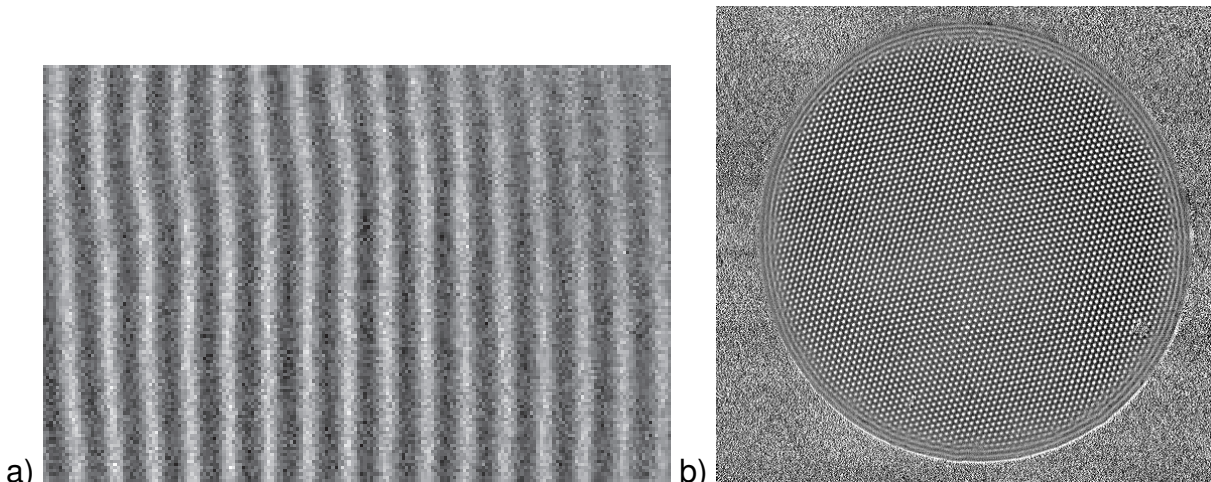


Figure 2: Convection patterns. a) Straight convection rolls in an inclined fluid layer. b) Hexagonal patterns in a horizontal fluid layer.

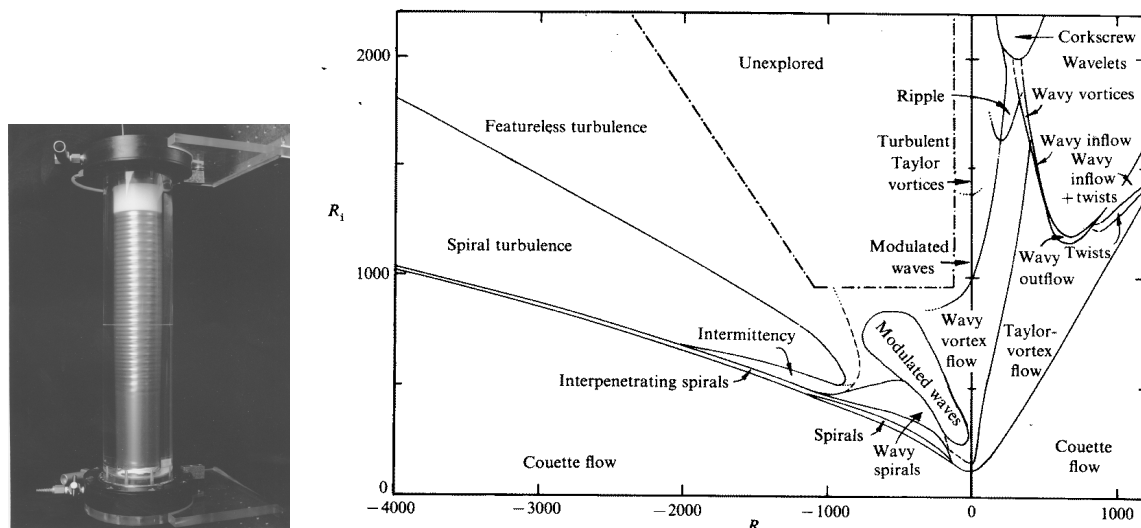


Figure 3: a) Taylor vortex flow between two cylinders. b) Depending on the rotation rate of the inner and the outer cylinder the fluid flow exhibits a bewildering multitude of qualitatively different behaviors when the rotation rates are changed (Andereck, Liu and Swinney, J. Fluid Mech. 164 (1986) 155).

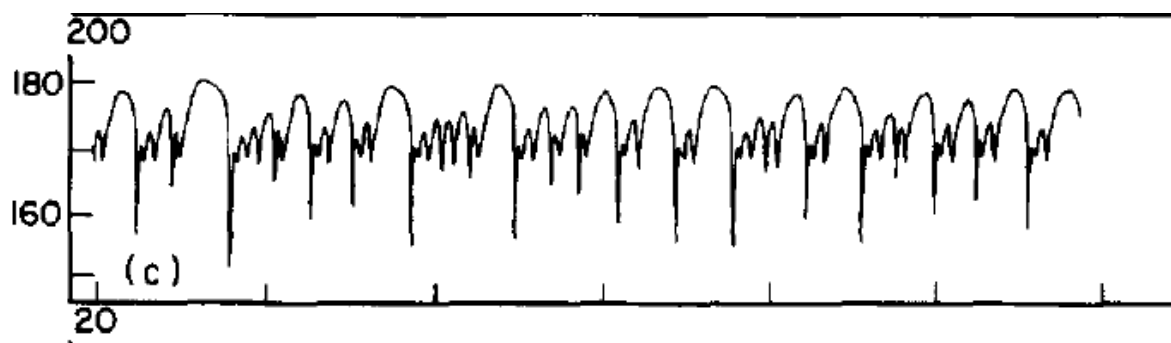


Figure 4: Chaotic oscillations in the Belousov-Zhabotinsky reaction (Schmitz, Graziani, and Hudson, J. Chem. Phys. 67 (1977) 3040).

## Possible Approaches

- Exact analytical solutions for nonlinear systems are available only in rare cases  
Even if an analytical solution is available, it is often so complicated that it is difficult to extract from it much insight about the mechanisms underlying the behavior of the system.
- Numerical solution
  - gives quantitative details for **specific** values of system parameters
    - \* allows testing/validation of the mathematical model by quantitative comparison with experiments  $\Rightarrow$  can be essential for model development.
    - \* many details may not be accessible in experiments: 3d fluid flows or thermal fields, turbulent, chemical concentrations of intermediate reactants, expression levels of genes,
  - insight into mechanisms by turning on or off specific aspects of the model (virtual ‘lesion experiments’)
  - **but** not very good at providing an overview of all solutions and how they are connected with each other
- Qualitative aspects:
  - transitions between different states
    - \* characterizing patterned vs unpatterned or oscillatory vs non-oscillatory rather than detailed quantitative predictions
  - behavior near transition points can often be captured by employing perturbation methods providing approximate solutions
- Visualization:
  - **geometry of dynamics**, phase plane, phase portraits
  - overview of **all** possible behaviors

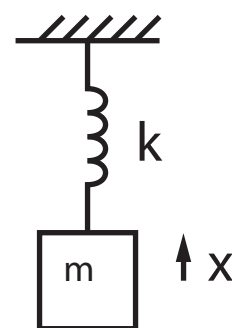
## Simple Example: Mass-spring-system

$$\frac{d^2x}{dt^2} = -\beta \frac{dx}{dt} - \frac{k}{m}x$$

with friction  $\beta$ .

We will write all differential equations as first-order systems:

$$\begin{aligned}\dot{x} &= v \\ \dot{v} &= -\beta v - \frac{k}{m}x\end{aligned}$$



**Note:**

- notation: we often write  $\dot{x}$  for  $\frac{dx}{dt}$

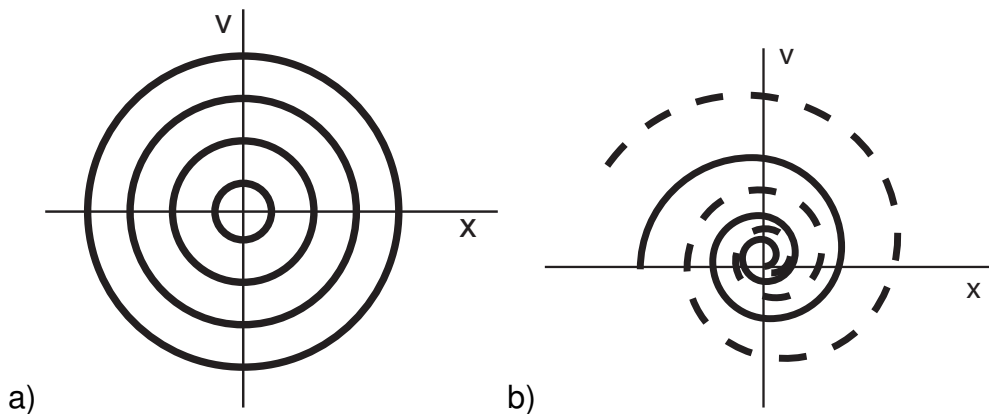


Figure 5: Phase portraits for a harmonic oscillator. a) without friction ( $\beta = 0$ ) any initial condition leads to harmonic oscillations. b) with damping ( $\beta > 0$ ) any initial condition leads to oscillatory convergence to a fixed point.

**Focus on the phase plane:**

- the phase portrait provides a **complete overview** of all possible solutions<sup>20</sup>

**Conservative Systems** (no friction/dissipation)

- almost all different initial condition lead to different states

**Dissipative Systems**

- a range of initial conditions leads to the same state: **attractors**
- **transitions**: **qualitative** change in the number and type of attractors

In this class we will mostly focus on dissipative systems.

## 2 1-d Flow

### 2.1 Flow on the Line<sup>21</sup>

Any first-order autonomous differential equation (i.e. without explicit time dependence),

$$\dot{x} = f(x),$$

can be solved exactly for any  $f(x)$  (by separation of variables).

---

<sup>20</sup>here linear  $\rightarrow$  not much going on.

<sup>21</sup>cf. Strogatz Ch.2 and Lecture 2

$$\int_{x_0}^x \frac{dx}{f(x)} = t - t_0$$

**Example:**

$$\dot{x} = \sin x$$

$$\begin{aligned} t &= \int \frac{dx}{\sin x} = \int \csc x \, dx \\ t &= -\ln |\csc x + \cot x| + C \end{aligned}$$

Now what? What have we learned?

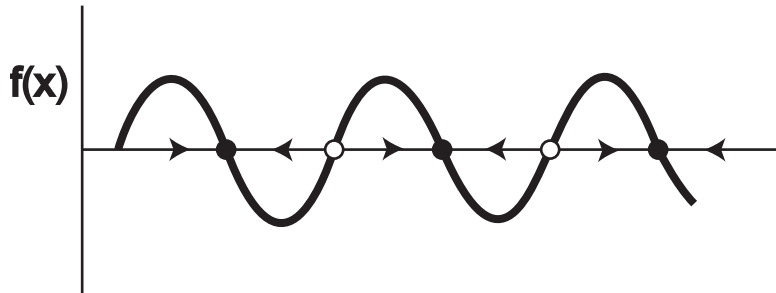
Even if we can solve for  $x$ , which we cannot always do, would we have an overview of the behavior of system for arbitrary initial conditions?

Geometrical picture: **phase space** (or phase line in 1 dimension)



$\dot{x} = f(x)$  defines a *flow* in phase space or a *vector field*

For 1d: plot in addition  $f(x)$



The phase portrait gives us a complete picture of the qualitative behavior of the system.

*Conclude:* any i.c. ends up in one of the **fixed points** at  $x_n = (2n + 1)\pi$ .  
Fixed points are **stagnation points** of the flow

**Stability:**

- flow *into*  $x_n = (2n + 1)\pi$ : *stable*
- flow *out of*  $x_n = 2n\pi$ : *unstable*

**Of course:** for **quantitative results** ('numbers') we need the detailed solution.

**Example:** Population Growth with Limited Resources

Write  $N$  for the number of animals (size of population)

$$\frac{dN}{dt} = g(N)N$$

with  $g(N) = \text{net birth/death rate}$

Limited food/space:

births decrease, deaths increase with increasing  $N$

Minimal model'

$$g(N) = \alpha - \beta N$$

$\Rightarrow$  Logistic growth model

$$\dot{N} = \alpha N - \beta N^2$$

Make dimensionless:

$$[\alpha] = \frac{1}{s} \quad [\beta] = \frac{1}{s} \frac{1}{\#}$$

$\frac{1}{\alpha}$  characteristic growth time

$\frac{\alpha}{\beta}$  characteristic population size

Introduce

$$\tau = \alpha t \quad n = \frac{\beta}{\alpha} N$$

**Question:** If the population goes to some non-zero equilibrium, what population size would you expect?

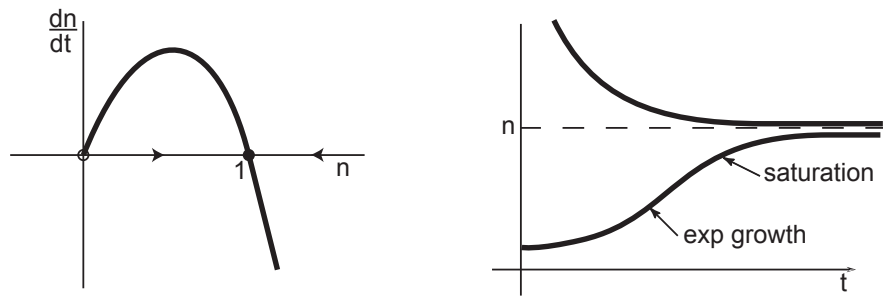
$\frac{\alpha}{\beta}$  is the only characteristic size after initial condition is forgotten  $\Rightarrow$  expect  $N \rightarrow \frac{\alpha}{\beta}$ .

Rewriting the differential equation in terms of  $n$  and  $\tau$  yields

$$\frac{dn}{d\tau} = n - n^2$$

Could solve the differential equation by partial fraction.

Instead, consider phase space:



fixed points:  $n = 0, n = 1$

flow indicates:  $n = 0$  unstable,  $n = 1$  stable

indeed: **all i.c.** go to  $n = 1$  i.e.  $N = \frac{\alpha}{\beta}$

In the one-dimensional plot the stability of the fixed points can be read off easily. In general (higher dimensions) much more difficult  $\Rightarrow$  determine the *linear* stability of the fixed points, i.e. consider small perturbations around them.

**Linear Stability:**

Study the effect of *small perturbations* away from the fixed point

Insert the expansion

$$n = n_0 + \epsilon n_1(\tau) + \epsilon^2 n_2(\tau) + \dots \quad \epsilon \ll 1$$

into the equation for  $n$

$$\frac{d(n_0 + \epsilon n_1(\tau) + \epsilon^2 n_2(\tau) + \dots)}{d\tau} = n_0 + \epsilon n_1(\tau) + \epsilon^2 n_2(\tau) + \dots - (n_0 + \epsilon n_1(\tau) + \epsilon^2 n_2(\tau) + \dots)^2$$

Expanding the square we get

$$\epsilon \frac{dn_1(\tau)}{d\tau} + \epsilon^2 \frac{dn_2(\tau)}{d\tau} + \dots = n_0 - n_0^2 + \epsilon (n_1(\tau) - 2n_0 n_1(\tau)) + \epsilon^2 (n_2(\tau) - 2n_0 n_2(\tau) - n_1(\tau)^2) + \dots$$

This equation has to be valid for any  $\epsilon \ll 1$ . Therefore it has to be valid also for  $\epsilon = 0$ ,

$$\begin{aligned} 0 &= n_0 - n_0^2 \\ \Rightarrow n_0 &= 1 \quad \text{or} \quad n_0 = 0 \end{aligned}$$

Insert this back into the equation above. Now we can cancel the overall factor of  $\epsilon$ ,

$$\frac{dn_1(\tau)}{d\tau} + 2\epsilon \frac{dn_2(\tau)}{d\tau} + \dots = + (n_1(\tau) - 2n_0 n_1(\tau)) + 2\epsilon (n_2(\tau) - 2n_0 n_2(\tau) - n_1(\tau)^2) + \dots$$

and set  $\epsilon = 0$  again

$$\begin{aligned} \frac{dn_1}{d\tau} &= n_1 - 2n_0 n_1 = (1 - 2n_0) n_1 \\ \Rightarrow n_1 &\propto e^{(1-2n_0)\tau} \end{aligned}$$

Thus,

$$\begin{aligned} n_0 = 1 \Rightarrow 1 - 2n_0 < 0 &\quad n_1 \text{ decays and that fixed point is stable} \\ n_0 = 0 \Rightarrow 1 - 2n_0 > 0 &\quad n_1 \text{ grows and that fixed point is unstable} \end{aligned}$$

**Notes:**

- One says a term  $a$  is of order  $\epsilon^n$ ,  $a = \mathcal{O}(\epsilon^n)$ , if  $a$  decreases at least as fast as  $\epsilon^n$  when  $\epsilon \rightarrow 0$ .  
Thus,  $\mathcal{O}(\epsilon) \ll \mathcal{O}(\epsilon^2)$  etc.  
A more formal definition is that  $a = \mathcal{O}(\epsilon^n)$  if  $a \leq C\epsilon^n$  as  $\epsilon \rightarrow 0$  for some constant  $C$ .
- For  $\epsilon \ll 1$  the terms involving  $n_2(\tau)$  etc. will be  $\mathcal{O}(\epsilon^2)$ , i.e. they will be much smaller than  $\epsilon n_1(\tau)$ , and can be neglected.
- Because the higher-order terms are neglected, this stability analysis is a *linear* stability analysis.

- Our procedure showed that because  $\epsilon$  is an arbitrary number, solving the expanded equation requires that the coefficients of like powers in  $\epsilon$  have to be equal on both sides of the equation.

**More generally:**

Consider

$$\dot{x} = f(x)$$

with a fixed point  $x_0$  satisfying

$$0 = f(x_0).$$

To determine the linear stability of  $x_0$  we make the ansatz:

$$x = x_0 + \epsilon x_1(t)$$

**Note:**

- for the linear stability analysis we do not need to introduce  $\epsilon^2 x_2(t)$  etc..

We use a Taylor expansion of  $f(x)$ ,

$$\dot{x}_0 + \epsilon \dot{x}_1 = f(x_0 + \epsilon x_1) = f(x_0) + f'(x_0) \epsilon x_1 + \frac{1}{2} f''(x_0) (\epsilon x_1)^2 + \dots$$

Again, equating like powers in  $\epsilon$  on both sides leads to

$$\begin{aligned} \mathcal{O}(\epsilon^0) : \quad 0 &= f(x_0) \\ \mathcal{O}(\epsilon^1) : \quad \dot{x}_1 &= f'(x_0) x_1 \end{aligned}$$

Thus,

$$x_1(t) \propto e^{f'(x_0)t}$$

and

the fixed point is stable:  $f'(x_0) < 0$

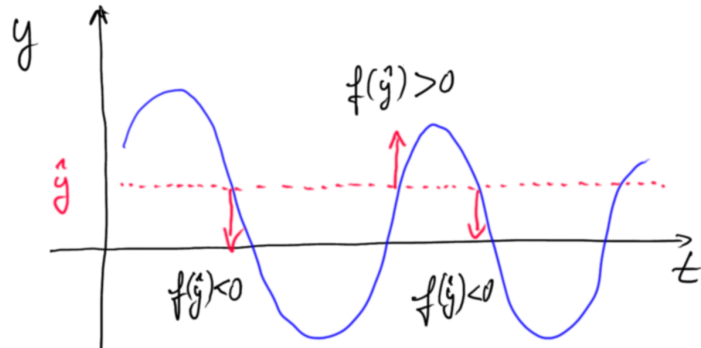
the fixed point is unstable:  $f'(x_0) > 0$

**Note:**

- for coupled systems  $f'(x)$  is replaced by Jacobian matrix:  
eigenvalues determine the stability (see below).

### 2.1.1 Impossibility of Oscillations

Does a 1-dimensional system allow oscillations? Can a fixed point be approached in an oscillatory fashion?



No! To get oscillations,  $x(t)$  would have to come back to an earlier value at a later time, i.e.  $x(t_2) = x(t_1)$  with  $t_2 > t_1$ . But the sign of  $\dot{x}(t)$  would have to be opposite at the two times, implying  $f(x(t_1)) \neq f(x(t_2))$ . This is not possible since  $x(t_2) = x(t_1)$  and  $f(x)$  is single-valued.

⇒ The system evolves monotonically.

It is the topology of the phase line that does not allow oscillations:

- in 1 dimension one can get back to a previous point only by *retracing* one's steps.
- in higher dimensions one can get back by taking a different path.

### More general concept: potential

For one-dimensional systems with time-independent coefficients one can always write

$$\dot{x} = f(x) = -\frac{dV(x)}{dx} \quad \text{with } V(x) = - \int f(x) dx$$

Consider:

$$\frac{dV}{dt} = \frac{dV}{dx} \dot{x} = -\dot{x}^2 \leq 0$$

Thus, any change in  $x$  reduces  $V \Rightarrow V$  cannot return to a previous, higher value  
⇒ no periodic motion possible.

In addition

$$\frac{dV}{dt} = 0 \quad \Rightarrow \quad \dot{x} = 0 \quad \text{fixed point}$$

Thus,  $x(t)$  either goes to a fixed point or  $V(x(t))$  diverges to  $-\infty$ .

**Note:**

- $V(x)$  is called a Lyapunov function for the differential equation.
- In an overdamped mechanical system  $V(x)$  is related to the potential energy

$$m\ddot{x} = -\beta\dot{x} + F(x) = -\beta\dot{x} - \frac{dV(x)}{dx}$$

For very small mass (no inertia) we get

$$\dot{x} = \frac{1}{\beta}F(x).$$

### Note:

- The concept of the potential is not limited to one-dimensional systems. If a higher-dimensional systems can be derived from a potential, the potential is a powerful tool to rule out oscillations. However, only few higher-dimensional systems allow a potential.

## 2.2 Existence and Uniqueness

So far we assumed that starting from a given initial condition we always get a **unique** solution for **all times**:

- at any time ‘we know where to go’
- we can continue this forever

Solutions to

$$\dot{x} = f(x)$$

1. do not have to exist for all times:  
for a given initial condition the solution may cease to exist beyond some time

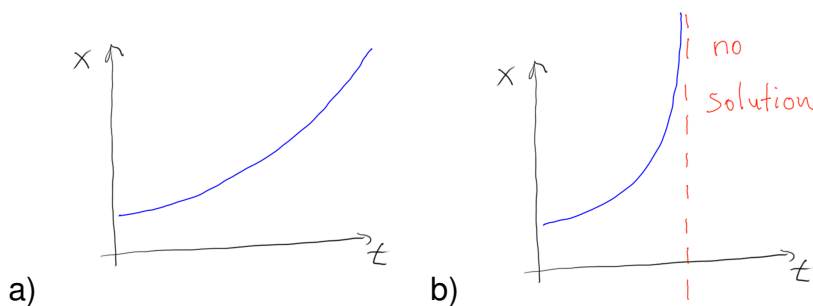


Figure 6: a) Linear equation: exponential growth can diverge in infinite time  $\Rightarrow$  solution exists for all finite times. b) Nonlinear equation: divergence in finite time  $\Rightarrow$  no solution beyond that time.

2. do not have to be unique:  
the same initial condition can lead to different states later.

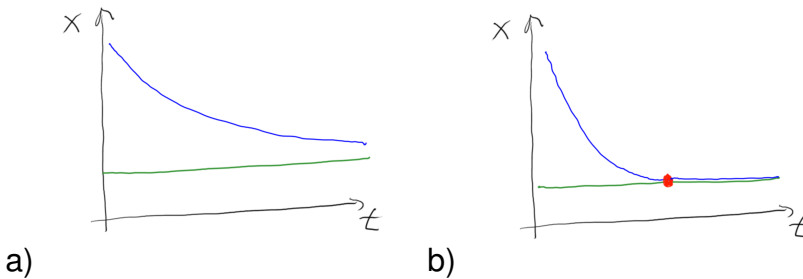


Figure 7: a) Linear equation: exponential convergence to fixed point in infinite time. b) Nonlinear equation: convergence to fixed point in finite time  $\Rightarrow$  in time-reversed system one can start at fixed point and stay there or depart from it: multiple solutions for the same initial condition.

### Theorem:

If  $f(x, t)$  and  $\frac{\partial f}{\partial x}$  are continuous in the vicinity of the initial condition  $x(t_0) = x_0$ , i.e. for  $|t - t_0| < \Delta t$  and  $|x - x_0| \leq \Delta x$ , then the solution exists for a finite time interval around  $t_0$  and is unique there.

### 1. Existence

Solution can disappear by becoming infinite. If this happens in *finite* time then there is no solution beyond that time

#### Example:

$$\dot{x} = +x^\alpha \quad \text{with} \quad x(0) = x_0 > 0$$

$$\begin{aligned} \int x^{-\alpha} dx &= \int \frac{dx}{x^\alpha} = t + C \\ \frac{1}{1-\alpha} x^{1-\alpha} &= t + C \end{aligned}$$

Initial conditions:

$$\begin{aligned} C &= \frac{1}{1-\alpha} x_0^{1-\alpha} \\ x(t) &= ((1-\alpha)t + x_0^{1-\alpha})^{\frac{1}{1-\alpha}} \end{aligned}$$

The solution diverges at

$$t^* = \frac{x_0^{1-\alpha}}{\alpha-1} > 0 \quad \text{if} \quad \alpha > 1$$

i.e. for  $\alpha > 1$  the divergence occurs in **finite time**.

#### Note:

- a divergence in *infinite* time represents no problem:  $x(t) = e^t$  exists for all times

## 2. Uniqueness

Consider the previous example for  $0 < \alpha < 1$

$$\Rightarrow x = 0 \quad \text{for} \quad t^* = \frac{x_0^{1-\alpha}}{\alpha - 1} < 0$$

This solution starts at  $t^*$  with  $x(t^*) = 0$  and grows from there.

**But:**  $\tilde{x}(t) \equiv 0$  is also a solution for all times.

**Thus:**

- The two *different* solutions  $\tilde{x}(t)$  and  $x(t)$  satisfy the *same* initial condition,  $x(t^*) = 0$ .

Moreover, we can construct another solution by starting with  $\tilde{x}(t) \equiv 0$  for  $t < t^*$  and 'switch' to  $x(t) > 0$  beyond  $t^*$ ,

$$\hat{x}(t) = \begin{cases} 0 & t \leq t^* \\ ((1-\alpha)t + x_0^{1-\alpha})^{\frac{1}{1-\alpha}} & t > t^* \end{cases}$$

The combined solution  $\hat{x}(t)$  is continuously differentiable everywhere, even at  $t^*$ , and satisfies the differential equation.

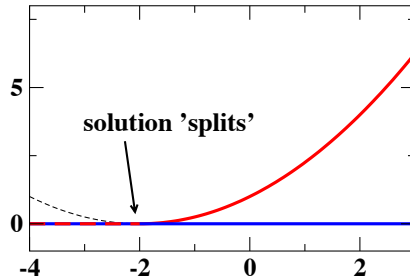


Figure 8: Non-uniqueness of an initial value problem: both, the blue and the red function satisfy the differential equation  $\dot{x} = x^{\frac{1}{2}}$  with the initial condition  $x(t_0) = 0$  for any  $t_0 \leq t^* = -2$ .

**Worse:**  $t^*$  varies with  $x_0$

$\Rightarrow \hat{x}(t)$  satisfies the initial condition  $x(t_{init}) = 0$  for any  $t^* < t_{init}$

$\Rightarrow$  infinitely many solutions that all satisfy the same initial conditions,  $x = 0$ .

**Note:**

- in the linear case,  $\alpha = 1$ , one would have  $x(t) \propto e^t$  and  $x = 0$  would be reached only in the *infinite past* ( $t \rightarrow -\infty$ ), which would not allow a connection to the solution  $x \equiv 0$ .

**Theorem<sup>22</sup>:**

If for  $\dot{x} = f(x, t)$

<sup>22</sup>see, e.g., Lin & Segel, *Mathematics applied to deterministic problems in the natural sciences*, p.57

- $f(x, t)$  is continuous in the vicinity of the initial condition  $x(t_0) = x_0$ , i.e. for  $|t - t_0| < \Delta t$  and  $|x - x_0| \leq \Delta x$ , and
- $f(x, t)$  satisfies Lipschitz condition within that vicinity,

$$|f(x_1, t) - f(x_2, t)| \leq K |x_1 - x_2| \quad \text{for all } |x_{1,2} - x_0| \leq \Delta x \text{ and for all } |t - t_0| \leq \Delta t$$

with some constant  $K$  ( $K$  can be thought of as a maximal slope in that vicinity)

then the solution exists for a finite time interval around  $t_0$ ,  $|t - t_0| \leq \Delta T$ , and is unique there. The interval is given by

$$\Delta T = \min \left( \Delta t, \frac{\Delta x}{M} \right)$$

where  $M$  is the maximum of  $|f(x, t)|$  within  $|t - t_0| < \Delta t$  and  $|x - x_0| \leq \Delta x$ .

### Notes:

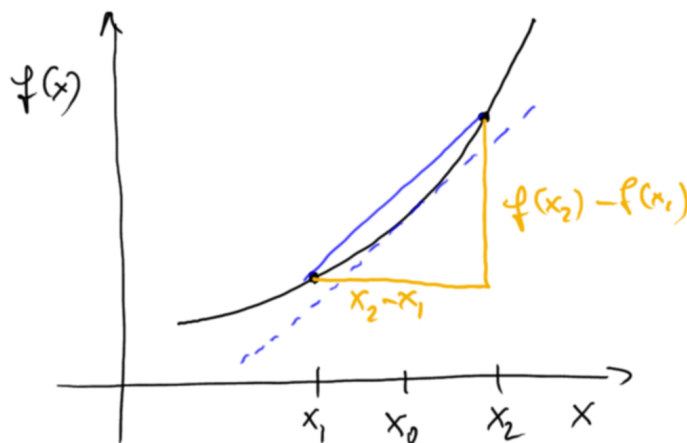
- $f(x) = |x|^\alpha$  does not satisfy Lipschitz condition at  $x = 0$  for  $0 < \alpha < 1$ : we would need

$$|x|^\alpha \leq K |x| \quad \text{for all } x \text{ near } x = 0$$

i.e.  $K \geq |x|^{\alpha-1}$ . But  $|x|^{\alpha-1} \rightarrow \infty$  for  $x \rightarrow 0$  and  $\alpha < 1$ .

$\Rightarrow$  the theorem does not guarantee the uniqueness of the solution; and, in fact, it is not unique.

- If  $f'(x)$  is continuous near  $x_0$ , then the slope of  $f'(x)$  has a maximum and  $f(x)$  satisfies the Lipschitz condition via the mean-value theorem and the solution is unique near  $x_0$ .



## 2.3 Bifurcations in 1 Dimension<sup>23</sup>

We had: in 1d final state always fixed point (if dynamics are bounded).

How many fixed points? How can the number of fixed points change?

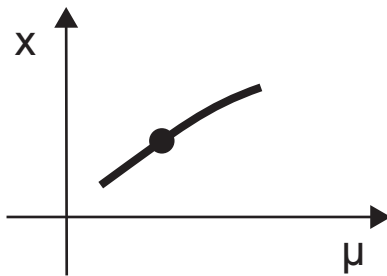
⇒ Introduce parameter  $\mu$

$$f(x, \mu) = 0$$

To study the creation or elimination of fixed point we need to study only small changes in  $\mu$

⇒ analysis in the *vicinity* of some specific value of  $\mu$ , i.e. *local* analysis

**Question:** Does the solution persist when the parameter is changed? Is it unique?



### 2.3.1 Implicit Function Theorem

*Local analysis* in the vicinity of a fixed point for small changes in  $\mu$ :

Consider the vicinity of  $x_0$  and  $\mu_0$ ,

$$x = x_0 + \Delta x \quad \mu = \mu_0 + \Delta \mu \quad \text{with } \Delta x \ll 1 \quad \Delta \mu \ll 1$$

At this point we do not know how the two small parameters  $\Delta x$  and  $\Delta \mu$  are related to each other.

For smooth  $f(x, \mu)$  we can use a Taylor expansion around  $x_0$  and  $\mu_0$

$$f(x_0 + \Delta x, \mu_0 + \Delta \mu) = \underbrace{f(x_0, \mu_0)}_{=0} + \frac{\partial f}{\partial x} \Delta x + \frac{\partial f}{\partial \mu} \Delta \mu + \frac{1}{2} \frac{\partial^2 f}{\partial x^2} \Delta x^2 + \frac{\partial^2 f}{\partial x \partial \mu} \Delta x \Delta \mu + \frac{1}{2} \frac{\partial^2 f}{\partial \mu^2} \Delta \mu^2 + \dots = 0$$

(All derivatives evaluated at  $x_0, \mu_0$ )

Since we are assuming  $x_0$  is a fixed point for  $\mu = \mu_0$ , we have  $f(x_0, \mu_0) = 0$ .

If  $\frac{\partial f}{\partial x}|_{x_0, \mu_0} \neq 0 \Rightarrow$  we can write

$$x - x_0 = \Delta x = -\Delta \mu \frac{\frac{\partial f}{\partial \mu}}{\frac{\partial f}{\partial x}} + \mathcal{O}(\Delta \mu^2) + \mathcal{O}(\Delta x^2) + \mathcal{O}(\Delta x \Delta \mu) .$$

<sup>23</sup>cf. Strogatz Ch.3 Lecture 2

Even without knowing any relation between  $\Delta\mu$  and  $\Delta x$  we know

$$\Delta x^2 \ll \Delta x \quad \Delta\mu^2 \ll \Delta\mu \quad \Delta x \Delta\mu \ll (\Delta x, \Delta\mu)$$

and we can ignore these terms. We see then that  $\Delta x = \mathcal{O}(\Delta\mu)$  and the higher-order terms  $\Delta x^2$  and  $\Delta x \Delta\mu$  are  $\mathcal{O}(\Delta\mu^2)$ .

Thus, we have obtained a unique solution for the fixed point for all values of  $\mu$  in the vicinity of  $\mu_0$

- If  $\frac{\partial f}{\partial x}|_{x_0, \mu_0} \neq 0$ , there is a *unique branch* of solutions.

More generally for higher dimensions:

### Implicit function theorem:

Consider the solutions of

$$\mathbf{f}(\mathbf{x}, \mu) = 0 \quad \mathbf{x} \in \mathbb{R}^n \quad \mathbf{f} \text{ smooth in } \mathbf{x} \text{ and } \mu$$

If

$$\mathbf{f}(\mathbf{x} = \mathbf{x}_0, \mu = \mu_0) = 0$$

and

$$\det \left( \frac{\partial f_i}{\partial x_j} \right) \neq 0 \quad \text{at } \mu = \mu_0 \text{ and } \mathbf{x} = \mathbf{x}_0,$$

then there is a **unique** differentiable  $\mathbf{X}(\mu)$  that satisfies

$$\mathbf{f}(\mathbf{X}(\mu), \mu) = 0 \quad \text{and} \quad \mathbf{X}(\mu = \mu_0) = \mathbf{x}_0$$

in the vicinity of  $\mu = \mu_0$ .

**Thus:** if  $\det \left( \frac{\partial f_i}{\partial x_j} \right) \neq 0$  there is a **unique branch** of solutions  $\mathbf{X}(\mu)$  going through  $\mathbf{x} = \mathbf{x}_0$  as  $\mu$  is varied.

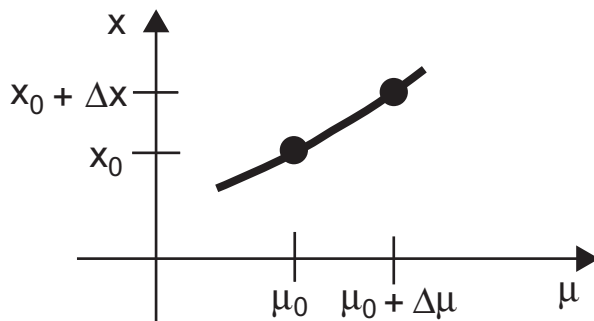


Figure 9: If  $\frac{\partial f}{\partial x} \neq 0$  at the fixed point  $(x_0, \mu_0)$ , there is a unique branch of solutions in the vicinity of  $\mu_0$ .

### Notes:

- In 1d:  $\det \frac{\partial f_i}{\partial x_j} \rightarrow \frac{df}{dx} = f'(x)$   
⇒ as seen in our explicit calculation: if  $f'(x) \neq 0$ , the branch persists uniquely.

- The change in  $x$  is smooth in  $\mu$  if  $\frac{\partial f}{\partial x} \neq 0$ ,

$$\Delta x \sim \Delta \mu \quad (1)$$

**Generic properties** are those properties that do not require **any tuning** of parameters.

When picking parameters at random one expects  $\frac{\partial f}{\partial x}|_{x_0, \mu_0} \neq 0$ ,

- i.e. we would need to *tune*  $\mu$  to get  $\frac{\partial f}{\partial x}|_{x_0, \mu_0} = 0$
- $\Rightarrow$  **generically** there is a smooth branch.

Putting back the dynamics in the vicinity of  $x_0$  at  $\mu_0$  and writing  $x(t) = x_0 + \Delta x(t)$  we have

$$\frac{d}{dt}(x_0 + \Delta x(t)) = f(x_0 + \Delta x, \mu) = \underbrace{f(x_0, \mu_0)}_{=0} + \left. \frac{\partial f}{\partial x} \right|_{x_0, \mu_0} \Delta x + \frac{1}{2} \frac{\partial^2 f}{\partial x^2} \Delta x^2 + \dots$$

Ignoring  $\mathcal{O}(\Delta x^2)$  we get

$$\frac{d}{dt} \Delta x(t) = \left. \frac{\partial f}{\partial x} \right|_{x_0, \mu_0} \Delta x(t).$$

Thus, the condition for the failure of the implicit function theorem,

$$\left. \frac{\partial f}{\partial x} \right|_{x_0, \mu_0} = 0,$$

is also the condition for a change in the linear stability of  $x_0$ .

**A change in the number of fixed points** requires a **change in the (linear) stability** of the fixed point.

### 2.3.2 Some Simple Examples: Normal Forms

Before considering a general function, consider the fixed points of some simple examples.

1.

$$\dot{x} = f(x, \mu) = \mu - x^2. \quad (2)$$

Explicit solution

$$x = \pm\sqrt{\mu}.$$

**Bifurcation diagrams:** plot all solution branches as a function of  $\mu$ .

In view of the implicit function theorem: is there a unique branch  $x(\mu)$  through  $(\mu_0, x_0)$  for all values of  $(\mu_0, x_0)$ ?

No, for  $\mu_0 = 0$  and  $x_0 = 0$  the solution cannot be continued to  $\mu < \mu_0$ .

Check  $\left. \frac{\partial f}{\partial x} \right|_{\mu_0, x_0} = -2x_0$ . Thus, the implicit function theorem is valid as long as  $x_0 \neq 0$ , consistent with the branch existing as long as  $x_0 \neq 0$ .

**Note:**

- At  $\mu_0 = 0$  the system (2) undergoes what is called a saddle-node bifurcation.
- In a saddle-node bifurcation two solutions annihilate each other.
- (2) is not just a made-up toy equation. It turns out to be, what is called the normal form of the saddle-node bifurcation. We will discuss this shortly more generally.

2.

$$\dot{x} = f(x, \mu) = x(\mu - x) \quad (3)$$

Explicit solutions

$$x_1 = 0 \quad \text{and} \quad x_2 = \mu$$

There is a unique branch  $x(\mu)$  through  $(\mu_0, x_0)$  for all values of  $\mu_0$  except for  $\mu_0 = 0$ . At  $\mu_0$  the branch continues, but it is not unique.

Now

$$\left. \frac{\partial f}{\partial x} \right|_{\mu, x} = \mu - 2x .$$

Thus,

$$\left. \frac{\partial f}{\partial x} \right|_{\mu, x_1} = \mu \quad \text{for} \quad x = x_1$$

$$\left. \frac{\partial f}{\partial x} \right|_{\mu, x_2} = \mu - 2\mu = -\mu \quad \text{for} \quad x = x_2$$

and the only point where the implicit function theorem breaks down is  $\mu = 0$ .

**Note:**

- At  $\mu = 0$  the system (3) undergoes a transcritical bifurcation.
- In a transcritical bifurcation the total number of solutions does not change, if one counts the solution for  $\mu = 0$  twice.

### 2.3.3 General Functions $f(x, \mu)$ : Saddle-Node Bifurcation

What happens in general when  $\frac{\partial f}{\partial x} = 0$ ?

To solve for  $x$  in  $f(x, \mu) = 0$  in the vicinity of  $(\mu_0, x_0)$  we need to go to higher order in the Taylor expansion (for simplicity choose  $x_0 = 0, \mu_0 = 0$ )

$$0 = f(x, \mu) = \underbrace{f(0, 0)}_{=0} + \underbrace{\frac{\partial f}{\partial x}}_{=0} x + \frac{\partial f}{\partial \mu} \mu + \frac{1}{2} \frac{\partial^2 f}{\partial x^2} x^2 + \frac{\partial^2 f}{\partial x \partial \mu} x \mu + \frac{1}{2} \frac{\partial^2 f}{\partial \mu^2} \mu^2 + \dots$$

Solve again:

$$x^2 = -\frac{2}{\frac{\partial^2 f}{\partial x^2}} \left\{ \frac{\partial f}{\partial \mu} \mu + \frac{\partial^2 f}{\partial x \partial \mu} x \mu + \frac{1}{2} \frac{\partial^2 f}{\partial \mu^2} \mu^2 + \dots \right\}$$

We are interested in the solution of this equation only for  $|x| \ll 1$  and  $|\mu| \ll 1$ . This implies

$$|x\mu| \ll |x| \quad \text{and} \quad \mu^2 \ll |\mu| .$$

We can therefore ignore the second and third and higher terms on the r.h.s and obtain

$$x^2 = -\frac{2}{\frac{\partial^2 f}{\partial x^2}} \frac{\partial f}{\partial \mu} \mu .$$

Except for the prefactor this is exactly the equation (2) for the saddle-node bifurcation and has the solutions

$$x_{1,2} = \pm \sqrt{-2 \frac{\frac{\partial f}{\partial \mu}}{\frac{\partial^2 f}{\partial x^2}} \mu} .$$

### Note:

- The prefactor  $\frac{2}{\frac{\partial^2 f}{\partial x^2}} \frac{\partial f}{\partial \mu}$  is just a number, since the derivatives are evaluated at  $(x_0 = 0, \mu_0 = 0)$ . Its sign determines whether the solutions arise for  $\mu > 0$  or for  $\mu < 0$ .

### Notes:

- If the implicit function theorem fails one gets a nonlinear, higher-order equation with multiple solutions (depending on the parameters)
- the change in  $x$  is **not smooth** in  $\mu$

### Dynamics:

$$\dot{x} = f(x, \mu) = a\mu + bx^2 + \text{h.o.t.} \quad (4)$$

with

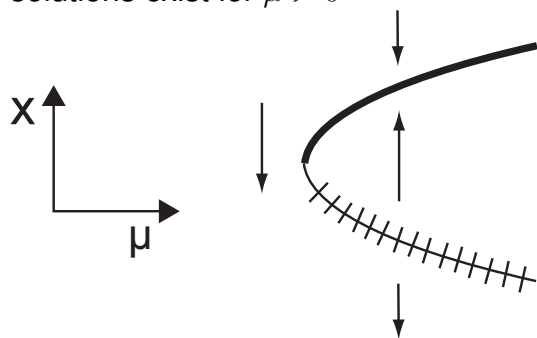
$$a = \left. \frac{\partial f}{\partial \mu} \right|_{x=x_0, \mu=\mu_0} \equiv \partial_\mu f \quad b = \left. \frac{\partial^2 f}{\partial x^2} \right|_{x=x_0, \mu=\mu_0} \equiv \partial_x^2 f$$

and *h.o.t.* denotes higher-order terms.

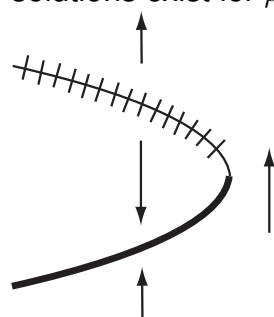
Relevant parameters:

$$\frac{a}{b} = \frac{\partial_\mu f}{\partial_x^2 f} = \frac{\frac{\partial f}{\partial \mu}}{\frac{\partial^2 f}{\partial x^2}}$$

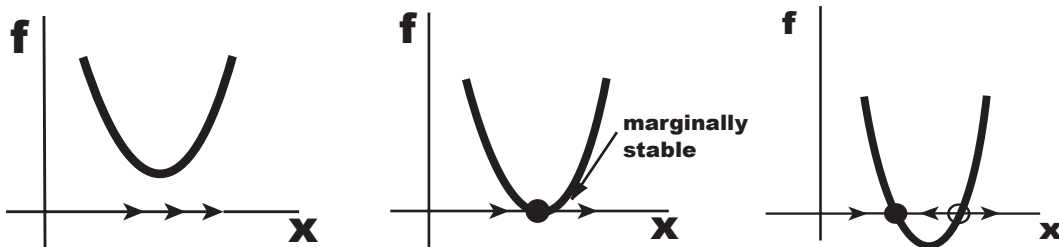
$\frac{a}{b} < 0$  and  $a > 0$   
solutions exist for  $\mu > 0$



$\frac{a}{b} > 0$  and  $a > 0$   
solutions exist for  $\mu < 0$



The  $x$ -direction in these  $(x, \mu)$ -plots corresponds to the phase line for a given value of  $\mu$ .  
The arrows indicate the flow on the phase line for that value of  $\mu$ .



### Notes:

- 2 fixed points are created/destroyed. Single solutions cannot simply pop up or disappear: instead 2 solutions merge and are annihilated.
- The coinciding fixed points at  $\mu = 0$  are linearly marginally stable:  $\partial f / \partial x$  changes sign going along the solution branch: **change in stability**
- The conditions for a saddle-node bifurcation to occur for some value  $\mu_0$  are
  - $f(x_0, \mu_0) = 0$ , which is the condition for  $x_0$  to be a fixed point,
  - $\frac{\partial f}{\partial x} \Big|_{\mu_0, x_0} = 0$ , which is the condition for **any** bifurcation to occur,
  - $\frac{\partial^2 f}{\partial x^2} \Big|_{\mu_0, x_0} \neq 0$ , which is to be expected unless some special conditions are met or some other parameter is tuned.

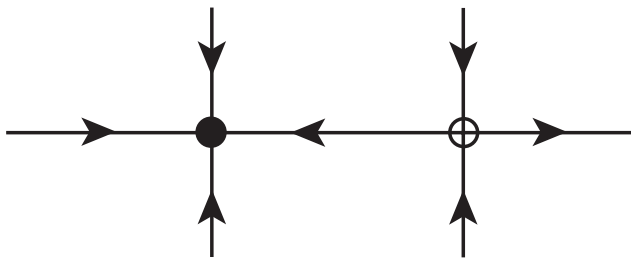
Therefore, unless the system has some special properties, if a bifurcation occurs, one should expect a saddle-node bifurcation.

- (4) is the universal form ('normal form') of the equation describing the dynamics near a saddle-node bifurcation
- The flow changes direction **only locally**: only when  $\mu$  goes through 0 and only near the bifurcation point  $x = 0$  does the flow

change direction.

Away from the bifurcation point the flow is qualitatively unchanged when  $\mu$  changes (arrows far away remain the same).

- The saddle-node bifurcation is sometimes also called “blue-sky bifurcation”, because two solutions seem to appear from nowhere as the parameter  $\mu$  is changed.
- in higher dimensions: saddle-node bifurcation



stable  $\sim$  node    unstable  $\sim$  saddle

### Example:

Find the fixed points and any bifurcations for<sup>24</sup>

$$\dot{x} = f(x, \mu) = \mu x + \frac{1}{1-x}. \quad (5)$$

Analyze this equation first graphically;

Fixed points satisfy

$$f(x, \mu) = 0 \quad g(x, \mu) = h(x, \mu) \quad \text{with} \quad g(x, \mu) = -\mu x \quad h(x, \mu) = \frac{1}{1-x}$$

At a bifurcation we have in addition

$$\frac{\partial f(x, \mu)}{\partial x} = 0 \quad \frac{\partial g(x, \mu)}{\partial x} = \frac{\partial h(x, \mu)}{\partial x}$$

i.e. the slopes of  $g$  and  $h$  are equal, the graphs are tangential to each other (Fig.10b). The resulting bifurcation is a saddle-node bifurcation.

There is only a single value for  $\mu$  for which the two curves are tangential; solutions disappear and appear individually (not in pairs) at infinity ( $x \rightarrow \infty$  or  $f \rightarrow \infty$  or  $g \rightarrow \infty$ ).

---

<sup>24</sup>In this example  $f(x, \mu)$  is not continuously differentiable at  $x = 1$  and therefore the solution does not exist for all times. E.g. for  $\mu = 0$  the solution is given by  $x(t) = 1 \pm \sqrt{1 - 2(t + C)}$  and ceases to exist for  $t + C > \frac{1}{2}$ , where  $C$  depends on the initial condition.

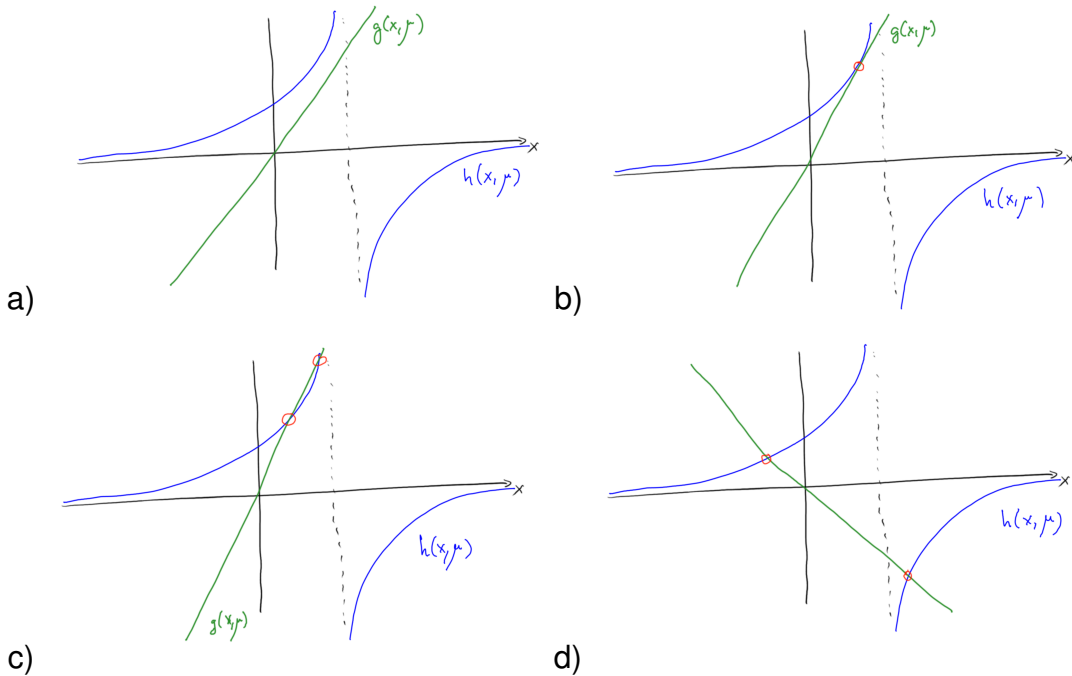


Figure 10: Graphical solution of (5) for different values of  $\mu$  for  $g(x, \mu) = -\mu x$ ,  $h(x, \mu) = (1 - x)^{-1}$ .

Algebraically, one gets

$$f(x, \mu) = -\mu x^2 + \mu x + 1 = 0 \quad \Rightarrow \quad x_{1,2} = \frac{-\mu \pm \sqrt{\mu^2 + 4\mu}}{-2\mu} = \frac{1}{2} \left( 1 \pm \sqrt{1 + \frac{1}{\mu}} \right)$$

$$\frac{\partial f(x, \mu)}{\partial x} = 0 = \mu + \frac{1}{(1 - x)^2}$$

Instead of plugging in  $x_{1,2}$  we can solve the fixed-point equation for  $\mu$ ,

$$\mu = -\frac{1}{x} \frac{1}{1 - x}$$

and insert it into the equation for the bifurcation

$$\frac{1}{(1 - x)^2} = \frac{1}{x} \frac{1}{1 - x} \quad x = 1 - x \quad x = \frac{1}{2} \quad \Rightarrow \quad \mu = -\frac{1}{4}.$$

Indeed, for  $\mu = \frac{1}{4}$  both solutions  $x_{1,2}$  coincide.

### Bifurcation diagram:

Often one can solve in the fixed-point equation for the control parameter  $\mu$  instead of  $x$ :

$$\mu = -\frac{1}{x} \frac{1}{1 - x}.$$

Then the bifurcation diagram is obtained by reflecting the graph across the diagonal.

### Notes:

- In this example the flow velocity  $\dot{x}$  diverges for  $x = 1$  and the flow direction changes sign.
- Thus: when identifying the stability of fixed points: the flow direction can (but need not) change sign only
  - at fixed points or
  - at locations where  $\dot{x}$  diverges.

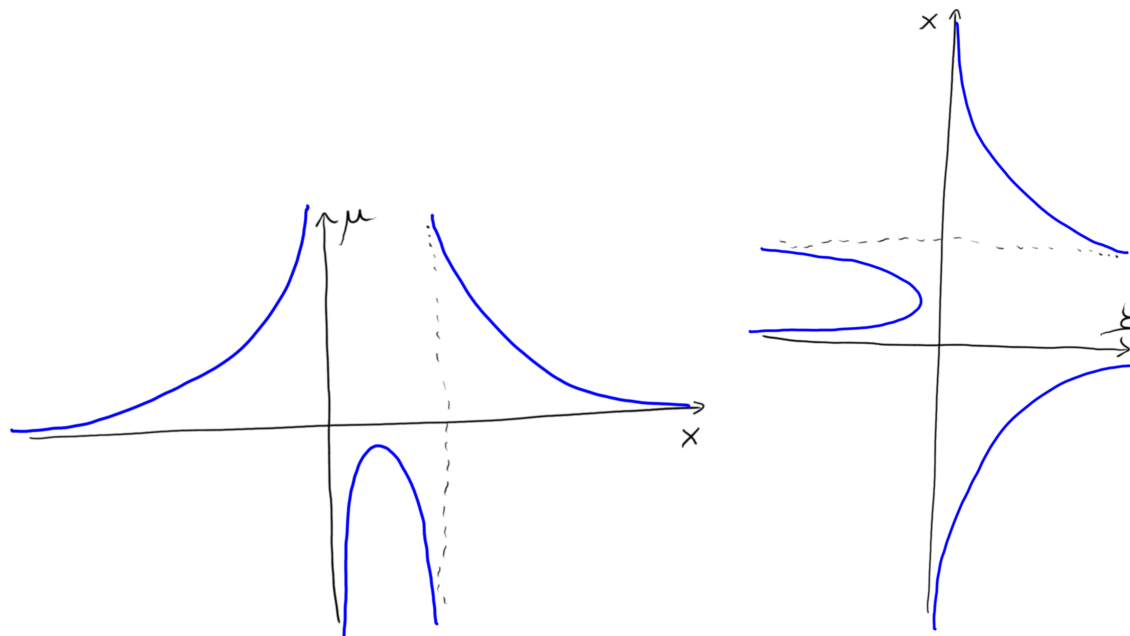


Figure 11: Bifurcation diagram obtained by reflecting  $\mu = \mu(x)$  across the diagonal. Note the range  $-\frac{1}{4} < \mu < 0$  for which there is no fixed point solution.

- In Taylor vortex flow in a short cylinder the transition to vortices arises through a saddle-node bifurcation and exhibits hysteresis.  
Here the saddle-node bifurcation is part of a larger bifurcation scenario

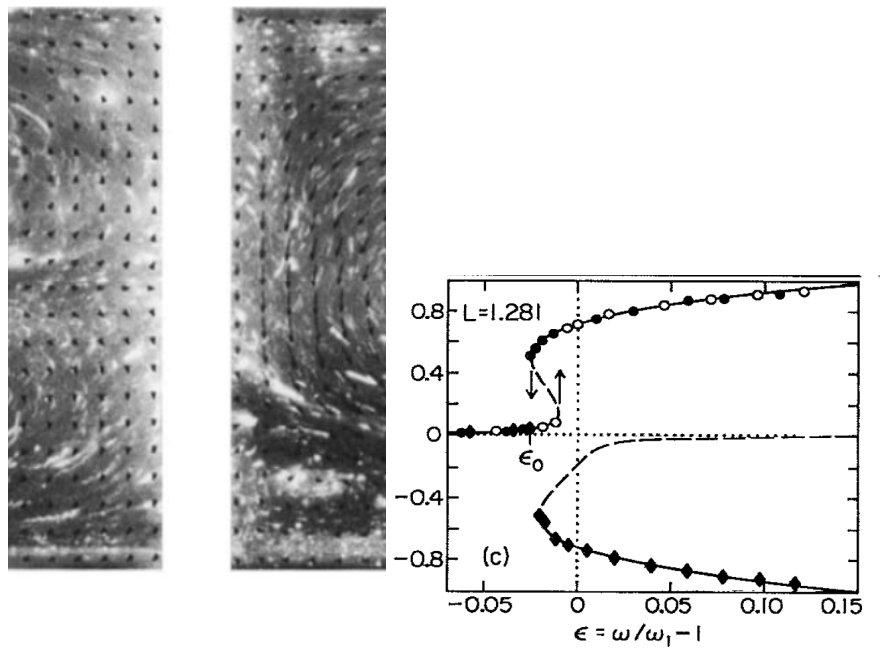


Figure 12: Two saddle-node bifurcations in Taylor vortex flow in a short cylinder. a) Symmetric vortices below the bifurcation and jump to asymmetric vortices above the transition (Lücke et al., 1984). b) Bifurcation diagram. The two saddle-node bifurcations lead to hysteresis when increasing/decreasing  $\epsilon$  (Aitta et al., 1985).

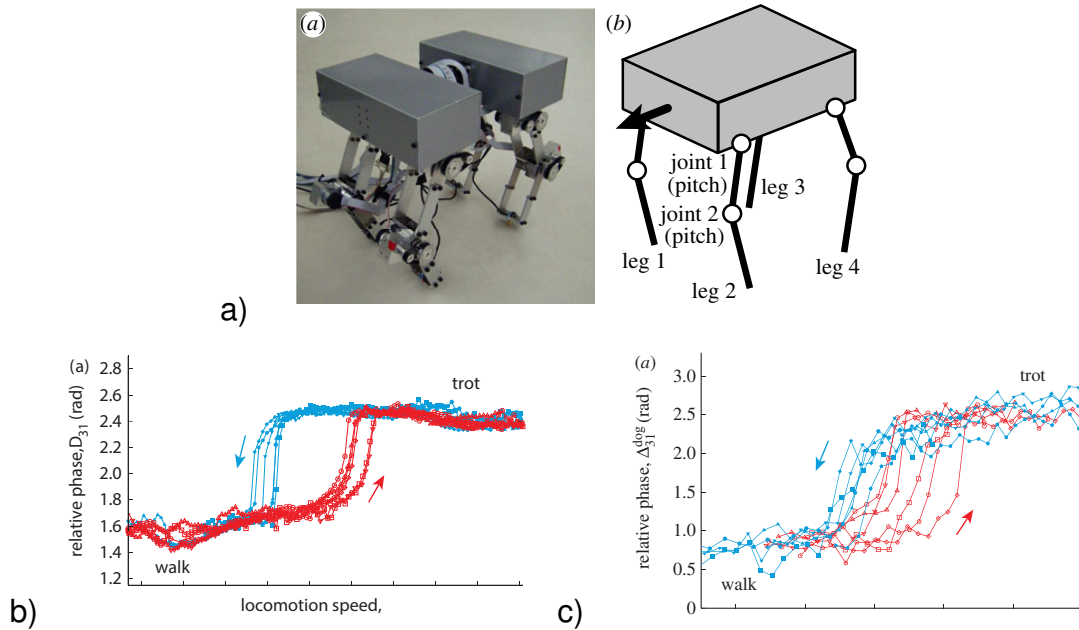


Figure 13: Hysteresis via saddle-node bifurcations in the transition between walk and trot gait as a function of locomotion speed. The gait is characterized by the phase difference between front and rear legs. a) 4-legged robot. b) hysteresis in the robot gait, c) hysteresis in dog gait.(Aoi et al., 2013)

### 2.3.4 Transcritical Bifurcation

Consider a system that satisfies an additional condition beyond that of the occurrence of a bifurcation:

Assume one fixed-point solution exists for all  $\mu$ . For simplicity assume that solution is  $x = 0$ :

$$f(0, \mu) = 0 \quad \text{for all } \mu$$

Taylor expansion around  $x = 0$  at the bifurcation point  $\mu = 0$

$$f(x, \mu) = \underbrace{f(0, 0)}_{=0} + \underbrace{\partial_x f(0, 0)}_{=0} x + \underbrace{\partial_\mu f(0, 0)}_{=0} \mu + \frac{1}{2} \underbrace{\partial_x^2 f(0, 0)}_{\neq 0} x^2 + \underbrace{\partial_{x\mu} f(0, 0)}_{=0} x\mu + \frac{1}{2} \underbrace{\partial_\mu^2 f(0, 0)}_{=0} \mu^2 + \dots$$

Vanishing terms

- $x = 0$  is a fixed point for  $\mu = 0$ :  $f(0, 0) = 0$
- a bifurcation occurs:  $\partial_x f(0, 0) = 0$
- $x = 0$  is a solution for all values of  $\mu$ :  $\partial_\mu f(0, 0) = 0$ ,  $\partial_\mu^2 f(0, 0) = 0$

Universal evolution equation

$$\dot{x} = x(a\mu + bx) + \dots$$

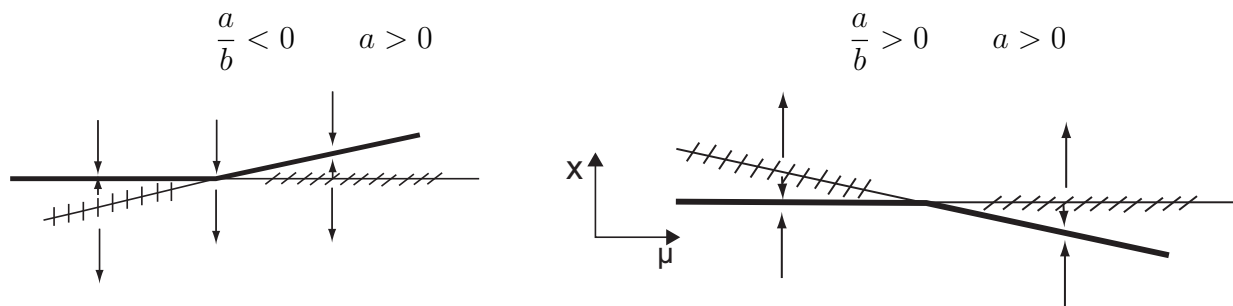
with

$$a = \partial_{x\mu}^2 f \Big|_{x=0, \mu=0} \quad b = \frac{1}{2} \partial_x^2 f \Big|_{x=0, \mu=0}$$

Two fixed points:

$$x_1 = 0 \quad x_2 = -\frac{a}{b}\mu \equiv -\frac{\partial_{x\mu}^2 f}{\frac{1}{2}\partial_x^2 f} \mu$$

There are four cases:



Two more cases for  $a < 0$ : the fixed point  $x_1 = 0$  is then stable for  $\mu > 0$  and unstable for  $\mu < 0$  with the corresponding other branch depending on the sign of  $a/b$ .

**Notes:**

- Both fixed points exist below and above the bifurcation ( $\mu < 0$  and  $\mu > 0$ )

- 'Exchange of stability' between the two branches of solutions
- Sufficiently large perturbation can lead away from the (linearly) stable fixed points.

### Examples:

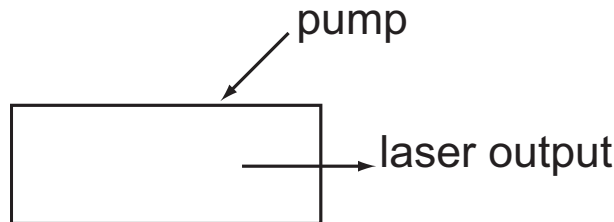
#### 1. Logistic equation for population dynamics

$$\dot{N} = \mu N - N^2$$

for  $\mu < 0$  the lower branch is unphysical since  $N > 0$  is required



#### 2. Simple Model for Laser



Optical cavity with excitable atoms

Dynamics of atoms:

- atoms are excited by the pump  $P$ <sup>25</sup>
- atoms emit photons and go to the ground state
  - spontaneously: spontaneous emission
  - due to other photon: **stimulated emission**  
a photon triggers the emission of a photon from excited atom

$$\dot{N} = P - fN - gnN$$

$N$ : number of excited atoms,  $P$ : pump,  $f$ : decay through spontaneous emission,  $g$ : 'collision' with photon takes atom to ground state (stimulated emission),  $n$ : number of photons in the cavity

Dynamics of photons:

---

<sup>25</sup>Atoms are also excited by photons already present; effect much smaller than pump ( $n$  is small near the onset of lasing).

- photons generated by **stimulated emission**
- photons leave through end mirrors

$$\dot{n} = gNn - \kappa n$$

$g$ : gain,  $\kappa$ : output/loss

**Note:**

- $n$  counts only photons that have the correct phase (only those generated by stimulated emission)

**Now:** We have 2 equations: *too difficult* for now

Model the  $N$ -equation *ad hoc*: the number of excited atoms in the steady state will be reduced by photons

$$N = N_0 - \alpha n.$$

Then

$$\dot{n} = g(N_0 - \alpha n) n - \kappa n = (gN_0 - \kappa) n - \alpha gn^2,$$

which is again same equation as for logistic growth.

To get lasing action the pump power must be large enough to generate enough excited atoms  $N_0$  to overcome the loss through the end mirrors,

$$N_0 > \frac{\kappa}{g}.$$

**Note:**

- We will learn under what conditions the model for  $N$  is justified: reduction from many ode's to few/single ode by *center-manifold reduction*.

### 3. Rayleigh-Benard convection in a fluid layer heated from below:

- The state without fluid flow (modeled with  $x = 0$ ) exists for all temperature differences
- Hexagonal flow patterns arise in a transcritical bifurcation connected with a saddle-node bifurcation
- Large perturbations can kick the solution without fluid flow above the unstable branch of the transcritical bifurcation and trigger the formation of hexagonal convection patterns.
- For  $\mu > 0$  the lower branch is unstable in a different way (instability not contained in the single equation)

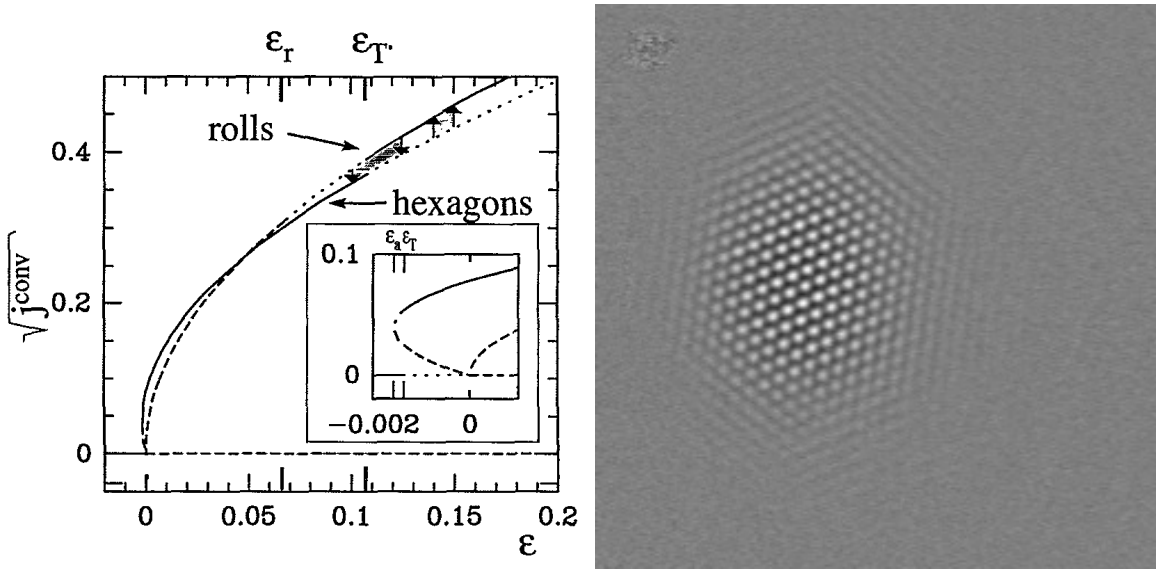


Figure 14: Convection in very thin fluid layers sets in via a transcritical bifurcation to hexagonal convection patterns. The root of the heat flux,  $\sqrt{j^{(conv)}}$ , plays the role of the magnitude  $|x|$  of the amplitude  $x$ . The hexagons and the convection-less state are simultaneously linearly stable in a (very small) range of parameters. If the heating is increased the pattern expands into the whole system (Bodenschatz et al., 1991).

### 2.3.5 Pitchfork Bifurcation

Consider systems with reflection symmetry  $x \rightarrow -x$ , i.e. systems for which, if  $x(t)$  is a solution,  $-x(t)$  is also a solution.

Thus, assume  $x(t)$  is a solution,

$$\dot{x} = f(x(t), \mu),$$

and require that the reflected function  $-x(t)$  is also a solution,

$$-\dot{x} = f(-x(t), \mu).$$

Thus we have

$$\dot{x} = -f(-x(t), \mu).$$

Since also  $\dot{x} = f(x(t), \mu)$ , we have that  $f(x, \mu)$  must be *odd* in  $x$

$$f(-x, \mu) = -f(x, \mu) \quad \text{for all } \mu.$$

Therefore, in a Taylor expansion around  $x = 0$  no even powers in  $x$  can appear

$$\begin{aligned} f(x, \mu) &= \underbrace{f(0, 0)}_{=0} + \underbrace{\partial_x f(0, 0)}_{=0} x + \underbrace{\partial_\mu f(0, 0)}_{=0} \mu + \underbrace{\partial_\mu^2 f(0, 0)}_{=0} \mu^2 + \\ &\quad + \underbrace{\partial_{x\mu}^2 f(0, 0)}_a x \mu + \frac{1}{2} \underbrace{\partial_x^2 f(0, 0)}_{=0} x^2 + \frac{1}{6} \underbrace{\partial_x^3 f(0, 0)}_b x^3 + \dots \end{aligned}$$

This yields

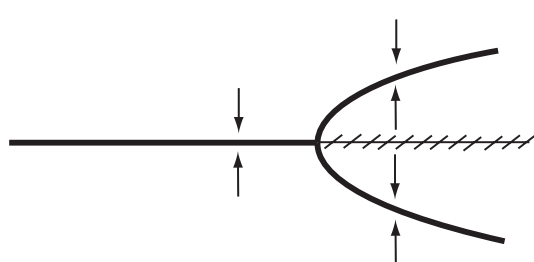
$$\dot{x} = a\mu x + bx^3$$

Depending on the value of  $\mu$  there are one or three fixed points:

$$\begin{aligned}x_0 &= 0 \\x_{1,2} &= \pm\sqrt{-\frac{a}{b}\mu}\end{aligned}$$

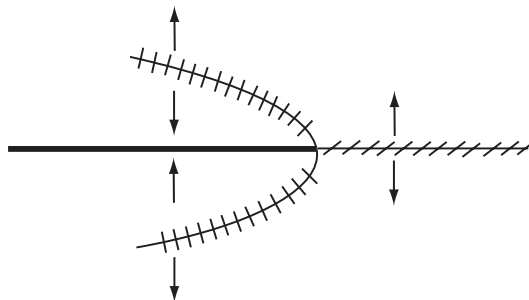
Consider the two cases:

$$\frac{a}{b} < 0 \quad a > 0$$



supercritical

$$\frac{a}{b} > 0 \quad a > 0$$



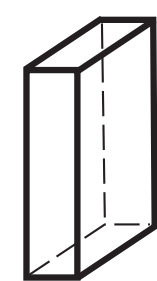
subcritical

### Notes:

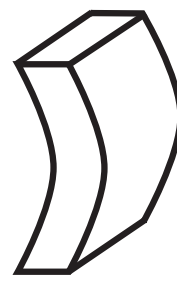
- Supercritical: the new branches arise on the side where the state  $x = 0$  is linearly unstable  $\Rightarrow$  the nonlinearity leads to a saturation of the instability.
  - Subcritical  $\Rightarrow$  no saturation to cubic order  $\Rightarrow$  we need higher-order terms to get a finite solution.
  - The system has the reflection symmetry  $x \rightarrow -x$ 
    - The solution  $x_0 = 0$  has that symmetry as well.
    - The solutions  $x_{1,2} = \pm\sqrt{-\frac{a}{b}\mu}$  break the reflection symmetry:  
The symmetry of the system is manifested in the fact that the two solutions are symmetrically related.
- $\Rightarrow$  The pitchform bifurcation is a *symmetry-breaking* bifurcation.

### Examples:

a) buckling of a beam



or



b) Electro-convection in nematic liquid crystals:

AC-voltage can induce a pitch-fork bifurcation to stripe-like convection patterns in nematic liquid crystals.

The reflection symmetry arises effectively from a translation symmetry: shifting by half a wavelength corresponds to a flipping of the velocity vector<sup>26</sup>:

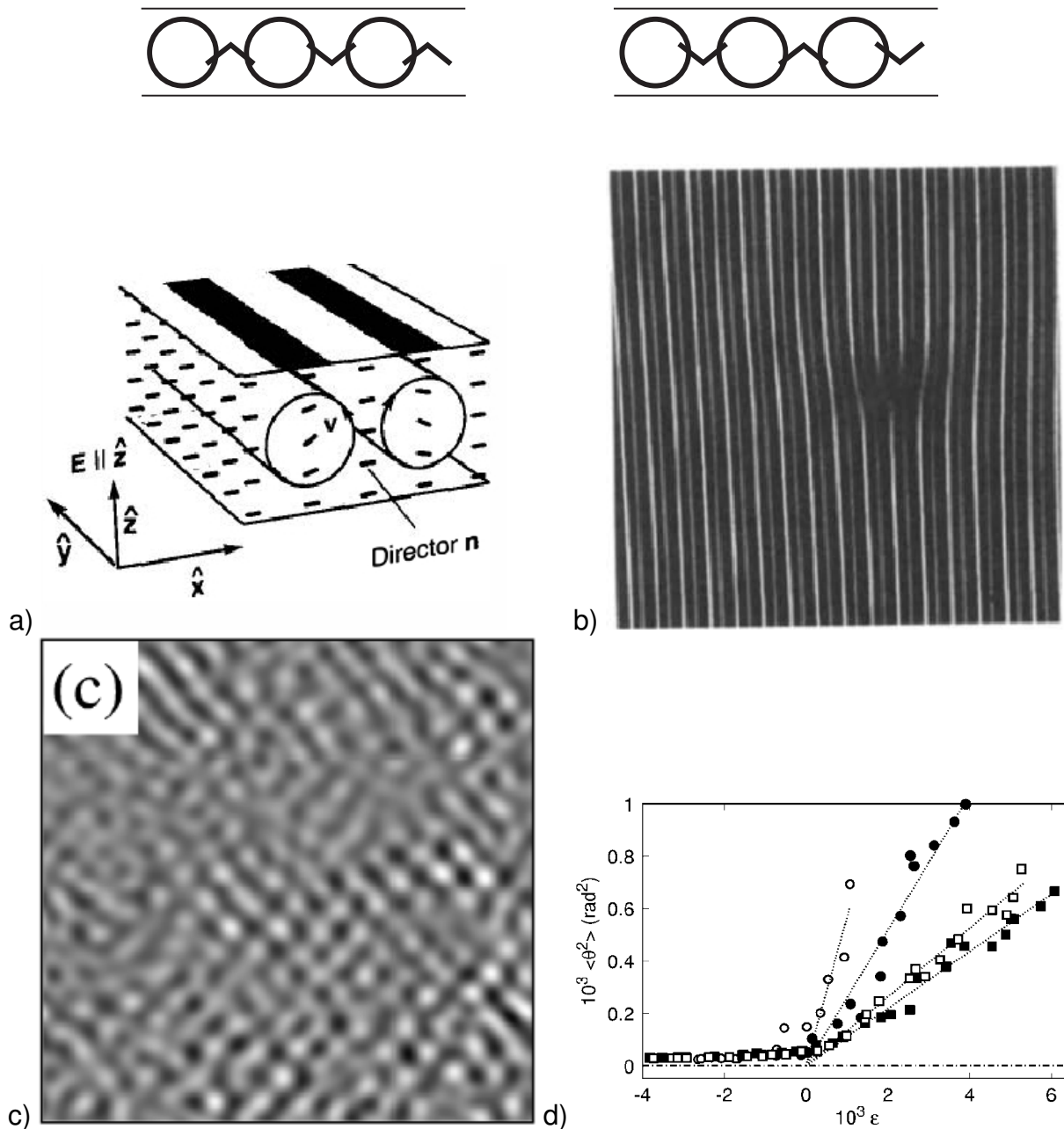


Figure 15: a) An AC electric field applied transversally to a thin layer of nematic liquid crystal can drive fluid flow in the form of rolls. b) Top view of a roll pattern with a dislocation defect. c) Disordered convection pattern slightly above the bifurcation point. d) The square  $x^2$  of the pattern amplitude grows linearly at the bifurcation point reflecting the square-root law for the amplitude. As the electrical conductivity of the liquid crystal is changed (different symbols) a tricritical point is approached (the line becomes vertical): the pitch-fork bifurcation eventually becomes subcritical. Scherer et al. (2000).

<sup>26</sup>intermediate positions are also possible  $\Rightarrow$  system has larger symmetry

### c) Ferromagnets

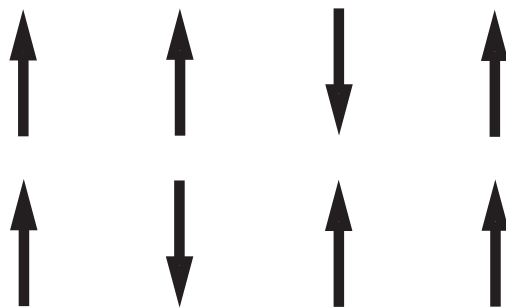
Bifurcations are closely related to phase transitions, they both describe qualitative changes in the behavior of the system, like from a liquid to a gas:

- Phase transitions can often be described in terms of a single scalar quantity, the *order parameter*, that describes the state of the system:
  - the density of a gas/liquid or the magnetization of a ferromagnet constitutes such an order parameter.
  - the order parameter typically satisfies a nonlinear equation, which exhibits bifurcations as the temperature, say, is changed.

Consider ferromagnets:

- as the temperature  $T$  is increased beyond the critical temperature  $T_c$  the magnet loses its magnetization, it goes from the ferromagnetic to the paramagnetic state.

Ising model: each atom carries a magnetic moment (spin):  $s_i = \pm 1$



An *overall* magnetization arises if the spins align on average in one direction or the other: this amounts to a *spontaneous symmetry breaking*

Thermal systems are described by statistical mechanics

- The state of the system is persistently fluctuating, reflecting the finite temperature.
- The probability of a state with energy  $E$  is given by the Boltzmann factor

$$P \propto e^{-\frac{E}{k_B T}}$$

with  $k$  being the Boltzmann constant and  $T$  the absolute temperature. The lower the energy of a state the higher is its probability.

The interaction of the spins is described via the energy

- with an external magnetic field:

$$E_H = -H s_i \quad \text{spins want to be parallel to field}$$

- between spins:

$$E_S = - \sum_{i,j} J_{ij} s_i s_j \quad J_{ij} > 0, \quad \text{want to be parallel to each other}$$

$\sum_{i,j}$  is a sum over neighbors

**Note:**

- Macroscopic magnets want to align anti-parallel: north is attracted by south.  
The parallel alignment in ferromagnets is a quantum-mechanical effect.

Total energy:

$$\begin{aligned} E(s_1, \dots, s_N) &= - \sum_i H s_i - \sum_{i,j} J_{ij} s_i s_j \\ &= - \sum_i \underbrace{\left( H + \sum_j J_{ij} s_j \right)}_{H_i^{eff}(\mathbf{s})} s_i, \end{aligned}$$

where  $\mathbf{s} = (s_1, \dots, s_N)$ .

Each spin  $s_i$  feels an effective field that depends on the state of its neighbors

$$H_i^{eff}(\mathbf{s}) = H + \sum_j J_{ij} s_j.$$

For finite temperature  $T$  the probability of a spin  $i$  to have value  $s_i$  depends on its energy  $E_i$  through the Boltzmann factor

$$P(s_i) \propto e^{-E_i/kT} = e^{H_i^{eff}(\mathbf{s}) s_i / kT}$$

The average value of  $s_i$  is then given by

$$\bar{s}_i = \sum_{s_i=\pm 1} s_i P(s_i) = P(1) - P(-1)$$

**However:**

$H_i^{eff}(\mathbf{s})$  still contains the unknown orientation of all the other interacting spins, which at any given moment will depend on the spin  $s_i$  under consideration  $\Rightarrow P(s_i)$  is in general very difficult to calculate.

**Note:**

- In one spatial dimension the model was solved by Ising in his thesis in 1925. In two dimensions it was solved by Onsager in 1944. In three dimensions no analytical solution is known.

**Mean Field Approximation:**

Replace the local spin value  $s_i$  by the average  $\bar{s}_i$ , which is the same for all spins since the system is spatially homogeneous,  $\bar{s}_i = \bar{s}$ ,

$$\begin{aligned} H_i^{eff}(\mathbf{s}) \rightarrow \bar{H} &= H + \sum_j J_{ij} \bar{s} \\ &= H + \bar{s} \underbrace{\sum_j J_{ij}}_{\bar{J}} \end{aligned}$$

Then

$$P(s_i) = \frac{1}{\mathcal{N}} e^{\bar{H} s_i / kT} \quad \text{with} \quad \bar{H} = H + \bar{s} \bar{J}$$

Normalization of probability:

$$1 = P(+1) + P(-1) \quad \Rightarrow \quad \mathcal{N} = e^{\bar{H}/kT} + e^{-\bar{H}/kT}$$

Thus, in this approximation the average magnetization satisfies:

$$\bar{s} = \frac{(+1) e^{\bar{H}/kT} + (-1) e^{-\bar{H}/kT}}{e^{\bar{H}/kT} + e^{-\bar{H}/kT}} = \tanh \left\{ \frac{(H + \bar{s} \bar{J})}{kT} \right\}$$

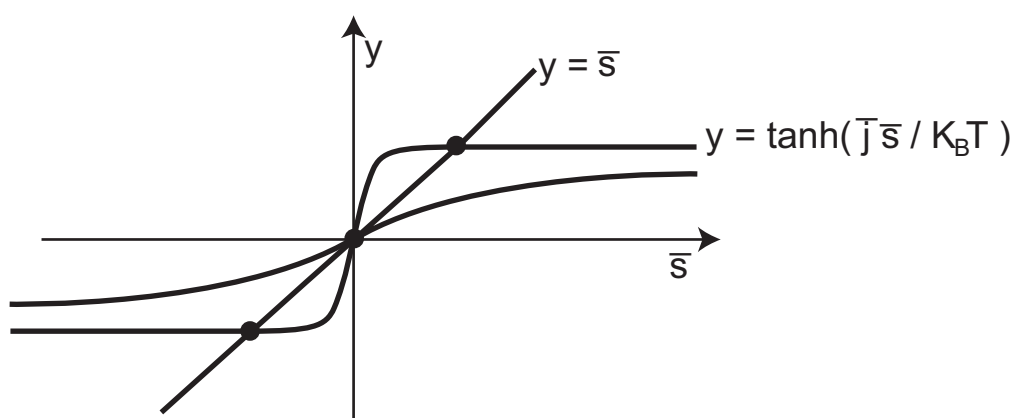
**Note:**

- In statistical physics the mean-field approximation is a very widely used approximation that is often very useful.

Consider  $H = 0$ :

$$\bar{s} = \tanh \left( \frac{\bar{s} \bar{J}}{kT} \right) \tag{6}$$

Graphically



Clearly,  $\bar{s} = 0$  is always a solution.

If the tanh is steep enough there can be two more solutions. They appear when the functions  $\bar{s}$  and  $\tanh(\frac{\bar{s}\bar{J}}{kT})$  have the same slope  $\Rightarrow$  take the derivative on both sides

$$1 = \left(1 - \tanh^2\left(\frac{\bar{s}\bar{J}}{kT}\right)\right) \left(\frac{\bar{J}}{kT}\right) \quad (7)$$

To obtain the ‘critical temperature’ at which the new solutions arise. eqs.(6,7) have to be solved simultaneously. Graphically, we see that this happens for

$$\bar{s} = 0$$

$\Rightarrow$

$$\frac{\bar{J}}{kT_c} = 1 \quad T_c = \frac{\bar{J}}{k}.$$

To get an approximate equation describing the solution close to the (pitchfork) bifurcation we can expand the tanh for small  $\theta$ ,

$$\tanh \theta = \theta - \frac{1}{3}\theta^3 + \mathcal{O}(\theta^5).$$

we get

$$\begin{aligned} \bar{s} &= \frac{\bar{s}\bar{J}}{kT} - \frac{1}{3} \left(\frac{\bar{s}\bar{J}}{kT}\right)^3 + \mathcal{O}(\bar{s}^5) \\ 0 &= \left(\frac{\bar{J}}{kT} - 1\right) \bar{s} - \frac{1}{3} \left(\frac{\bar{J}}{kT}\right)^3 \bar{s}^3 + \mathcal{O}(\bar{s}^5) \end{aligned}$$

i.e. to leading order

$$0 = \mu\bar{s} + b\bar{s}^3$$

with

$$\mu = \frac{\bar{J}}{kT} - 1 \quad b = -\frac{1}{3} \left(\frac{\bar{J}}{kT}\right)^3$$

Since the bifurcation (phase transition) occurs at  $\mu = 0$  the critical temperature  $T_c$  is given by

$$T_c = \frac{\bar{J}}{k}$$

### Note:

- The assumption of small  $\theta$  requires  $|\mu| \ll 1 \Rightarrow$  we can set  $T = T_c$  in  $b$

$$b = -\frac{1}{3}$$

### Notes:

- The transition is a pitchfork bifurcation because of the reflection symmetry  $\bar{s} \rightarrow -\bar{s}$

- buckling, thermal convection, ferromagnets are very different physical systems: **but** the transitions are described by the same equation because they have the same symmetries.
- Supercritical pitchfork bifurcation  $\Leftrightarrow$  phase transition of 2<sup>nd</sup> order.
- $H \neq 0$  breaks reflection symmetry  $\Rightarrow$  the pitchfork bifurcation is perturbed  $\Rightarrow$  see Section 2.3.7.

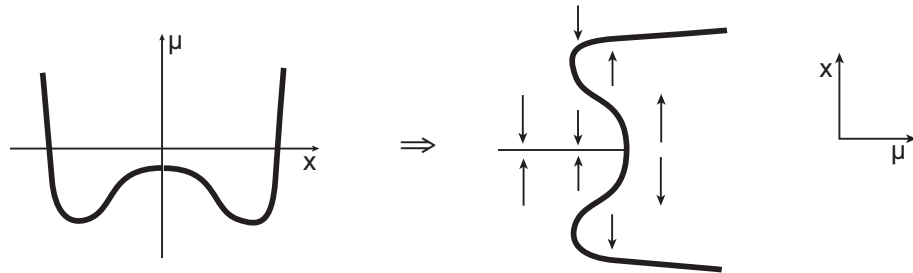
### 2.3.6 Subcritical Pitchfork Bifurcation:

If the cubic term does not lead to a saturation of the amplitude it is natural to go to higher orders in the expansion in  $x$  to include a quintic term:

$$\dot{x} = \mu x + \underbrace{bx^3}_{\text{destabilizing for } b>0} - \underbrace{cx^5}_{\text{stabilizing for } c>0}$$

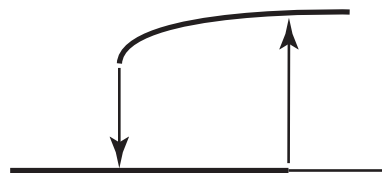
**Assume**  $c > 0$ . In general this need not be the case, there may not be any saturate at quintic order.

To get the bifurcation diagram: plot  $\mu = \mu(x)$



**Note:**

- Characteristic features of the subcritical pitchfork bifurcation
  - 2 saddle-node bifurcations
  - hysteresis loop & bistability



Question: are the conclusions about the saddle-node bifurcations based on this analysis guaranteed to be valid? For all previous bifurcation cases we know that the results are correct in the limit  $\mu \rightarrow 0$  and  $x \rightarrow 0$ .

- Taylor expansion in  $x$ :

On the upper branch the analysis is strictly valid only, if even there  $x$  is sufficiently small.

Since

$$x_{1,2}^2 = \frac{b \pm \sqrt{b^2 - 4\mu c}}{c},$$

the validity requires that  $b$  be small, i.e. we need to expand around the ‘tricritical’ point  $b = 0$ : the bifurcation has to be *weakly subcritical*. In particular, at the saddle-node bifurcation we have

$$x_{1,2}^2 = \frac{b}{c} \quad \Rightarrow \quad b = \mathcal{O}(x^2)$$

Thus, we have

$$bx^3 \sim cx^5$$

and the cubic and the quintic terms balance.

In other words: the nonlinear growth through the cubic term is saturated by the quintic term. For that to be possible the coefficient  $b$  of the cubic term has to be sufficiently small.

If  $b$  is not small enough, one may not be able to stop the expansion at quintic order. As a result, it could be that there is no saddle-node bifurcation even if  $c > 0$ .

### 2.3.7 Imperfect Bifurcations

The saddle-node bifurcation requires only the tuning of a single parameter.

For the transcritical and for the pitch-fork bifurcation to occur we needed 2 conditions

- bifurcation occurs:  $\partial_x f|_{x_0, \mu_0} = 0$
- additional coefficients ‘happen to vanish’, e.g., because of some symmetry

#### Question:

- What happens when the additional conditions are only satisfied approximately, e.g. the symmetries are **weakly broken**?

#### Example:

In the ferromagnet, without external field we have the reflection symmetry  $\bar{s} \rightarrow -\bar{s}$ , which leads to a pitchfork bifurcation. If we apply an external external field  $H$ , that symmetry is broken even if that magnetic field is very weak. What happens to the pitchfork bifurcation for such a small perturbation? How does the pitchfork bifurcation disappear?

A similar question can be asked about the transcritical bifurcation.

We had:

$$\bar{s} = \tanh(\beta(H + \bar{J}\bar{s}))$$

with  $\beta = \frac{1}{k_B T}$ . Using again

$$\tanh \theta = \theta - \frac{1}{3}\theta^3 + \mathcal{O}(\theta^5)$$

the equation for the magnetization  $\bar{s}$  becomes

$$\bar{s} = \beta(H + \bar{J}\bar{s}) - \frac{1}{3} (\beta(H + \bar{J}\bar{s}))^3 + O((\beta(H + \bar{J}\bar{s}))^5).$$

For small  $\bar{s}$  and  $H$  the quintic term can be neglected.

With  $\mu \equiv \beta\bar{J} - 1$  one has near the bifurcation

$$|\mu| \ll 1$$

and one obtains to leading order in  $\mu$ ,  $\bar{s}$ , and  $H$

$$0 = \mu\bar{s} - \frac{1}{3}\beta^3\bar{J}^3\bar{s}^3 + \beta H$$

Therefore, consider the perturbed pitchfork bifurcation

$$\dot{x} = \mu x - x^3 + h,$$

i.e.  $f(x, \mu) + f(-x, \mu) \neq 0$ , but the symmetry breaking by  $h$  is weak,  $h$  small.

Solving this cubic equation directly for fixed points is cumbersome (although possible).

Graphical solution of

$$\mu x - x^3 = -h.$$

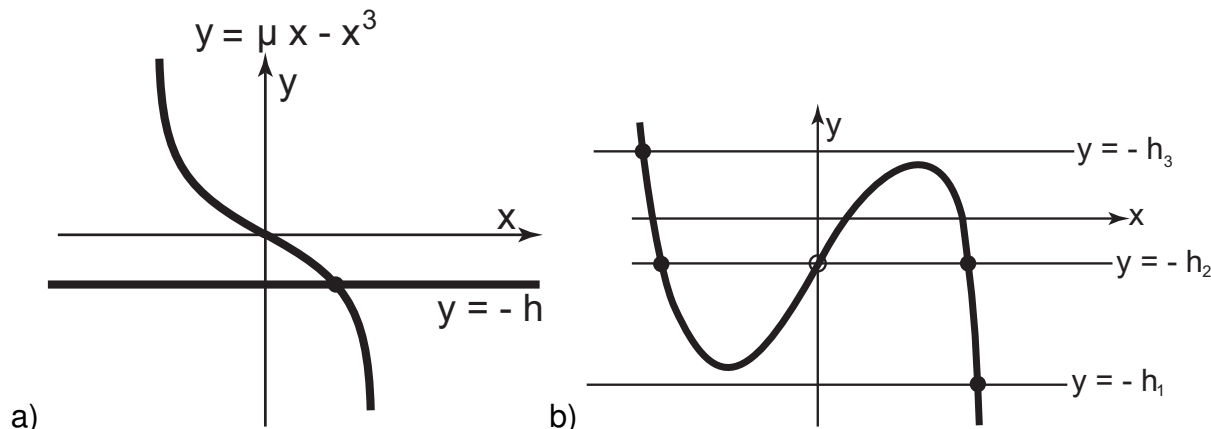


Figure 16: Graphical solution of  $\mu x - x^3 = -h$  for  $\mu < 0$  (a) and for  $\mu > 0$  (b).

Vary  $h$  for fixed  $\mu$ :

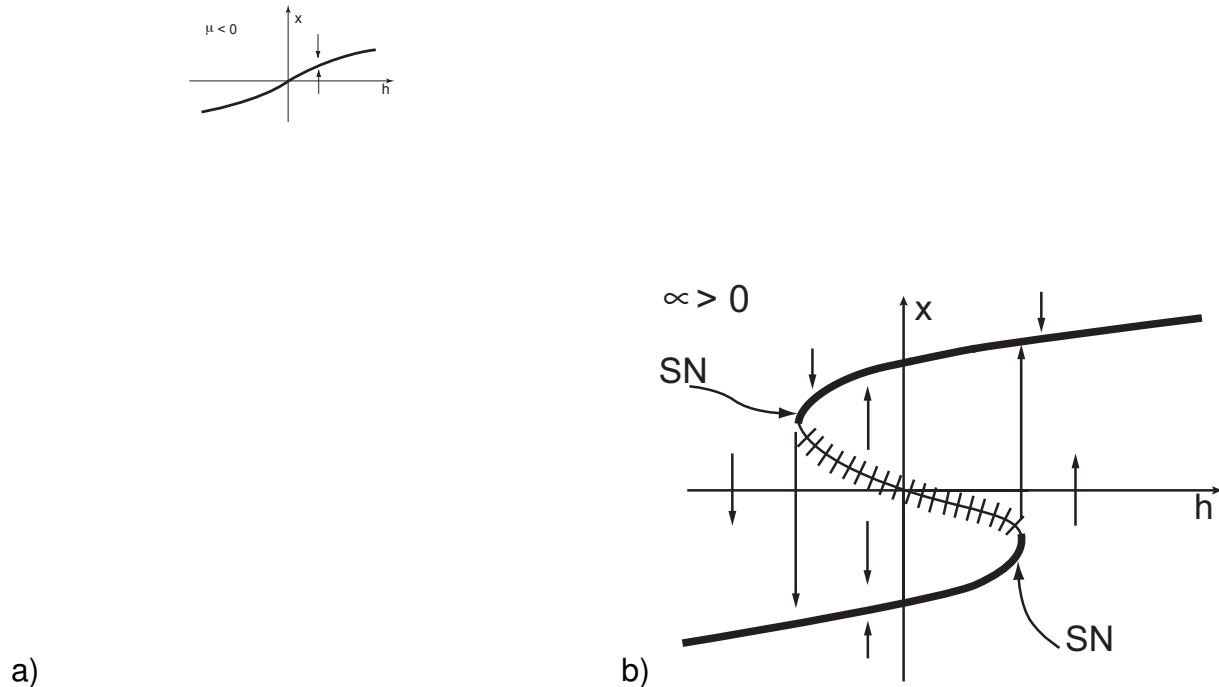


Figure 17: Bifurcation diagrams obtained when varying  $h$  for  $\mu < 0$  fixed (a) and for  $\mu > 0$  (b).

**Note:**

- varying  $h$  up and down beyond the saddle-node bifurcations induces a *hysteresis loop*: in the magnetic system the magnetization jumps and switches sign.

How does the bifurcation diagram in Fig.17a change to that in Fig.17b?

To visualize that consider the solution surface over the 2-parameter plane  $(\mu, h)$ .

For that it is useful to identify the saddle-node bifurcations in the  $(\mu, h)$ -plane. We need to solve simultaneously<sup>27</sup>

$$\begin{aligned} h &= -\mu x + x^3 && \text{fixed point} \\ \mu &= 3x^2 && \text{bifurcation} \end{aligned}$$

which yields

$$x_{SN} = \pm \sqrt{\frac{1}{3}\mu} \quad h_{SN}(\mu) = \pm 2 \left(\frac{\mu}{3}\right)^{\frac{3}{2}} \quad \text{for } \mu > 0. \quad (8)$$

<sup>27</sup>One can obtain the saddle-node bifurcations also by noting that they occur at the extrema of  $\mu x - x^3$ .

For  $|h| < h_{SN}(\mu)$  there are 3 solutions, otherwise there is only 1 solution (cf. Fig.18). Plotting the solution above the  $(\mu, h)$ -plane yields the picture of the *cusp catastrophe* (Fig.19). The saddle-node lines (8) are (roughly) sketched in Fig.19 on the parameter plane underneath the surface.

The term *catastrophes* was introduced somewhat dramatically to express that as a saddle-node bifurcation is crossed the solution **jumps** to another branch, i.e. **minute** changes in the parameters lead to **drastic** results in the solution.

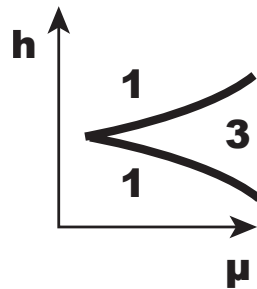


Figure 18: Saddle-node bifurcation lines in the  $(h, \mu)$ -plane. The numbers indicate how many fixed point solutions exist in the respective parameter regime.

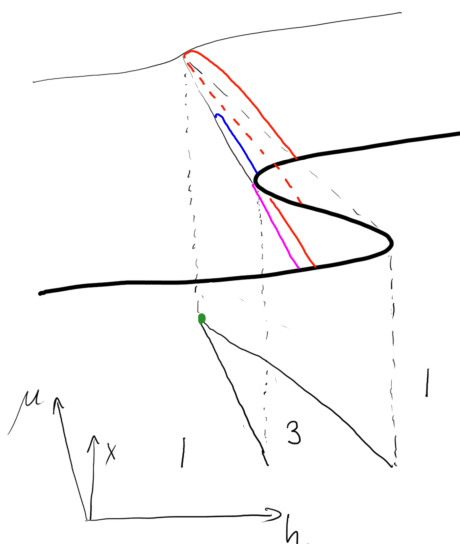


Figure 19: The cusp catastrophe solution surface. The pitchfork bifurcation occurs when increasing  $\mu$  through the codimension-2 point  $(\mu = 0, h = 0)$  along the two red solid lines. The unstable state  $x = 0$  is denoted with the dashed solid line. The blue line denotes a path in which two solutions are generated by a saddle-node bifurcation at the ‘knee’ of the solution surface. The magenta line denotes the solution that does not undergo a bifurcation as  $\mu$  is increased.

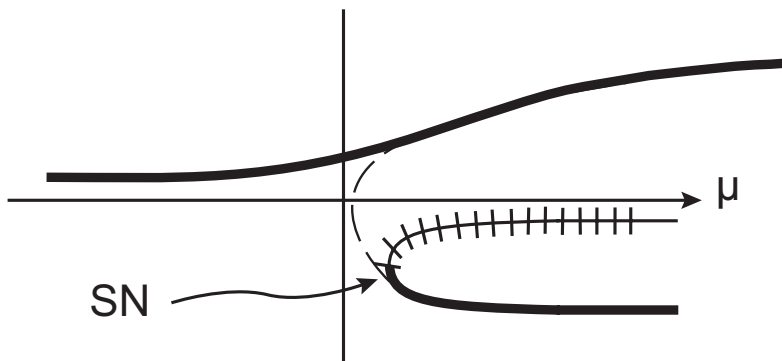


Figure 20: For  $h \neq 0$  increasing  $\mu$  leads to two qualitative different solution branches: one without any bifurcation (cf. magenta line in Fig.19) and one in which 2 fixed points are generated in a saddle-node bifurcation (cf. blue line in Fig.19).

### Notes:

- A bifurcation is called *degenerate* if additional conditions “happen” to be satisfied, i.e. if additional coefficients in the Taylor vanish due to the tuning of some parameter
  - in a system that does not have a reflection symmetry a pitch-fork bifurcation would be degenerate.
- *Unfolding* of a degenerate bifurcation:  
introduce sufficiently many parameters so that no degeneracy is left.

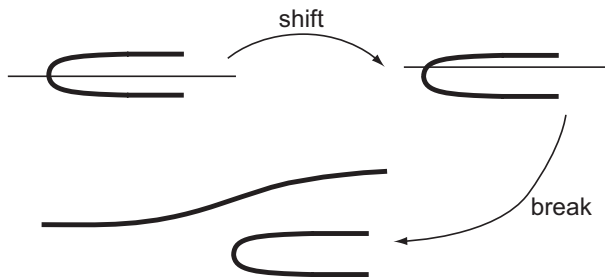


Figure 21: Unfolding a pitchfork bifurcation.

Unfolding the pitchfork bifurcation:

- break the symmetry  $x \rightarrow -x$ , but keep the solution  $x = 0$  for all  $\mu \Rightarrow$  transcritical bifurcation
- break the transcritical bifurcation by dropping the condition that  $x = 0$  is always a solution  $\Rightarrow$  only saddle-node bifurcation remains

### Note:

- the number of parameters that have to be tuned to get a certain bifurcation is called the *codimension* of that bifurcation: if the system has  $N$  parameters and the bifurcation has codimension  $d$  then the bifurcation occurs on a  $N - d$ -dimensional surface (‘manifold’) in the  $N$ -dimensional parameter space.

- to get an unperturbed pitch-fork bifurcation in a system without reflection symmetry we have to tune 2 parameters

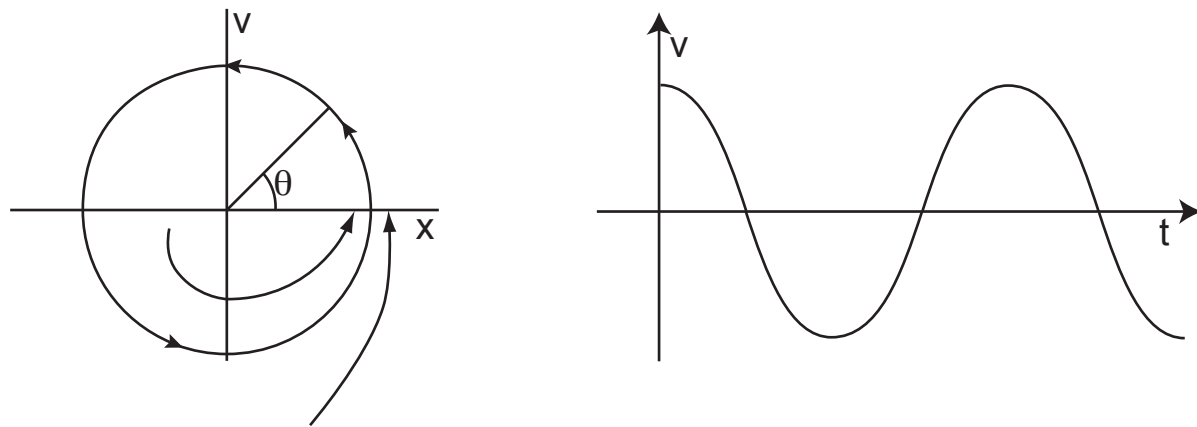
$$\mu = 0 \quad \& \quad h = 0$$

*codimension-2 bifurcation*

- in systems with reflection symmetry the pitch-fork bifurcation has codimension 1

## 2.4 Flow on a Circle<sup>28</sup>

For oscillations to be possible the system needs to allow a return: two dimensions needed



Consider the dynamics on the periodic orbit:

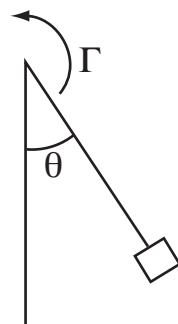
### Flow on a circle

$$\dot{\theta} = f(\theta) \quad \theta \in [0, 2\pi]$$

### Notes:

- $f(\theta)$  cannot be arbitrary: has to be single-valued, i.e.  $2\pi$ -periodic
- $f(\theta)$  gives the instantaneous frequency

### Example: Overdamped Pendulum with Torque



$$m\ell^2\ddot{\theta} + \beta\dot{\theta} = -mg\ell \sin \theta + \tilde{\Gamma}$$

consider large damping

$$\dot{\theta} = \Gamma - a \sin \theta$$

with  $a = mg\ell/\beta$  and  $\Gamma = \tilde{\Gamma}/\beta$

---

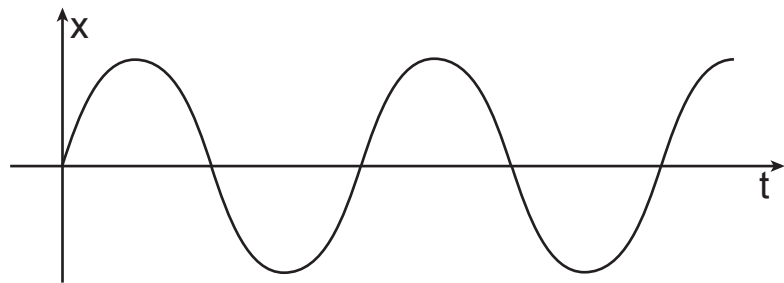
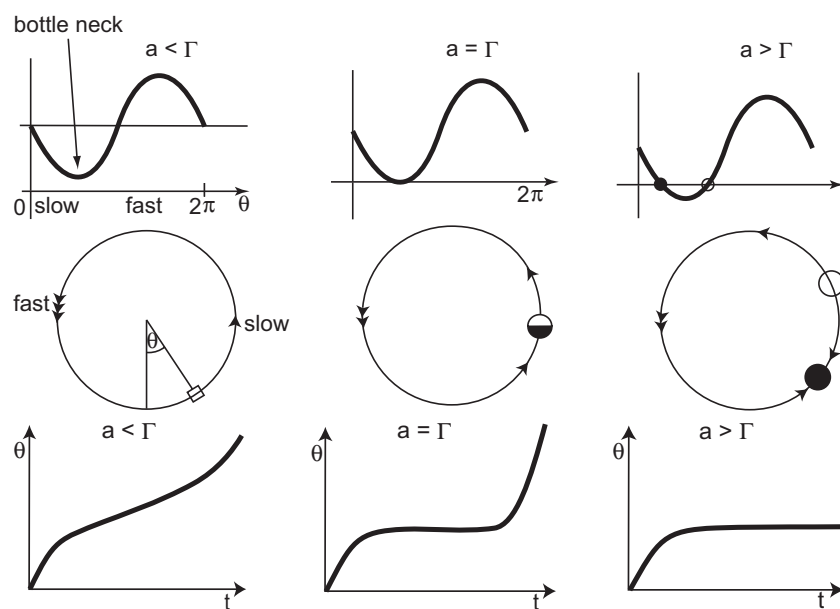
<sup>28</sup>cf. Strogatz Ch.4

i)  $a = 0$  (no gravity)

$$\theta = \theta_0 + \Gamma t \quad \text{whirling motion}$$

oscillation in horizontal coordinate:

$$x = \ell \sin \theta = \ell \sin(\theta_0 + \Gamma t)$$

ii)  $a > 0$  (with gravity)

'Ghost' of the saddle-node bifurcation:

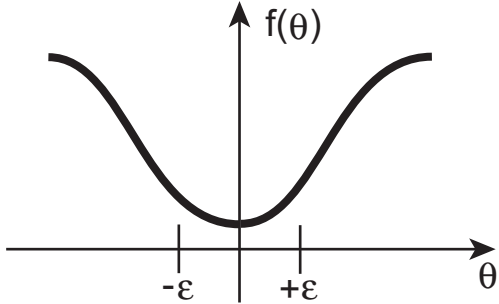
for  $a$  just below the saddle-node bifurcation,  $a \lesssim \Gamma$ , the evolution becomes extremely slow near the location on the orbit where the two saddle and the node are 'borne' at  $a = \Gamma$ .

**Note:**

- quite generally: near a steady bifurcation the dynamics become slow: growth/decay rates go to 0 ('critical slowing down').

Estimate the period near the bifurcation point:

$$T = \int dt = \int_0^{2\pi} \frac{d\theta}{\dot{\theta}} = \int_0^{2\pi} \frac{d\theta}{\Gamma - a \sin \theta}$$



Consider the general case near a saddle-node bifurcation

$$\dot{\theta} = f(\theta, \mu)$$

assume that bifurcation occurs at  $\mu = 0$  and  $\theta = 0$ :

$$f(\theta, \mu) = f(0, 0) + \underbrace{\partial_\mu f}_{=0 \text{ bifurcation}} \mu + \underbrace{\frac{1}{2} f''(0)}_b \theta^2 + \mathcal{O}(\theta^3)$$

$$\begin{aligned} T &= \int_{-\pi}^{\pi} \frac{d\theta}{f(\theta)} \underset{f(\theta) \text{ periodic}}{\approx} \int_{-\pi}^{-\epsilon} \frac{d\theta}{f(\theta)} + \int_{-\epsilon}^{+\epsilon} \frac{d\theta}{\underbrace{\mu + b\theta^2 + \mathcal{O}(\theta^3)}_{\text{diverges as } \mu \rightarrow 0}} + \int_{\epsilon}^{\pi} \frac{d\theta}{f(\theta)} \underset{\text{finite as } \mu \rightarrow 0}{=} \\ &= \int_{-\epsilon}^{+\epsilon} \frac{d\theta}{\mu + b\theta^2} + T_0 \end{aligned}$$

extract the divergence for  $\mu \rightarrow 0$  (at fixed  $\epsilon$ ) using  $\psi = \frac{\theta}{\sqrt{\mu}}$

$$T = \frac{1}{\mu} \int_{-\frac{\epsilon}{\mu^{1/2}}}^{\frac{\epsilon}{\mu^{1/2}}} \frac{\mu^{1/2} d\psi}{1 + b\psi^2} + T_0 \rightarrow \frac{1}{\mu^{1/2}} \int_{-\infty}^{\infty} \frac{d\psi}{1 + b\psi^2} + T_0 \propto \mu^{-1/2}$$

### Notes:

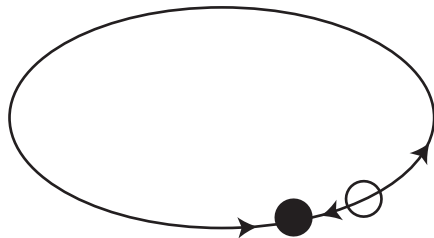
- A saddle-node bifurcation on an invariant circle is **one** way to generate oscillations. This bifurcation is often called a SNIC bifurcation. Generically one has for this bifurcation

$$T \propto \mu^{-1/2}$$

- other types of bifurcations to oscillatory behavior lead to different  $T(\mu)$ , e.g. at a Hopf bifurcation one has

$$T(\mu = 0) = T_0 \text{ finite.}$$

- the fact that the saddle-node bifurcation leads to oscillations is a **global** feature of the system:  
one needs a **global connection** between from saddle to the node (in addition to the direct connection)



### 2.4.1 Examples for SNIC Bifurcations

#### Synchronization of Oscillators

Videos:

- synchronized fireflies  
<https://www.youtube.com/watch?v=a-Vy7NZTGos>
- metronomes falling into lock-step  
<https://www.youtube.com/watch?v=5v5eBf2KwF8>

Such synchronization is not just curious, but technologically and scientifically relevant:

- Coupled lasers achieve much higher power: the synchrony refers to the fact that the light from all individual lasers is in phase (cf. stimulated emission discussed earlier).
- Synchronous activity of heart muscle cells is essential for functioning of the heart: asynchrony (fibrillation) can be deadly.
- Rhythmic activity is pervasive in the brain in the form of EEG brain waves (measured with scalp electrodes) or local field potentials (measuring the electric potential invasively without patching onto any specific neuron)
  - synchronized firing by multiple neurons has more impact on neurons reading this output.
  - synchronization has been associated with attention to stimuli
  - too much synchrony bad: epileptic seizure

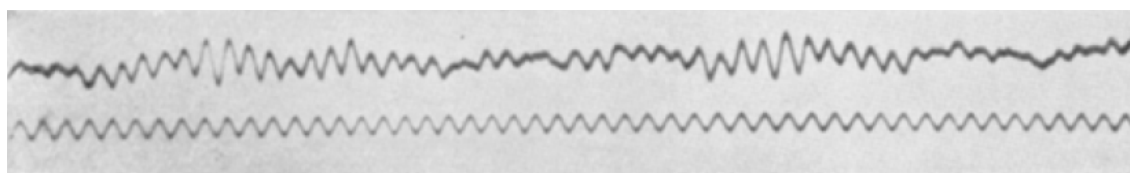


Figure 22:  $\alpha$ -wave in EEG (Berger).

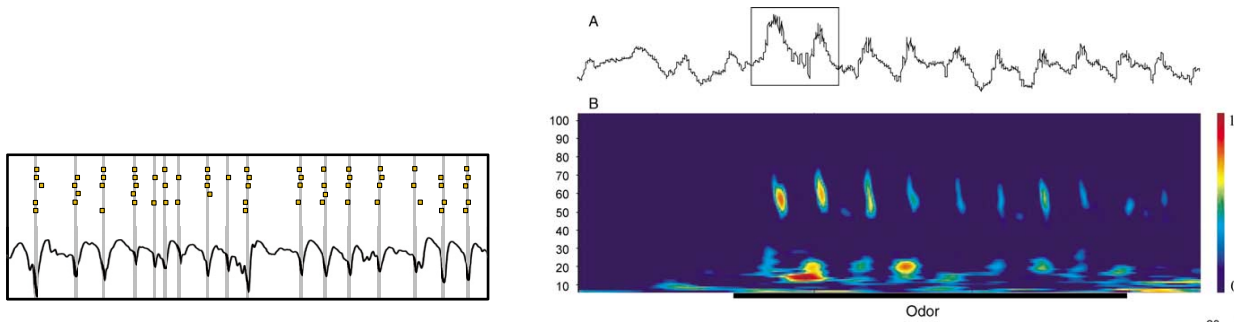


Figure 23: Brain rhythms arise from the synchronized activity of large ensembles of neurons. a) Local field potential peaks (lower curve) are associated with the synchronized spiking of neurons (symbols) in a hippocampal brain slice (Ainsworth et al., 2012). b) In the olfactory bulb local field potential show three rhythms: breathing (slow),  $\beta$ -rhythm (intermediate), and  $\gamma$ -rhythm (fast). The  $\gamma$ - and  $\beta$ -rhythms alternate and ride on top of the breathing rhythm (Buonviso et al., 2003).

For any periodic oscillation one can characterize the state at any time in terms of the oscillator's phase, which traces out the periodic orbit in phase space. Simplest case

$$x = A \cos \omega t \quad \phi = \omega t$$

When the coupling between oscillators is weak, the shape of the periodic orbit is only slightly modified by the interaction. But the relative phase between the oscillators is strongly affected by the interaction. In this regime the interaction between the oscillators can be reduced to an interaction between the phases  $\phi_j(t)$  of the oscillators

$$\begin{aligned} \dot{\phi}_1 &= \omega_1 + F_1(\phi_1, \phi_2) \\ \dot{\phi}_2 &= \omega_2 + F_2(\phi_1, \phi_2) \end{aligned}$$

where  $\omega_{1,2}$  are the frequencies of the uncoupled oscillators and the coupling functions  $F_{1,2}$  are  $2\pi$ -periodic in  $\phi_{1,2}$ . For sufficiently weak coupling one can show that  $F_{1,2}$  only depend on the difference of the phases

$$\begin{aligned} \dot{\phi}_1 &= \omega_1 + F_1(\phi_2 - \phi_1) \\ \dot{\phi}_2 &= \omega_2 + F_2(\phi_2 - \phi_1) \end{aligned}$$

Combine into an equation for the phase difference

$$\dot{\phi}_2 - \dot{\phi}_1 = \omega_2 - \omega_1 + F_2(\phi_2 - \phi_1) - F_1(\phi_2 - \phi_1).$$

A minimal model for the synchronization of oscillators is then

$$\dot{\theta} = \Gamma - a \sin(\theta) \quad \theta = \phi_2 - \phi_1 \quad \Gamma = \omega_2 - \omega_1,$$

i.e. the overdamped pendulum.

$\Gamma$ : frequency mismatch = detuning

Consider  $\Gamma > 0$ :

- oscillator 2 is faster than oscillator 1, i.e. the phase difference  $\theta$  would keep increasing without coupling.

- If  $a > 0$  and  $\theta \gtrsim 0$  the phase difference decreases due to the coupling and the oscillators approach each other
- *Fixed point:* oscillators are synchronized if their detuning is not too large

$$\underbrace{|\omega_2 - \omega_1|}_{\text{range of synchronization}} < a \quad \text{and} \quad \theta_0 = \arcsin \frac{\omega_2 - \omega_1}{a} \neq 0$$

The slower oscillator lags behind the faster one, but their phase difference is fixed:  
**phase-locked state**

- “Whirling” motion:  $|\omega_2 - \omega_1| > a$   
oscillators are not synchronized; they go in and out of phase.

### Notes:

- The same equations could model the coupling between an external perturbation that oscillates at a *fixed* frequency, which *entrains* an oscillator

$$\begin{aligned}\dot{\phi}_1 &= \omega_1 + F_1(\phi_1, \phi_2) \\ \dot{\phi}_2 &= \omega_2\end{aligned}$$

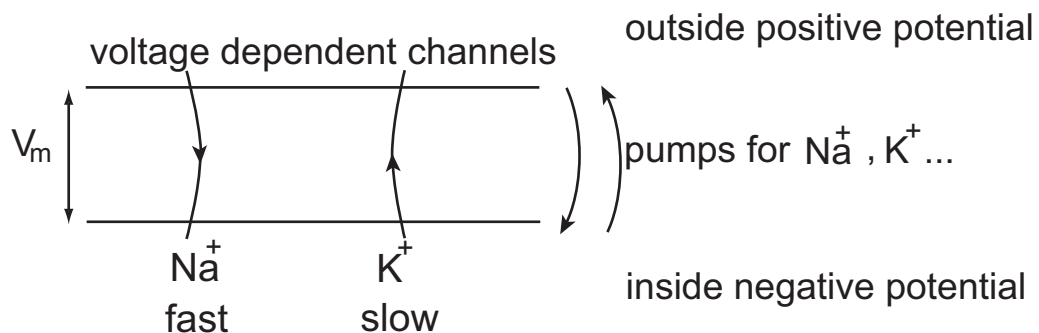
For the fireflies  $\phi_2$  could represent an external, periodically flashing light.

### Excitable Neurons

A large class of individual (uncoupled) neurons can also be captured with the equations describing a SNIC bifurcation.

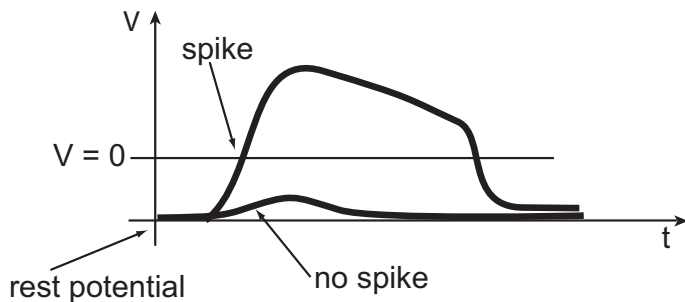
Main features of the neurons that are to be modeled

- The voltage across the membrane of the nerve cell plays a central role: the communication between neurons is mostly achieved via voltage pulses ('action potentials')



- Neurons are excitable:
  - Brief small stimulations evoke only small responses.

- Brief super-threshold stimulations evoke large voltage excursions: action potential



- Steady stimulation can lead to periodic firing of action potentials

Biophysical model:

Voltage-dependent membrane currents ‘charge’ the ‘capacitance’. In addition, there are in general currents representing synaptic inputs from other neurons.

The voltage-dependent membrane currents follow Ohm’s law with a bias due to different ion concentrations inside and outside of the cell

$$\begin{aligned} C \frac{dV}{dt} &= -\underbrace{g_{Na} m^3 h (V - V_{Na})}_{\text{sodium current}} - \underbrace{g_K n^4 (V - V_K)}_{\text{potassium current}} - \underbrace{g_L (V - V_L)}_{\text{leak current}} + I_{input} \\ \tau_n(V) \frac{dn}{dt} &= n_\infty(V) - n \\ \tau_h(V) \frac{dh}{dt} &= h_\infty(V) - h \\ \tau_m(V) \frac{dm}{dt} &= m_\infty(V) - m \end{aligned}$$

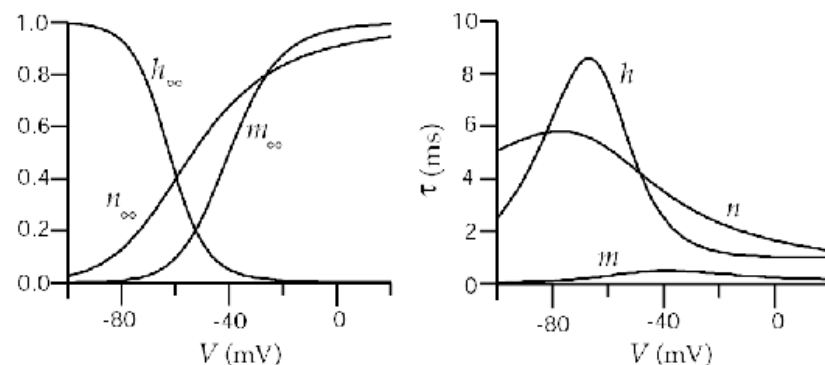


Figure 24: Steady-state values of the gating variables  $m$ ,  $n$ ,  $h$  (left) and the corresponding time constants (right) for the potassium and the sodium channels, respectively.

### Generation of the action potential

- Sufficiently large depolarization ( $V$  less negative)  $\Rightarrow Na^+$  channels open fast ( $m$  increases)  $\Rightarrow$  the cell becomes rapidly yet more depolarized
- Depolarization of the neuron  $\Rightarrow$  the slower  $K^+$  channels open ( $n$  increases),  $V$  becomes negative: cell becomes hyperpolarized again

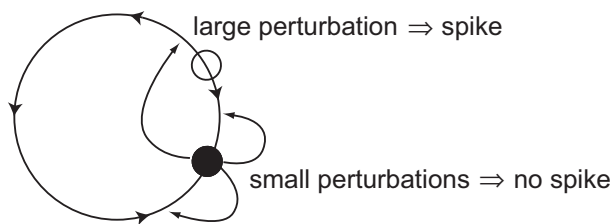
Depending on details of the various ion currents, periodic spiking in response to a steady external current input can arise through a SNIC bifurcation. In that case the normal form for the description of the system dynamics for parameter values near the bifurcation is the  $\theta$ -model Ermentrout and Kopell (1986) (see also article in Scholarpedia [http://www.scholarpedia.org/article/Ermentrout-Kopell\\_canonical\\_model](http://www.scholarpedia.org/article/Ermentrout-Kopell_canonical_model))

$$\begin{aligned}\dot{\theta} &= 1 - \cos \theta + (1 + \cos \theta)(-r + I_{inj}) \\ &= 1 - r + I_{inj} - (1 + r - I_{inj}) \cos \theta \equiv f(\theta)\end{aligned}$$

where  $\theta$  characterizes the phase on the cycle.

SNIC bifurcation occurs at  $f(\theta) = 0 = f'(\theta)$ , i.e.

$$\theta = 0 \quad I_{inj} = r$$



### Notes:

- Near the SNIC the conductance model shows the same power-law scaling of the period with the distance to the bifurcation point as the  $\theta$ -model and the generic SNIC bifurcation.

### 3 Two-dimensional Systems

New aspects:

- ‘true’ oscillations without periodic ‘boundary’ conditions
- reduction of dynamics to lower dimension

#### 3.1 Classification of Linear Systems<sup>29</sup>

We would like to obtain a complete overview of the dynamics of a two-dimensional system. For linear systems this is possible and we will see that for nonlinear systems this will provide valuable information about the local neighborhood of fixed points.

Therefore consider first a general linear system

$$\dot{\underline{x}} = \underline{\underline{L}} \underline{x} \quad \text{with} \quad \underline{x}(0) = \underline{x}_0$$

One can give the formal solution in terms of a matrix exponential

$$\underline{x}(t) = e^{\underline{\underline{L}} t} \underline{x}_0$$

which is defined via the expansion

$$e^{\underline{\underline{L}} t} = 1 + \underline{\underline{L}} t + \frac{1}{2} \underline{\underline{L}}^2 t^2 + \dots$$

We can simplify  $\underline{\underline{L}}$  by similarity transformation:

If the eigenvalues of  $\underline{\underline{L}}$  are distinct  $\underline{\underline{L}}$  can be diagonalized

$$\underline{\underline{S}}^{-1} \underline{\underline{L}} \underline{\underline{S}} = \begin{pmatrix} \lambda_1 & 0 \\ 0 & \lambda_2 \end{pmatrix}$$

The eigenvectors of  $\underline{\underline{L}}$  are given by the columns of  $\underline{\underline{S}}$

$$\underline{\underline{L}} \underline{v}_{1,2} = \lambda_{1,2} \underline{v}_{1,2}$$

since

$$\begin{aligned} \underline{\underline{S}}^{-1} \underline{\underline{L}} \underline{\underline{S}} \begin{pmatrix} 1 \\ 0 \end{pmatrix} &= \lambda_1 \begin{pmatrix} 1 \\ 0 \end{pmatrix} \\ \Rightarrow \underline{\underline{L}} \underbrace{\underline{\underline{S}} \begin{pmatrix} 1 \\ 0 \end{pmatrix}}_{\underline{v}_1} &= \lambda_1 \underbrace{\underline{\underline{S}} \begin{pmatrix} 1 \\ 0 \end{pmatrix}}_{\underline{v}_1} \end{aligned}$$

---

<sup>29</sup>cf. Strogatz Ch.5 and Lecture 5

**Note:**

- In general the eigenvectors need not be orthogonal to each other

The dynamics in the eigendirections are simple

$$\begin{aligned} e^{\underline{\underline{L}}t} \underline{v}_i &= \left\{ 1 + \frac{1}{2}(\underline{\underline{L}}t)^2 + \dots \right\} \underline{v}_i = \\ &= \left\{ 1 + \lambda_i t + \frac{1}{2}\lambda_i^2 t^2 + \dots \right\} \underline{v}_i = \\ &= e^{\lambda_i t} \underline{v}_i \end{aligned}$$

i.e. the eigenvectors of  $\underline{\underline{L}}$  are also eigenvectors of  $e^{\underline{\underline{L}}t}$  and along the eigendirections we have simple exponential time dependence.

The general solution can be written in terms of the eigenvectors

$$\underline{x}(t) = e^{\lambda_1 t} \underline{v}_1 A_1 + e^{\lambda_2 t} \underline{v}_2 A_2$$

with the amplitudes  $A_i$  determined by the initial conditions

$$x_0 = A_1 \underline{v}_1 + A_2 \underline{v}_2$$

**Notes:**

- The eigenvalues can be complex

$$\begin{aligned} \lambda_{1,2} &= \sigma_{1,2} + i\omega_{1,2} \\ \underline{x}(t) &= A_1 e^{\sigma_1 t} e^{i\omega_1 t} \underline{v}_1 + A_2 e^{\sigma_2 t} e^{i\omega_2 t} \underline{v}_2 \end{aligned}$$

If  $\underline{\underline{L}}$  is a real matrix the eigenvalues and eigenvectors are complex conjugates of each other,  $\sigma_1 = \sigma_2$ ,  $\omega_1 = -\omega_2$ , and the solution is real

$$\underline{x}(t) = e^{\sigma t} (A_1 e^{i\omega t} \underline{v}_1 + A_1^* e^{-i\omega t} \underline{v}_1^*)$$

- If  $\underline{\underline{L}}$  has repeated eigenvalues it cannot always be diagonalized. But it always can be reduced to the Jordan normal form

$$\underline{\underline{S}}^{-1} \underline{\underline{L}} \underline{\underline{S}} = \begin{pmatrix} \lambda & 1 \\ 0 & \lambda \end{pmatrix}$$

We are interested in the trajectories (orbits)  $y(x)$  in the phase plane, which are parametrized by the time  $t$ . Consider for simplicity a diagonal  $\underline{\underline{L}}$  with two distinct real eigenvalues,

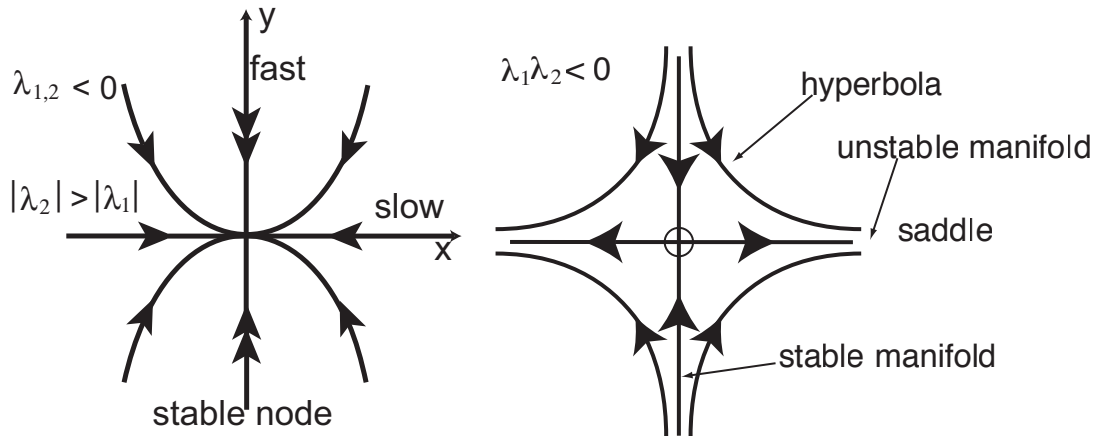
$$\begin{pmatrix} \dot{x} \\ \dot{y} \end{pmatrix} = \begin{pmatrix} \lambda_1 & 0 \\ 0 & \lambda_2 \end{pmatrix} \begin{pmatrix} x \\ y \end{pmatrix} \Rightarrow \begin{aligned} x &= e^{\lambda_1 t} x_0 \\ y &= e^{\lambda_2 t} y_0 \end{aligned}$$

$$\Rightarrow e^t = \left( \frac{x}{x_0} \right)^{1/\lambda_1}$$

$$y(t) = \left( \left( \frac{x}{x_0} \right)^{1/\lambda_1} \right)^{\lambda_2} y_0 = y_0 \left( \frac{x}{x_0} \right)^{\frac{\lambda_2}{\lambda_1}}$$

Thus

$$y(t) = C x(t)^{\frac{\lambda_2}{\lambda_1}}$$



### Definitions:

- Stable manifold of a fixed point  $x_0$ :

$$W^{(s)} = \{ \underline{x} \mid \underline{x}(0) = \underline{x} \Rightarrow \underline{x}(t) \rightarrow \underline{x}_0 \text{ for } t \rightarrow +\infty \}$$

- Unstable manifold of a fixed point  $x_0$ :

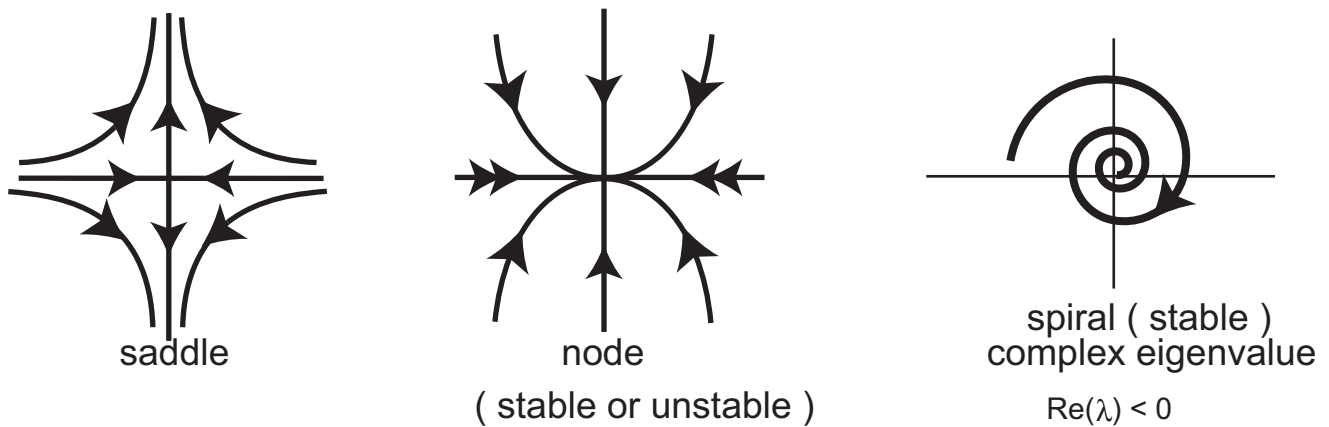
$$W^{(u)} = \{ \underline{x} \mid \underline{x}(0) = \underline{x} \Rightarrow \underline{x}(t) \rightarrow \underline{x}_0 \text{ for } t \rightarrow -\infty \}$$

### Note:

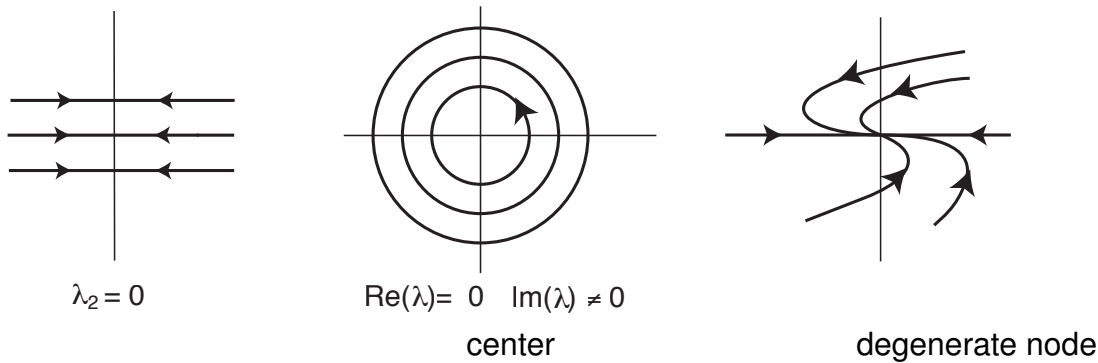
- The stable and unstable manifolds of a fixed point are quite informative for the flow in the vicinity of the fixed point.

**Possible Phase Portraits:**

- i) Generic cases, i.e. the phase portraits do not change qualitatively when a parameter is changed slightly; they are robust:



- ii) Special cases, i.e. a parameter has to be tuned to a special value to obtain these diagrams. Small changes in a parameter can change the diagrams qualitatively:



At a degenerate node the linearization has a double eigenvalue with only a single eigenvector

$$\underline{\underline{L}} = \begin{pmatrix} \lambda & 1 \\ 0 & \lambda \end{pmatrix}$$

the system is *almost* oscillating:

$$\underline{\underline{L}} = \begin{pmatrix} \lambda & 1 \\ \epsilon & \lambda \end{pmatrix} \quad (\lambda - \sigma)^2 = \epsilon \quad \sigma = \lambda \pm \sqrt{\epsilon}$$

In two dimensions the eigenvalues can be written simply in terms of  $\det \underline{\underline{L}}$  and  $\text{tr} \underline{\underline{L}}$

$$\det L = \det(\underline{\underline{S}}^{-1} \underline{\underline{L}} \underline{\underline{S}}) = \lambda_1 \lambda_2 \quad \text{tr} \underline{\underline{S}}^{-1} \underline{\underline{L}} \underline{\underline{S}} = \lambda_1 + \lambda_2$$

$$\lambda_{1,2} = \frac{\text{tr} \underline{\underline{L}} \pm \sqrt{(\text{tr} \underline{\underline{L}})^2 - 4 \det \underline{\underline{L}}}}{2}$$

**Change in stability:**  $\text{Re}(\lambda_i) = 0$

- i)  $\text{tr } \underline{\underline{L}} = 0$  and  $\det \underline{\underline{L}} > 0 \Rightarrow \lambda = \pm i\omega$  complex pair crossing imaginary axis
- ii)  $\text{tr } \underline{\underline{L}} < 0$  and  $\det \underline{\underline{L}} = 0 \Rightarrow \lambda_1=0, \lambda_2 < 0$  single zero eigenvalue

**Change in character:**

Transition between real  $\leftrightarrow$  complex

$$(\text{tr } \underline{\underline{L}})^2 = 4 \det \underline{\underline{L}}$$

Saddle  $\iff \det L < 0$

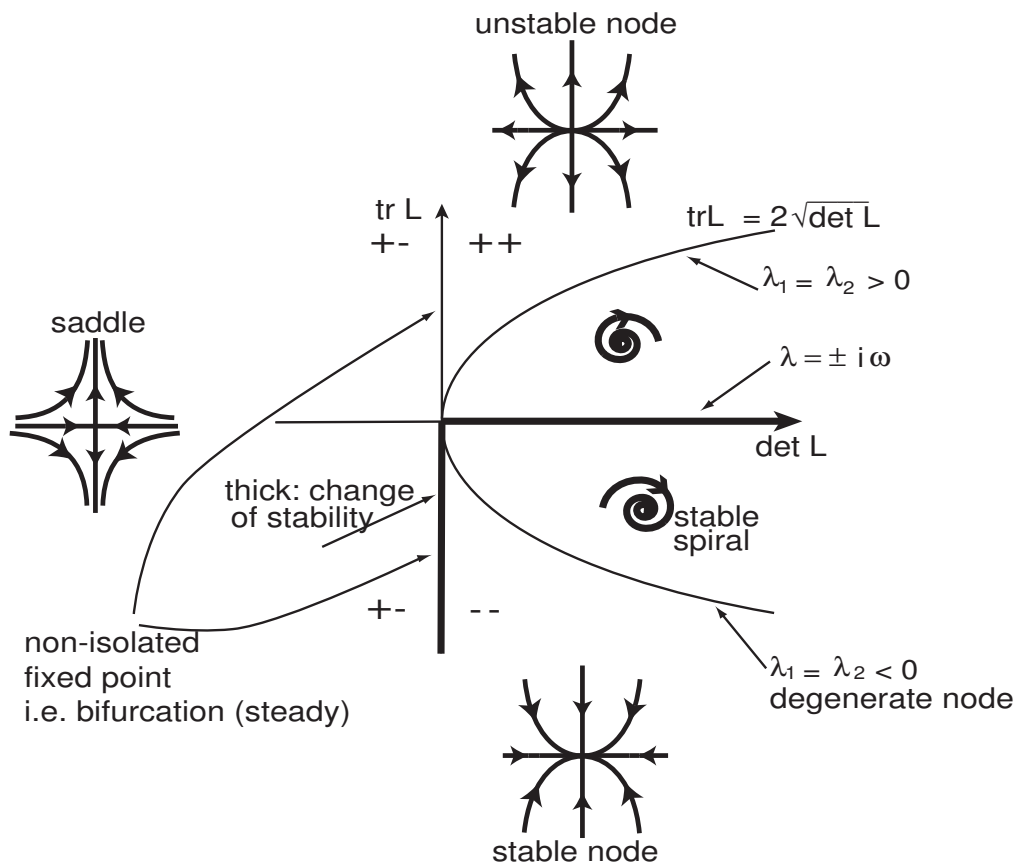


Figure 25: Dependence of the eigenvalues on the trace and determinant of the  $2 \times 2$ -matrix.

### Notes:

- Degenerate node  $\Rightarrow$  border between nodes and spirals, does not quite oscillate
- Non-isolated fixed points: steady bifurcation, one or more fixed points are created/annihilated (details depend on the nonlinearities).

## 3.2 Stability<sup>30</sup>

So far we have considered only linear stability. There are also other notions of stability.

Linear stability in a nonlinear system

- all *infinitesimal* perturbations decay eventually
- the dynamics of infinitesimal perturbations can be determined by a *linearization* of the equations around the points in question

**Example:** Damped-driven pendulum

$$m\ell^2 \ddot{\theta} + \beta \dot{\theta} = -mg\ell \sin \theta + \Gamma$$

rewrite as first-order system using  $x = \theta$  and  $y = \dot{\theta}$ :

$$\begin{aligned}\dot{x} &= y \equiv F_x(x, y) \\ \dot{y} &= -\frac{\beta}{m\ell^2}y - \frac{mg\ell}{m\ell^2} \sin x + \Gamma \equiv F_y(x, y)\end{aligned}$$

Fixed points:

$$y_0 = 0 \quad \& \quad mg\ell \sin x_0 = \Gamma$$

Expand around the fixed points

$$\begin{aligned}x &= x_0 + \epsilon x_1(t) \quad \epsilon \ll 1 \\ y &= y_0 + \epsilon y_1(t)\end{aligned}$$

Insert the expansion

$$\begin{aligned}\epsilon \dot{x}_1 &= F_x(x_0 + \epsilon x_1(t), y_0 + \epsilon y_1(t)) = \\ &= \underbrace{F_x(x_0, y_0)}_0 + \epsilon x_1 \partial_x F_x|_{(x_0, y_0)} + \epsilon y_1 \partial_y F_x|_{(x_0, y_0)} + \mathcal{O}(\epsilon^2)\end{aligned}$$

Analogously for  $\dot{y}_1$ .

In matrix form:

$$\begin{pmatrix} \dot{x}_1 \\ \dot{y}_1 \end{pmatrix} = \underbrace{\begin{pmatrix} \partial_x F_x & \partial_y F_x \\ \partial_x F_y & \partial_y F_y \end{pmatrix}}_{\text{Jacobian } \underline{\underline{L}}} \begin{pmatrix} x_1 \\ y_1 \end{pmatrix}$$

⇒ the linear stability is determined by the eigenvalues of the Jacobian

For the pendulum we have

$$\underline{\underline{L}} = \begin{pmatrix} 0 & 1 \\ -\frac{g}{\ell} \cos x_0 & -\frac{\beta}{m\ell^2} \end{pmatrix}$$

Thus, the eigenvalues are given by

$$\det(\underline{\underline{L}} - \lambda \underline{\underline{I}}) = 0$$

---

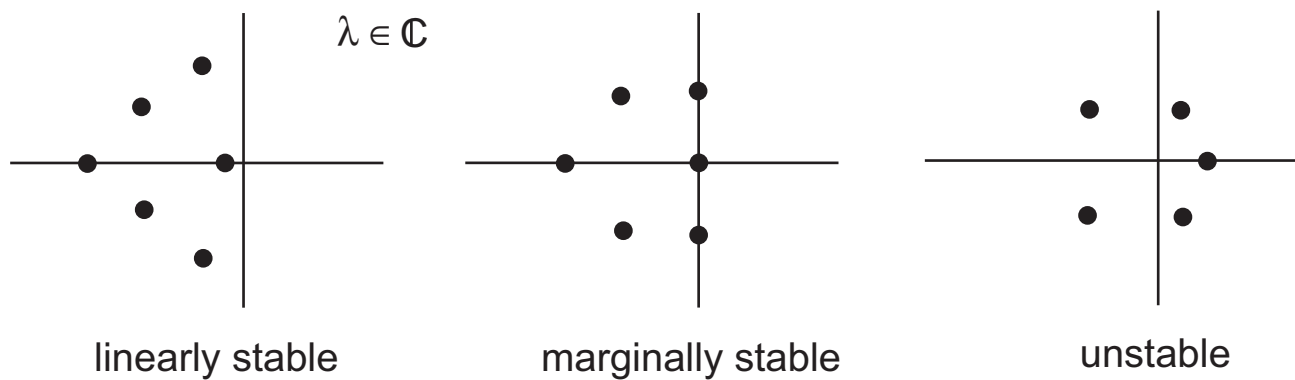
<sup>30</sup>Strogatz 6.3

yielding in this case

$$(-\lambda)(-\lambda - \frac{\beta}{m\ell^2}) + \frac{g}{\ell} \cos x_0 = 0$$

$$\begin{aligned}\lambda^2 &+ \lambda \frac{\beta}{m\ell^2} + \frac{g}{\ell} \cos x_0 = 0 \\ \lambda_{1,2} &= -\frac{\beta}{2m\ell^2} \pm \frac{1}{2} \sqrt{\left(\frac{\beta}{m\ell^2}\right)^2 - 4\frac{g}{\ell} \cos x_0}\end{aligned}$$

In general, for  $n$  first-order equations the Jacobian of the linearization is an  $n \times n$  matrix and has  $n$  eigenvalues in the complex plane:

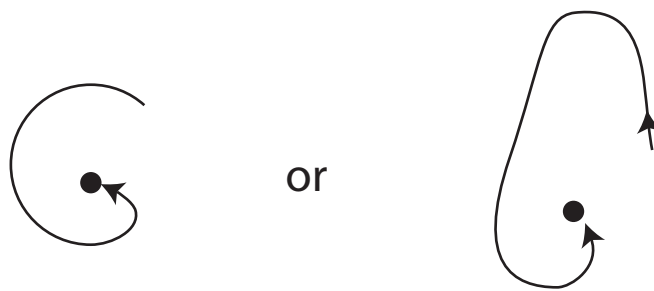


### Other stability notions:

#### Attractor:

A set of points (e.g. a fixed point) is attracting if all trajectories that start close to it converge to it, i.e.

for all  $\mathbf{x}(0)$  near  $\mathbf{x}_{FP}$  :  $\mathbf{x}(t) \rightarrow \mathbf{x}_{FP}$  for  $t \rightarrow \infty$



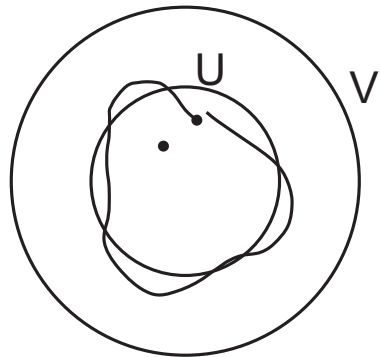
#### Note:

- The trajectory need not approach the attractor right away.
- The set of points that eventually reach the attractor form the *basin of attraction* of the attractor.

- The attractor can also be a periodic orbit or something more complicated (oscillating with multiple frequencies, say, or chaotic).

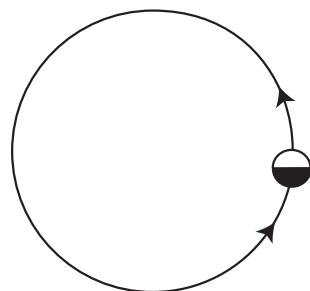
### Lyapunov Stability:

A set is (Lyapunov) stable if all orbits that start close to it remain close to it for all times. Technically, for any neighborhood  $V$  of  $x_{FP}$  one can find a  $U \subseteq V$  such that if  $x(0) \in U$  then  $x(t) \in V$  for all times.



### Notes:

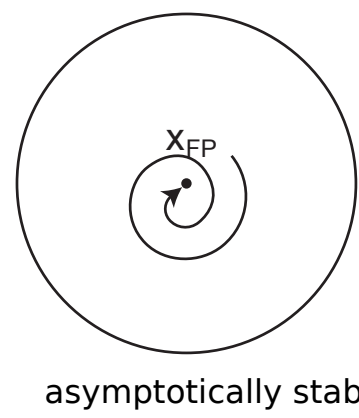
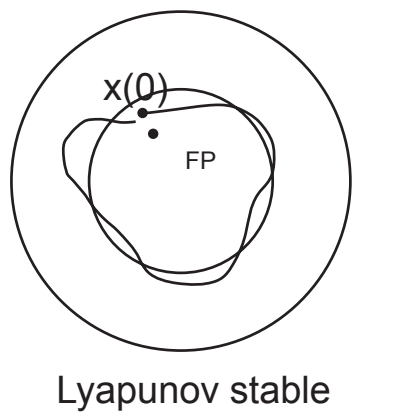
- Lyapunov stability of a set does not imply that the set is an attractor:
- An attractor does not have to be Lyapunov stable



This fixed point is not Lyapunov stable (one cannot find a neighborhood to which excursions are confined), but due to the global connection it is attracting.

### Asymptotic Stability:

A set is asymptotically stable if it is attracting and Lyapunov stable, i.e. if all orbits that start sufficiently close to a fixed point converge to it as  $t \rightarrow \infty$  without leaving its neighborhood.

**Notes:**

- A fixed point is asymptotically stable  $\Rightarrow$  the fixed point is attracting, it is an attractor.
- Linear stability  $\Rightarrow$  asymptotic stability  $\Rightarrow$  Lyapunov stability
- Linear instability  $\Rightarrow$  instability
- **But:** asymptotic or Lyapunov stability **do not imply** linear stability

**Examples:** see homework

### 3.3 General Properties of the Phase Plane

#### 3.3.1 Hartman-Grobman theorem<sup>31</sup>

Linear systems: can be completely understood

How much of that can be transferred to nonlinear systems? The linearization is only an approximation. What aspects of the linear system are exactly valid in the nonlinear system?

**Definition:** A fixed point  $\underline{x}_0$  of  $\dot{\underline{x}} = \underline{f}(\underline{x})$  is called hyperbolic if all eigenvalues of  $\frac{\partial f_i}{\partial x_j}$  have non-zero real parts.

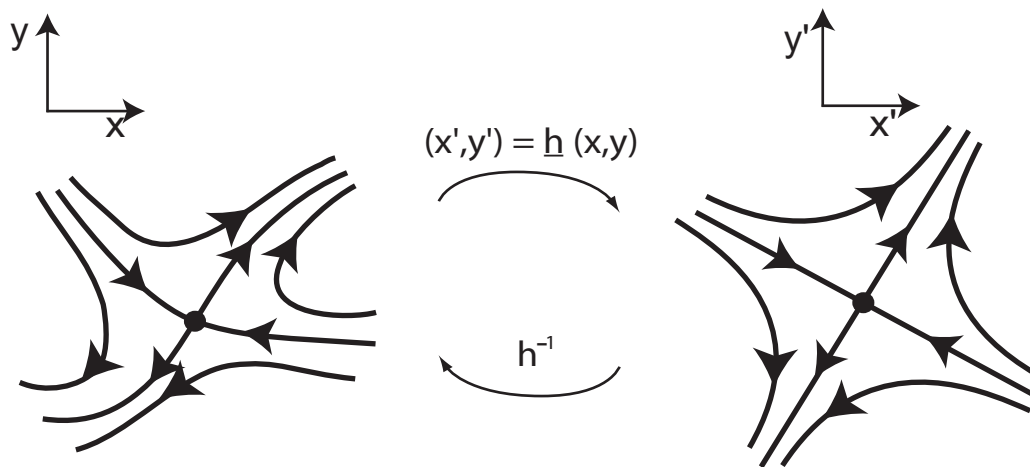
**Thus:** in all directions a hyperbolic fixed point is either linearly attractive or repulsive. No marginal direction.

#### Hartman-Grobman Theorem:

If  $\underline{x}_0$  is a hyperbolic fixed point of  $\dot{\underline{x}} = \underline{f}(\underline{x})$  then there exists a continuous invertible function  $h(\underline{x})$  that is defined on some neighborhood of  $\underline{x}_0$  and maps all orbits of the nonlinear flow into those of the linear flow. The map can be chosen so that the parameterization of orbits by time is preserved.

---

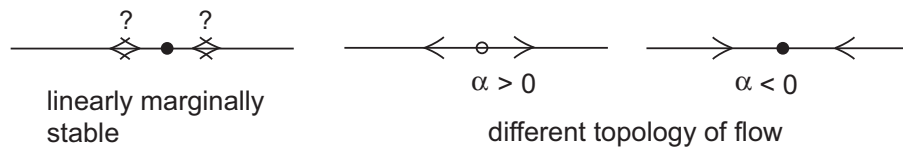
<sup>31</sup>Strogatz Ch 6.3



Thus:

- For a hyperbolic fixed point  $\underline{x}_0$  the linearization of the flow gives the **topology** of the nonlinear flow in a neighborhood of  $\underline{x}_0$ .
- If the fixed point is not hyperbolic, the linearization does not give sufficient information:

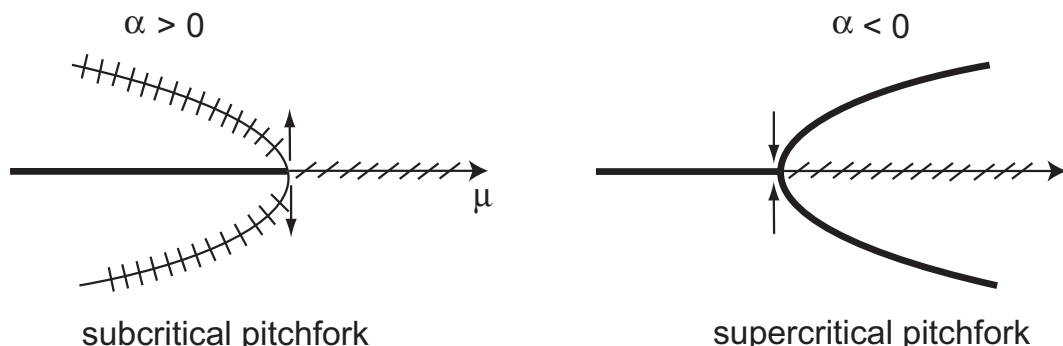
$$\dot{x} = \alpha x^3$$



- At any bifurcation the fixed point is not hyperbolic.

$$\dot{x} = \mu x + \alpha x^3$$

at  $\mu = 0$  the linear systems are equal for all  $\alpha$ .



- Away from the bifurcation point the nonlinear terms are negligible compared to the linear terms if one focuses on a sufficiently small neighborhood of the fixed point.

**Note:**

- the flow in the vicinity of a hyperbolic fixed point is structurally stable, i.e. small perturbations do not change the topology (qualitative features) of the flow . This is not the case without hyperbolicity, e.g. for centers or fixed points undergoing bifurcations.

**3.3.2 Phase Portraits<sup>32</sup>**

A phase portrait captures all relevant features of the phase plane.

**Example:**

$$\begin{aligned}\dot{x} &= f(x, y) = y \\ \dot{y} &= g(x, y) = x(1 + y) - 1\end{aligned}$$

1. Nullclines are lines along which the time derivative of one of the variables vanishes. They can only be crossed parallel to the coordinate axis corresponding to the other variable.

$$\begin{aligned}f(x, y) = 0 &\Rightarrow y = 0 \\ g(x, y) = 0 = x(1 + y) - 1 &\Rightarrow y = \frac{1}{x} - 1\end{aligned}$$

2. Fixed Points are at the intersections of the nullclines.

$$y = 0 \quad x = 1$$

3. Linear stability of fixed point:

$$x(t) = 1 + \epsilon x_1(t) \quad y = \epsilon y_1(t)$$

$$\begin{pmatrix} \dot{x}_1 \\ \dot{y}_1 \end{pmatrix} = \begin{pmatrix} 0 & 1 \\ 1 & 1 \end{pmatrix} \begin{pmatrix} x_1 \\ y_1 \end{pmatrix}$$

Eigenvalues:

$$\lambda_{1,2} = \frac{1 \pm \sqrt{5}}{2} \quad \text{saddle point}$$

Eigenvectors:

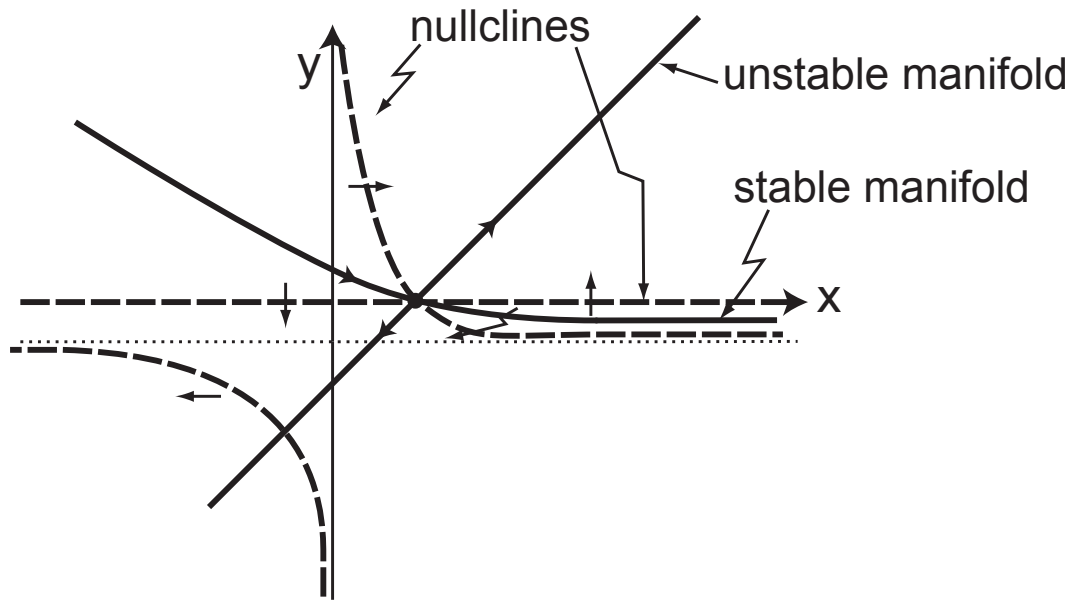
$$\begin{pmatrix} x_0^{(1,2)} \\ y_0^{(1,2)} \end{pmatrix} = \begin{pmatrix} 2 \\ 1 \pm \sqrt{5} \end{pmatrix}$$

**Note:**


---

<sup>32</sup>Strogatz Ch. 6.1

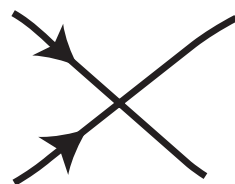
- This fixed point is hyperbolic  $\Rightarrow$  the eigenvectors of the linear stability analysis give the directions of the stable and unstable manifolds of the nonlinear flow.



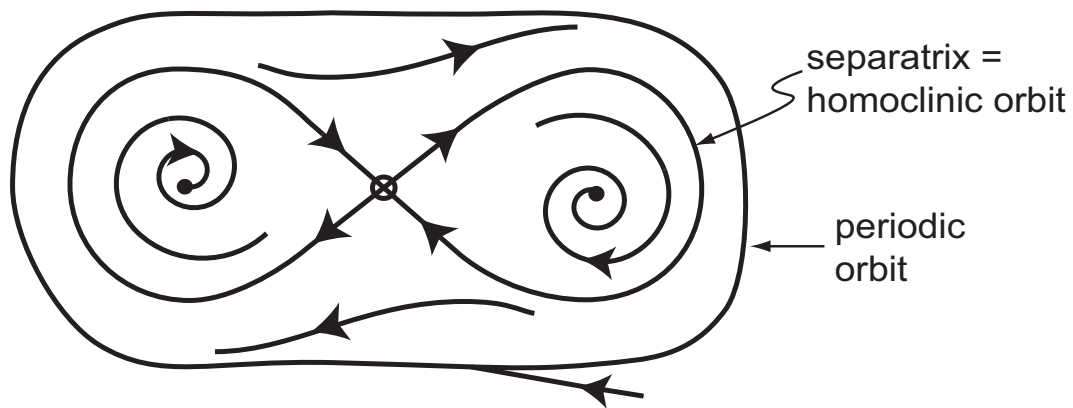
### Notes:

- For  $\dot{x} = f(x)$  the solutions are unique if all partial derivatives  $\frac{\partial f_i}{\partial x_j}$  are continuous

$\Rightarrow$  orbits do not intersect. An intersection would imply a non-unique solution: starting with an initial condition at the intersection the system could go into two different directions. Thus, the lines denoting orbits can cross only at fixed points.



Phase portraits can be more complicated:



Phase portraits can contain

- nullclines
- fixed points with their stable/unstable manifolds
- periodic orbits
- separatrices: a separatrix separates basins of attraction of different attractors
- heteroclinic orbits: trajectories that connect two different fixed points. If two fixed points are connected by a heteroclinic orbit the unstable manifold of one fixed point is the stable manifold of the other.
- homoclinic orbits: a trajectory that returns to the same fixed point. In this case the unstable manifold coincides with the stable manifold of the fixed point.

### 3.3.3 Ruling out Persistent Dynamics<sup>33</sup>

For what kind of systems can one rule out persistent dynamics like periodic orbits?

#### Bendixson-Dulac theorem

For two-dimensional systems there is a useful simple criterion arising from Green's theorem:

Consider

$$\begin{aligned}\frac{dx}{dt} &= f(x, y) \\ \frac{dy}{dt} &= g(x, y)\end{aligned}$$

and assume there is a periodic solution  $(x(t), y(t))$ . It describes a closed contour  $\mathcal{C}$  in the phase plane. Use Green's theorem for that contour

$$\int \int_D \frac{\partial f}{\partial x} + \frac{\partial g}{\partial y} dx dy = \int_{\mathcal{C}} -g dx + f dy$$

Along the contour we have

$$\begin{aligned}\frac{dx}{dt} = f &\quad \Rightarrow \quad dx = f dt \\ \frac{dy}{dt} = g &\quad \Rightarrow \quad dy = g dt\end{aligned}$$

implying

$$\int_{\mathcal{C}} -g dx + f dy = \int -g f dt + f g dt = 0.$$

Therefore we have the **Bendixson-Dulac Theorem**:

If  $\frac{\partial f}{\partial x} + \frac{\partial g}{\partial y}$  has the same sign everywhere in a two-dimensional

<sup>34</sup> domain  $D$ , the dynamical system cannot have a periodic orbit that lies completely in  $D$ .

#### Note:

---

<sup>33</sup>Strogatz Ch. 7.2 and Lecture 9

<sup>34</sup>The domain cannot have any holes.

- It is easy to show the more general condition:  
If there is a smooth function  $\phi$  such that

$$\frac{\partial(\phi f)}{\partial x} + \frac{\partial(\phi g)}{\partial y} > 0$$

everywhere inside a simply connected region  $\mathcal{D}$  then there cannot be any periodic orbit inside of  $\mathcal{D}$ .

## Potential Systems

In the one-dimensional case we discussed already **Gradient Systems (Potential Systems)**

Thus, if

$$\dot{x} = -\nabla V(x) \quad \text{i.e.} \quad \dot{x}_i = -\frac{\partial V}{\partial x_i}$$

with  $V \geq V_0$  for all  $x$  (bounded from below)

then

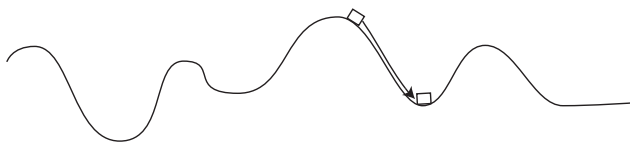
$$\frac{dV}{dt} = \sum_i \frac{\partial V}{\partial x_i} \dot{x}_i = - \sum_i \left( \frac{dx_i}{dt} \right)^2 \leq 0.$$

Thus,  $V$  eventually reaches a (local) minimum and

$$\frac{dV}{dt} = 0 \Leftrightarrow \dot{x}_i = 0 \quad \text{for all } i$$

Thus, the system always goes to a fixed point.

**Example:** Mechanical overdamped particle in potential



## Lyapunov Function

To rule out persistent dynamics, one does not have to require that the dynamics are given by the gradient of the potential,  $\dot{x} = -\nabla V$ .

More generally:

Assume there is a continuously differentiable function  $V(x)$  with  $V(x) > V_0 \equiv V(x_0)$  for all  $x \neq x_0$  where  $x_0$  is a fixed point. Then one has the following statements:

- if  $\frac{dV}{dt} \leq 0$  for all  $x \neq x_0$  in a neighborhood  $\mathcal{U}$  of  $x_0$  then  $x_0$  is Lyapunov stable,  
i.e. if  $V(x(t))$  is non-increasing in time,  $x(t)$  cannot escape.

- if  $\frac{dV}{dt} < 0$  for all  $\underline{x} \neq \underline{x}_0$  in  $\mathcal{U}$  of  $\underline{u}_0$  then  $\underline{x}_0$  is asymptotically stable,  
i.e. if  $V(\underline{x}(t))$  is strictly decreasing in time,  $\underline{x}(t)$  must approach the fixed point.

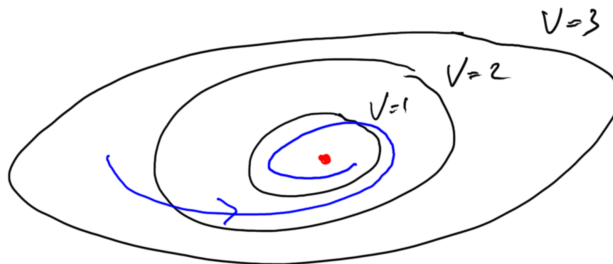


Figure 26: If the system has a Lyapunov function  $V$ , that function decreases along the trajectory even though the dynamics need not be given by its gradient.

### Note:

- Such a  $V(\underline{x})$  is called a *Lyapunov function*.

### Example:

a) Damped particle in a bounded potential  $\mathcal{U}(x)$

$$\ddot{x} + \beta \dot{x} = -\frac{d\mathcal{U}}{dx}$$

i.e.

$$\begin{aligned}\dot{x} &= v \\ \dot{v} &= -\beta v - \frac{d\mathcal{U}}{dx}\end{aligned}$$

Try the total energy as a Lyapunov function

$$V = \frac{1}{2}\dot{x}^2 + \mathcal{U} = \frac{1}{2}v^2 + \mathcal{U}$$

$$\frac{dV}{dt} = v\dot{v} + \frac{d\mathcal{U}}{dx}\dot{x} = v(-\beta v - \frac{d\mathcal{U}}{dx}) + \frac{d\mathcal{U}}{dx}v = -\beta v^2 < 0 \quad \text{for } v \neq 0$$

$\Rightarrow$  there are no periodic orbits and the system always ends up in a stable fixed point.

### Note:

- For finite damping, the dynamics are not given by the gradient of the Lyapunov function

$$\frac{\partial V}{\partial x} = \frac{\partial U(x)}{\partial x} \neq v,$$

i.e. this system is not a potential system.

In the limit of  $\beta \rightarrow \infty$  the system becomes a potential system

$$\frac{dx}{dt} = v = -\frac{1}{\beta} \frac{dU}{dx}.$$

b)

$$\begin{aligned}\dot{x} &= -x + 4y \\ \dot{y} &= -x - y^3\end{aligned}$$

This system is not a gradient system. Try a function  $V(x, y)$ . We would need then

$$\dot{x} = -\frac{\partial V}{\partial x} = -x + 4y$$

implying

$$V = \frac{1}{2}x^2 - 4xy + f(y).$$

As soon as  $V(x, y)$  is given, it would also determine  $\dot{y}$  via  $\partial V / \partial y$ ,

$$\frac{\partial V}{\partial y} = -4x + \frac{df}{dy} \neq -\dot{y} = x + y^3.$$

Simplest attempt to find a Lyapunov function: try a quadratic function that is bounded from below:

$$V = x^2 + ay^2 \quad \text{with } a > 0.$$

The parameter  $a$  can be chosen as needed. Check whether  $V$  is monotonically decreasing under the dynamics,

$$\begin{aligned}\frac{dV}{dt} &= 2x(-x + 4y) + 2ay(-x - y^3) \\ &= \underbrace{-2x^2}_{\leq 0} + \underbrace{xy(8 - 2a)}_{\text{undetermined}} - \underbrace{2ay^4}_{\leq 0}\end{aligned}$$

$\Rightarrow$  choose  $a = 4 \Rightarrow \frac{dV}{dt} < 0$  for  $x \neq 0 \neq y$

$\Rightarrow (0, 0)$  is asymptotically stable and this system has no periodic orbits.

**Note:**

- Lyapunov functions rule out persistent dynamics in **arbitrary dimensions**.

In this two-dimensional case we could also have tried the Bendixson-Dulac theorem. Since

$$\frac{\partial f}{\partial x} + \frac{\partial g}{\partial y} = -1 - 3y^2 < 0 \quad \text{for all } x, y,$$

there cannot be any periodic orbit.

### 3.3.4 Poincaré-Bendixson Theorem: No Chaos in 2 Dimensions<sup>35</sup>

- How complex can the dynamics be in 2 dimensions?

---

<sup>35</sup>cf. Strogatz Ch.7.3

- Can we guarantee a periodic orbit without explicitly calculating it?

### Poincaré-Bendixson Theorem:

If

- $R$  is a closed bounded subset of the plane
- $\dot{x} = f(x)$  with  $f(x)$  continuously differentiable on an open set containing  $R$

then

- any orbit that remains in  $R$  for all  $t$  either converges to a fixed point or to a periodic orbit.

### Simple Illustration:

- In one dimension we had: no periodic orbits and not even an oscillatory approach to a fixed point because
  - an oscillatory approach would require that the orbit goes across the fixed point.
  - however, because the solutions are unique, trajectories cannot cross each other.

To get oscillations the trajectory would need to *spiral* into the fixed point: we would need 2 dimensions

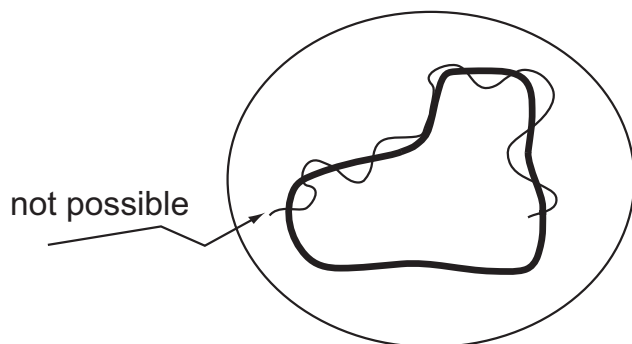
- In two dimensions:  
What is more "complicated" than periodic orbit?  
a periodic orbit has single fundamental frequency  $\omega$

$$x(t) = A_1 \cos \omega t + A_2 \cos 2\omega t + A_3 \cos 3\omega t + \dots$$

Can we have 2 incommensurate frequencies? I.e.

$$x(t) = A \cos \omega_1 t + B \cos \omega_2 t + \text{higher harmonics} \quad \text{with} \quad \frac{\omega_1}{\omega_2} \neq \frac{m}{n} \quad \text{irrational}$$

Consider the approach to a periodic orbit in two dimensions:



The periodic orbit *divides* the phase plane into *inside* and *outside*. An oscillatory approach to the periodic orbit would require going from inside to outside and back. This is not possible without crossing the periodic orbit, which is not possible due to the uniqueness of the solution  $\Rightarrow$  No second independent frequency.

The system has to go to a fixed point or a periodic orbit.

To get an oscillatory approach to the periodic orbit the trajectory would have to *spiral* around the periodic orbit: we would need 3 dimensions.

### Consequence of the Poincaré-Bendixson Theorem:

- The only attractors of 2d-flows are fixed points or periodic orbits
- **There is no chaos in 2 dimensions.**

### Example 2: Glycolysis Oscillations

Yeast cells break down sugar by glycolysis, which can proceed in an oscillatory fashion.

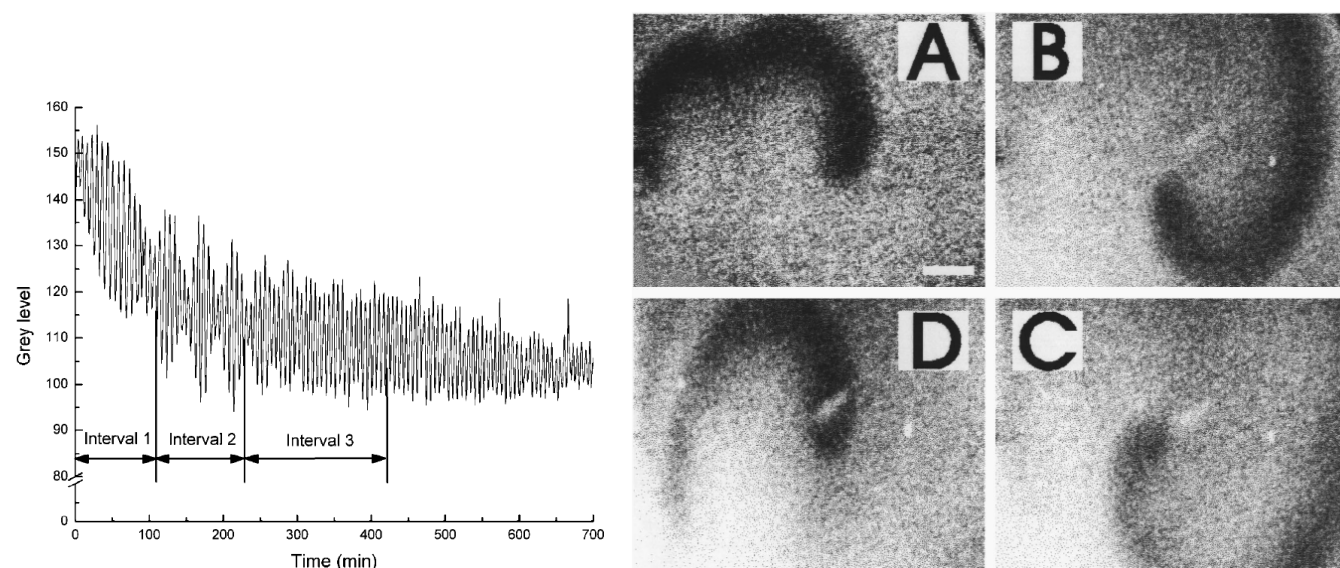


Figure 27: Glycolytic oscillations in an unstirred yeast extract leads to spiral waves (Müller et al., 1998; Bagyan et al., 2008).

Simple model(Selkov, 1968; Edelstein-Kesher, 2005):

Phosphorylation of fructose-6-phosphate  $F6P$  to fructose-6-diphosphate  $FDP$

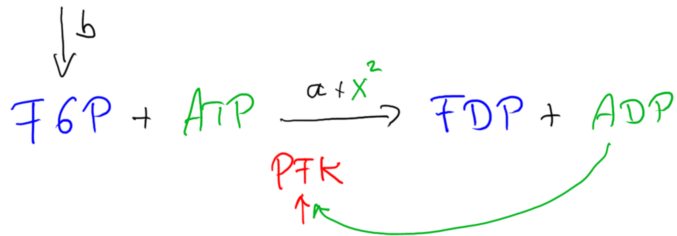


Figure 28: Glycolysis. This reaction is catalyzed by the enzyme phosphofructokinase PFK and accompanied by the conversion of adenosine triphosphate ATP into adenosine diphosphate ADP. PFK is stimulated by binding with several ADP molecules, i.e. the phosphorylation of F6P is enhanced by the presence of multiple ADP molecules.

$$\begin{array}{ll}
 & \text{non-enhanced phosphorylation} \\
 \text{ADP adenosine diphosphate} & \dot{x} = -x + \overbrace{ay} \\
 \text{F6P fructose-6-phosphate} & \dot{y} = b - ay - \underbrace{x^2y} \\
 & \text{enhanced phosphorylation}
 \end{array}
 \quad
 \begin{aligned}
 +x^2y &= f(x, y) \\
 &= g(x, y)
 \end{aligned}$$

$b$  represents another reaction that resupplies the F6P.

Are there parameter ranges for which one can guarantee the existence of a stable periodic orbit?

### Phase portrait:

study nullclines:  $\dot{x} = 0$  or  $\dot{y} = 0$

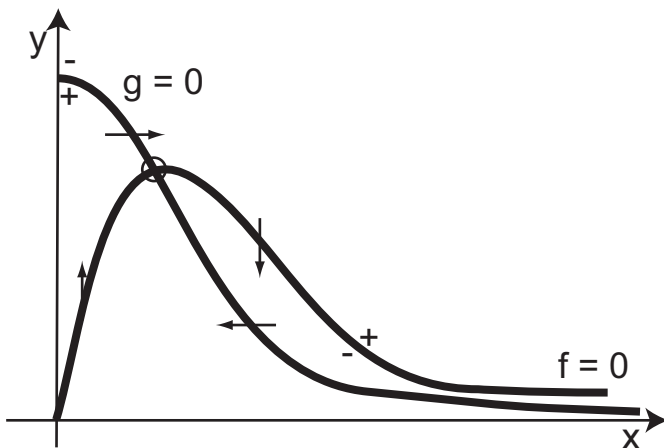
$$\begin{aligned}
 f &= 0 \quad \Rightarrow y = \frac{x}{a+x^2} \\
 g &= 0 \quad \Rightarrow y = \frac{b}{a+x^2}
 \end{aligned}$$

$\Rightarrow$  the fixed point is at

$$y = \frac{x}{a+x^2} = \frac{b}{a+x^2}$$

$$\Rightarrow x = b \quad \text{and} \quad y = \frac{b}{a+b^2}.$$

The fixed point exists for all  $b > 0, a > 0$



Nullclines show: spiraling motion

- to fixed point?
- to periodic orbit? which?
- to infinity?

Use the Poincaré-Bendixson theorem to show that there is a periodic orbit. To use the Poincaré-Bendixson theorem we need to make sure the assumptions underlying the theorem are satisfied.

1. We need a trapping region  $\mathcal{R}$ , i.e. a region in the phase plane from which the orbit cannot escape. We know then that any initial condition inside  $\mathcal{R}$  leads either to a fixed point or a periodic orbit.
2. To guarantee that the solution goes to a periodic orbit, we need to make sure that there are no fixed points in  $\mathcal{R}$ .

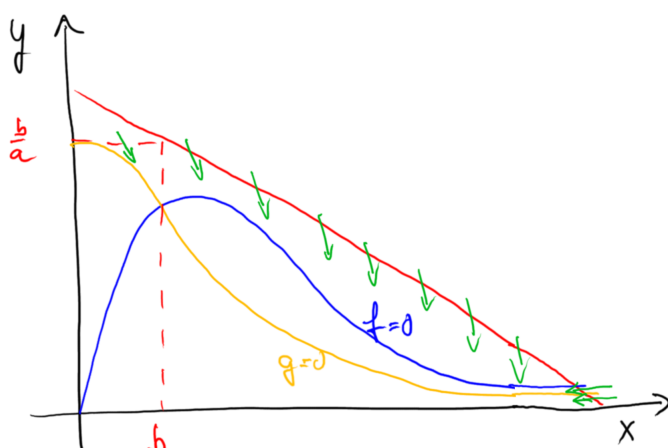


Figure 29: Identifying the trapping region.

## 1. Trapping Region:

- (a) For  $y > \frac{b}{a}$  we have  $g < 0$  for any value of  $x > 0 \Rightarrow$  flow inward for  $y > \frac{b}{a}$ . This limits the region in the  $y$ -direction, but it is not bounded in the  $x$ -direction yet.
- (b) Consider a general orbit

$$\frac{dy}{dx} = \frac{\frac{dy}{dt}}{\frac{dx}{dt}} = -\frac{-g}{f} = -\frac{x^2y + ay - b}{x^2y + ay - x}$$

For  $x > b$ , i.e. to the right of the fixed point:

For  $x^2y + ay - x > 0$ , i.e. above the nullcline  $f = 0$ , one has

$$\frac{dy}{dx} < -1$$

the trajectories enter the trapping region along  $y = -x + C$

Below the nullcline  $f = 0$  we have  $\dot{x} < 0$ :

the trajectories enter the trapping region along  $x = x_r$  with  $x_r$  being the  $x$ -coordinate of the intersection of the straight line and  $f = 0$

Alternatively one can compare  $|\dot{x}|$  with  $|\dot{y}|$  like this

$$\begin{aligned}\dot{x} - (-\dot{y}) &= -x + ay + x^2y + b - ay - x^2y \\ &= b - x\end{aligned}$$

$\Rightarrow$  for  $x > b \quad |\dot{x}| < |\dot{y}|$

$\Rightarrow$  flow inward along  $y = -x + C$  for  $x > b$  and  $C$  large enough

## 2. Fixed Points:

There is only a single fixed point  $(b, \frac{b}{a+b^2})$ . To guarantee oscillations we need to exclude this fixed point from  $\mathcal{R}$ .

The linear stability analysis shows that the fixed point is unstable for

$$1 - 2a - \sqrt{1 - 8a} < 2b^2 < 1 - 2a + \sqrt{1 - 8a}.$$

Therefore an orbit starting in  $\mathcal{R}$  cannot converge onto that fixed point  $\Rightarrow$  a limit cycle is guaranteed for this range of  $b$ , which exists<sup>36</sup> as long as  $a \leq \frac{1}{8}$

Formally, we could exclude a small neighborhood  $\mathcal{U}$  around the unstable fixed point from  $\mathcal{R}$  and because the fixed point is linearly unstable we would know that no orbits can escape from  $\mathcal{R}$  into  $\mathcal{U}$ . If the fixed point was only marginally stable according to the linear stability calculation, nonlinear terms would become relevant: we would then need to establish that orbits can only cross the border from  $\mathcal{U}$  to  $\mathcal{R}$  but not in the other direction (as we did for the line  $y = -x + C$  in the example).

<sup>36</sup>The instability at  $2(b_H^{(1,2)})^2 = 1 - 2a \pm \sqrt{1 - 8a}$  is a Hopf bifurcation. Oscillations occur for  $b_H^{(1)} < b < b_H^{(2)}$ . No steady bifurcation is possible.

### 3.4 Relaxation Oscillations<sup>37</sup>

Class of systems for which one can see the periodic orbit relatively easily:

Fast-slow systems with *N*-shaped nullcline

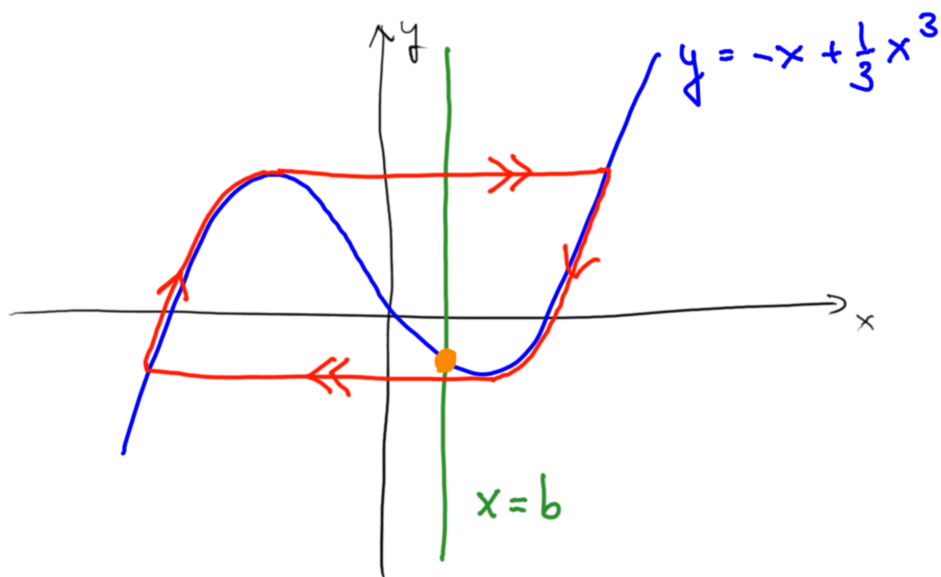
Example:

Consider for  $\mu \gg 1$ :

$$\begin{aligned}\dot{x} &= \mu(y - F(x)) \\ \dot{y} &= b - x\end{aligned}$$

with

$$F(x) = -x + \frac{1}{3}x^3$$



For  $\mu \gg 1$  the variable  $x$  evolves much faster than  $y$  except near the nullcline  $y = F(x)$ :

- except near the nullcline  $y = F(x)$  the vector field is essentially horizontal

$$\frac{dy}{dx} = \frac{\dot{y}}{\dot{x}} = \frac{b - x}{\mu(y - F(x))} \rightarrow 0 \quad \text{for } \mu \rightarrow \infty$$

the horizontal trajectories constitute two *fast* branches

- near the nullcline  $y = F(x)$  the trajectory is pushed towards the nullcline: the nullcline  $y = F(x)$  represents two *slow* branches

---

<sup>37</sup>Strogatz Ch. 7.5

Fixed point:

$$x_0 = b \quad y_0 = b - \frac{1}{3}b^3$$

Linear stability of the fixed point: expand around  $(b, b - \frac{1}{3}b^3)$

$$x = x_0 + \epsilon x_1(t) \quad y = y_0 + \epsilon y_1(t)$$

$$\begin{aligned}\epsilon \dot{x}_1 &= \mu \left( y_0 + \epsilon y_1 + x_0 + \epsilon x_1 - \frac{1}{3} (x_0 + \epsilon x_1)^3 \right) \\ \epsilon \dot{y}_1 &= b - x_0 - \epsilon x_1.\end{aligned}$$

Collecting all terms at  $\mathcal{O}(\epsilon)$  yields

$$\begin{pmatrix} \dot{x}_1 \\ \dot{y}_1 \end{pmatrix} = \mathbf{L} \begin{pmatrix} x_1 \\ y_1 \end{pmatrix}$$

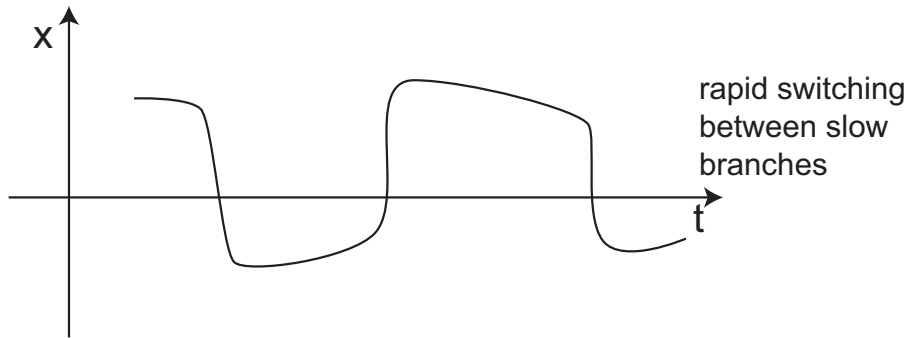
with

$$\mathbf{L} = \begin{pmatrix} \mu(1-b^2) & \mu \\ -1 & 0 \end{pmatrix}$$

In terms of the trace and the determinant of  $\mathbf{L}$  the eigenvalues are given by

$$\lambda_{1,2} = \frac{1}{2} \left( \text{trace} \mathbf{L} \pm \sqrt{(\text{trace} \mathbf{L})^2 - 4 \det \mathbf{L}} \right) = \frac{1}{2} \left( \mu(1-b^2) \pm \sqrt{\mu^2(1-b^2)^2 - 4\mu} \right).$$

Thus, since  $\mu > 0$ , the fixed point becomes unstable with a complex pair of eigenvalues at  $|b| = 1$ . For these two values of  $b$  the fixed point is at either of the two extrema of  $F(x)$ .



The period of the periodic orbit is essentially determined by the time spent on the slow branches.

On the right slow branch (nullcline) (i.e. for  $x > 0$ )  $y$  and  $x$  are tightly connected

$$y \sim F(x) \quad \Rightarrow \quad \dot{y} \sim \frac{dF}{dx} \dot{x}.$$

Thus, together with

$$\dot{y} = g(x, y) = b - x,$$

we have two equations for  $\dot{y}$ . We therefore can eliminate  $y$  from those equations and obtain a single single differential equation for  $x$ ,

$$\dot{x} = \frac{\dot{y}}{\frac{dy}{dx}} = \frac{g(x, y)}{\frac{dy}{dx}} = \frac{g(x, F(x))}{\frac{dF}{dx}}.$$

We can then approximate the period  $T$  by

$$T = \int dt = \int \frac{dt}{dx} dx = \int \frac{1}{\dot{x}} dx \sim \int_{C_1+C_2} \frac{1}{\frac{g(x, F(x))}{\frac{dF(x)}{dx}}} dx.$$

For simplicity, consider the symmetric case  $b = 0$ , for which the fixed point is at  $(0, 0)$ . Then we get

$$T \sim 2 \int_{\mathcal{C}} \frac{1}{\dot{x}} dx = 2 \int_{\mathcal{C}} \frac{dF}{-x} dx = 2 \int_{x_r}^{x_{min}} \frac{-1+x^2}{-x} dx,$$

where  $\mathcal{C}$  is the portion of the trajectory along the nullcline  $y = F(x)$  from  $x = x_r > 0$  to  $x = x_{min}$  with  $x_{min} > 0$  given by the minimum of  $F(x)$ :

$$\frac{dF}{dx} = 0 = -1 + x^2 \quad x_{min} = 1 \quad y_{min} = -\frac{2}{3} \quad x_{max} = -1 \quad y_{max} = \frac{2}{3}$$

The upper limit  $x_r$  is given by the condition

$$y_{max} \equiv \frac{2}{3} = F(x_r) = -x_r + \frac{1}{3}x_r^3$$

We know that  $F(x_r) = y_{max}$  has a double zero at  $x_{max} = -1$ . The cubic can therefore be factorized easily to obtain  $x_r = 2$ .

Thus

$$T \sim 2 \left[ \ln x - \frac{1}{2}x^2 \right] \Big|_2^1 = 2 \left\{ -\ln 2 + \frac{3}{2} \right\}$$

**Note:**

- This *fast-slow analysis* of identifying slow and fast portions of the dynamics is a powerful approach to analyze many systems that exhibit complex dynamics with multiple time scales.

### 3.5 Weakly Nonlinear Oscillators<sup>38</sup>

We would like to determine solutions for non-linear oscillators like

$$\ddot{x} + \beta \dot{x} + x + \alpha x^2 \dot{x} + \gamma x^3 = 0.$$

Exact nonlinear solutions usually impossible to get.

To make *analytical* progress we try to obtain *systematic approximate* solutions for

- the periodic orbits and
- the transients approaching periodic orbits.

---

<sup>38</sup>Strogatz Ch. 7.6

### 3.5.1 Failure of Regular Perturbation Theory

Consider first a simple linear example to demonstrate the problem,

$$\ddot{x} + 2\epsilon\beta\dot{x} + (1 + \epsilon\Omega)^2x = 0 \quad \text{with} \quad \epsilon \ll 1$$

with some initial condition like  $x(0) = 0, \dot{x}(0) = 1$ .

For this simple linear problem we can calculate the exact solution:

$$x_e = Ae^{\lambda t} \quad \Rightarrow \quad \lambda^2 + 2\epsilon\beta\lambda + (1 + \epsilon\Omega)^2 = 0$$

$$\lambda_{1,2} = \frac{-2\epsilon\beta \pm \sqrt{4\epsilon^2\beta^2 - 4(1 + \epsilon\Omega)^2}}{2} = -\epsilon\beta \pm i\sqrt{(1 + \epsilon\Omega)^2 - \epsilon^2\beta^2}.$$

We therefore have

$$x_{exact} = e^{-\epsilon\beta t} (Ae^{i\omega t} + A^*e^{-i\omega t}) \quad \text{with} \quad \omega = \sqrt{(1 + \epsilon\Omega)^2 - \epsilon^2\beta^2}.$$

To find out how we could try to solve the nonlinear problem approximately, attempt to get a perturbation solution using

$$x_a = x_0 + \epsilon x_1 + h.o.t.$$

Insert this ansatz into the differential equation,

$$\begin{aligned} \frac{d^2}{dt^2}(x_0 + \epsilon x_1 + \dots) &+ 2\epsilon\beta \frac{d}{dt}(x_0 + \epsilon x_1 + \dots) \\ &+ (1 + \epsilon\Omega)^2(x_0 + \epsilon x_1 + \dots) = 0 \end{aligned}$$

Collect the different orders in  $\epsilon$ :

$\mathcal{O}(\epsilon^0)$ :

$$\begin{aligned} \frac{d^2}{dt^2}x_0 + x_0 &= 0 \\ x_0 = Ae^{it} + A^*e^{-it} &= 2A_r \cos t - 2A_i \sin t \end{aligned}$$

At this order we have lost the friction and the change  $\Omega$  in the frequency. Go therefore to the next order:

$\mathcal{O}(\epsilon^1)$ :

$$\begin{aligned} \frac{d^2}{dt^2}x_1 + 2\beta \frac{d}{dt}x_0 + 2\Omega x_0 + x_1 &= 0 \\ \frac{d^2}{dt^2}x_1 + x_1 &= \underbrace{-2i\beta Ae^{it} - 2\Omega Ae^{it}}_{\sim \text{resonant forcing}} + c.c. \equiv \alpha e^{it} + c.c. \end{aligned}$$

This is a second-order constant-coefficient *inhomogeneous* differential equation: its general solution is given by

$$x_1(t) = x_h(t) + x_p(t)$$

with

$$\frac{d^2}{dt^2}x_h + x_h = 0 \quad \Rightarrow x_h = A_1 e^{it} + c.c.$$

Try undetermined coefficients for the particular solution (since the inhomogeneity is a simple exponential function):

$$x_p = B e^{it} + c.c.$$

However:

$$\frac{d^2}{dt^2}B e^{it} + B e^{it} = 0 \quad \Rightarrow \text{we cannot balance the inhomogeneity on the r.h.s.}$$

### Note:

- At  $\mathcal{O}(\epsilon)$  the inhomogeneous term is forcing the oscillator  $x_1$  at its resonance frequency: *resonant forcing*

We could now use the method of *variation of parameters*  $x_p = B(t)e^{it}$  and reduce the order of the equation and solve the resulting first-order equation by integration

$$\begin{aligned} x_p &= B(t)e^{it} \\ \ddot{x}_p &= \ddot{B}e^{it} + 2i\dot{B}e^{it} - Be^{it} + c.c. \end{aligned}$$

Thus,

$$\ddot{B}e^{it} + 2i\dot{B}e^{it} - Be^{it} + Be^{it} = \alpha e^{it}$$

with  $V = \dot{B}$  we get

$$\dot{V} + 2iV = \alpha$$

and using an integrating factor

$$\begin{aligned} \frac{d}{dt}(e^{2it}V) &= e^{2it}\alpha \\ V &= e^{-2it} \int e^{it}\alpha dt = \frac{1}{2i}\alpha \end{aligned}$$

and

$$\begin{aligned} B &= \frac{1}{2i}t\alpha + C \\ x_p(t) &= \frac{1}{2i}(-2i\beta - 2\Omega)te^{it}A + c.c. \end{aligned}$$

Alternatively, having some experience we can try directly the ansatz:

$$x_p = B t e^{it} + c.c.$$

Insert:

$$\begin{aligned} \frac{d^2}{dt^2}x_p + x_p &= \\ B(2ie^{it} - te^{it} + te^{it}) + c.c. &= -2i\beta Ae^{it} - 2\Omega Ae^{it} + c.c. \\ \Rightarrow B &= \frac{1}{2i}(-2i\beta - 2\Omega)A \end{aligned}$$

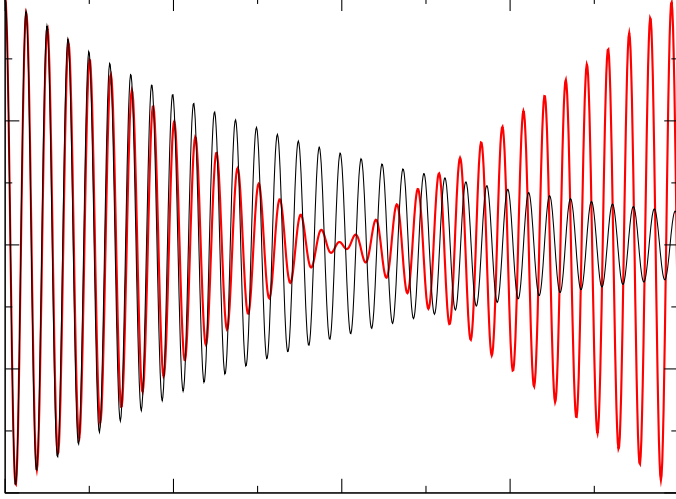
Put together the two orders together we have

$$x_a(t) = x_0(t) + \epsilon x_1(t) = Ae^{it} + \epsilon(-\beta + i\Omega)te^{it}A + c.c. = (1 - \epsilon\beta t + i\epsilon\Omega t)Ae^{it} + c.c.$$

### Notes:

- Initially, the oscillation amplitude of  $x_a(t)$  is decaying like that of the exact solution.
- For larger times the oscillation amplitude of  $x_a$  grows linearly, while the exact solution  $x_e(t)$  decays to 0.

Resonant forcing leads to (linear) growth without bounds: *secular terms*<sup>39</sup>



- for  $t = \mathcal{O}(\epsilon^{-1})$  the perturbation  $\epsilon x_1$  becomes as large as  $x_0$ : this contradicts the assumptions of the approach  $\Rightarrow$  the perturbation approach breaks down for  $t = \mathcal{O}(\epsilon^{-1})$ .

However: the approximation is indeed an expansion of the exact solution in  $\epsilon$ :

$$x_e = \underbrace{e^{-\epsilon\beta t}}_{1-\epsilon\beta t+\mathcal{O}(\epsilon^2)} (Ae^{i\omega t} + c.c.)$$

with

$$\omega = \underbrace{\sqrt{(1 + \epsilon\Omega)^2 - \epsilon^2\beta^2}}_{1+\epsilon\Omega+\mathcal{O}(\epsilon^2)}$$

$$\begin{aligned} x_e &= Ae^{it} + \epsilon(-\beta t + i\Omega t)Ae^{it} + \mathcal{O}(\epsilon^2) + c.c. \\ &= (1 + \epsilon(-\beta t + i\Omega t))Ae^{it} + \mathcal{O}(\epsilon^2) + c.c. \end{aligned}$$

### Thus:

- The straightforward perturbation expansion captures

---

<sup>39</sup>The term comes from perturbation calculations of planetary motion: some of their errors are of the same type and accumulate over the course of centuries (saeculum).

- the slow growth/decay
- the small change in frequency

but only initially.

Over longer times it keeps growing forever. It does not even capture the periodic solution for large times (for  $\beta = 0$ )

- The secular terms suggest what the true solution is doing.
- We need to expand in a more intelligent way that captures the change in frequency and the exponential decay for larger times.

### 3.5.2 Multiple Scales

The exact solution suggests that there are two time scales

$$x_{\text{exact}} = \mathcal{A}e^{-\epsilon\beta t+i\omega_0 t} + \text{c.c.} = \mathcal{A}e^{-\epsilon\beta t+i(1+\Omega\epsilon)t} + \text{c.c.} = \underbrace{\mathcal{A}e^{-\beta\epsilon t+i\Omega\epsilon t}}_{A(\epsilon t)} e^{it} + \text{c.c.}$$

The fast oscillation  $e^{i\omega_0 t}$  with frequency  $\omega_0 = 1$  has an amplitude that varies slowly with time since its argument changes only little as time progresses,  $A = A(\epsilon t)$ .

Introduce this slower time scale explicitly as a ‘separate time’,

$$T = \epsilon t$$

and let the function  $x$  depend on two time variables:  $\hat{t} = t$  and  $T$

$$x_e = x_e(\hat{t}, T).$$

#### Note:

- In this approach the two times  $\hat{t}$  and  $T$  are assumed to be essentially *independent* variables:

$$\begin{aligned} \frac{d}{dt}x(\hat{t}, T) &= \frac{\partial x}{\partial \hat{t}} \frac{d\hat{t}}{dt} + \frac{\partial x}{\partial T} \frac{dT}{dt} = \frac{\partial x}{\partial \hat{t}} + \epsilon \frac{\partial x}{\partial T} \\ \frac{d^2}{dt^2}x(\hat{t}, T) &= \frac{d}{dt} \left( \frac{\partial x}{\partial \hat{t}} + \epsilon \frac{\partial x}{\partial T} \right) = \frac{\partial^2 x}{\partial \hat{t}^2} + 2\epsilon \frac{\partial^2 x}{\partial \hat{t} \partial T} + \epsilon^2 \frac{\partial^2 x}{\partial T^2}. \end{aligned}$$

Thus, the ordinary differential equation becomes a partial differential equation.

- Of course, the two times  $\hat{t}$  and  $T$  are not really independent of each other. The assumption amounts therefore to making an approximation. The nature of that approximation is subtle.

Try again the same linear problem:

Expand again

$$x_a = x_0(\hat{t}, T) + \epsilon x_1(\hat{t}, T) + \dots$$

$$\left( \frac{\partial^2}{\partial \hat{t}^2} + 2\epsilon \frac{\partial^2}{\partial \hat{t} \partial T} + \epsilon^2 \frac{\partial^2}{\partial T^2} \right) (x_0 + \epsilon x_1 + \dots) + 2\epsilon \beta \left( \frac{\partial}{\partial \hat{t}} + \epsilon \frac{\partial}{\partial T} \right) (x_0 + \epsilon x_1 + \dots) + (1 + \epsilon \Omega)^2 (x_0 + \epsilon x_1 + \dots) = 0$$

$\mathcal{O}(\epsilon^0)$ :

$$\frac{d^2}{d\hat{t}^2} x_0 + x_0 = 0$$

$$x_0 = A e^{i\hat{t}} + A^* e^{-i\hat{t}} = 2A_r \cos \hat{t} - 2A_i \sin \hat{t}$$

**Note:**

- Previously,  $A$  was a constant. Now we have two independent variables; the differential equation only involved  $\hat{t}$ . Therefore  $A$  cannot depend on  $\hat{t}$ , but it is still allowed to depend on the slow time  $T$ :  $A = A(T)$

$\mathcal{O}(\epsilon^1)$ <sup>40</sup>:

$$2\partial_{\hat{t}}\partial_T x_0 + \partial_{\hat{t}}^2 x_1 + 2\beta\partial_{\hat{t}}x_0 + 2\Omega x_0 + x_1 = 0.$$

$$\partial_{\hat{t}}^2 x_1 + x_1 = -2 \left( i \frac{d}{dT} A + i\beta A + \Omega A \right) e^{i\hat{t}} + c.c.$$

Need to avoid secular terms  $\Rightarrow$  require

$$\frac{d}{dT} A = -\beta A + i\Omega A \quad (9)$$

then no secular terms arise that would grow linearly in time.

The solution of the amplitude equation (9) is given by

$$A = \mathcal{A} e^{-\beta T + i\Omega T}$$

$$x_0 = \mathcal{A} e^{-\beta T} e^{i\hat{t} + i\Omega T} + c.c. = \mathcal{A} e^{-\epsilon \beta t} e^{i(1 + \epsilon \Omega)t} + c.c.$$

**Thus:**

- Two-timing (multiple scales) avoids secular terms and gets frequency shift and slow damping correct to the order considered : no secular growth.
- Key is that in the expansion in  $\epsilon$  the amplitude function  $A(\epsilon t)$  is not expanded with respect to its argument, although it contains  $\epsilon$ . This is avoided by introducing the additional slow time  $T = \epsilon t$  and writing  $A = A(T)$ .
- The calculation is easier using complex exponentials than using trig functions.

<sup>40</sup>Use the shorthand notation  $\partial_T x$  for  $\frac{\partial x}{\partial T}$ , etc.

**Example:** Nonlinear Duffing oscillator

$$\ddot{x} + x + x^3 = 0.$$

How to deal with the nonlinear term? Consider instead the inhomogeneous equation

$$\ddot{x} + x = e^{i\omega t}.$$

This inhomogeneous equation is easily solved. If we could consider  $x^3$  as a small perturbation,

$$\ddot{x} + x = -\epsilon x^3,$$

we could expand

$$x = x_0 + \epsilon x_1 + \dots$$

We would get at  $\mathcal{O}(\epsilon^0)$

$$\ddot{x}_0 + x_0 = 0,$$

i.e.

$$x_0 = A e^{it} + A^* e^{-it}.$$

At  $\mathcal{O}(\epsilon)$  we would obtain an inhomogeneous equation for  $x_1$ ,

$$\begin{aligned}\ddot{x}_1 + x_1 &= -x_0^3 = - (A e^{it} + A^* e^{-it})^3 \\ &= -A^3 e^{3it} - 3|A|^2 A e^{it} - 3|A|^2 A^* e^{-it} - A^{*3} e^{-3it}.\end{aligned}$$

Now, the inhomogeneous term  $e^{3it}$  is easily taken care of, but the term with  $e^{it}$  generates again secular terms. Therefore introduce again a slow time variable  $T$  and allow  $x$  to depend on  $\hat{t}$  and  $T$  independently. Thus, we make the Ansatz:

$$\begin{aligned}x &= x_0(\hat{t}, T) + \epsilon x_1(\hat{t}, T) + \dots \\ \left( \frac{d}{dt} \right)^2 &\rightarrow \partial_{\hat{t}}^2 + 2\epsilon \partial_{\hat{t}} \partial_T + O(\epsilon^2)\end{aligned}$$

$\mathcal{O}(\epsilon^0)$ :

$$\partial_{\hat{t}}^2 x_0 + x_0 = 0 \quad x_0 = A e^{i\hat{t}} + A^* e^{-i\hat{t}}$$

with  $A = A(T)$ .

$\mathcal{O}(\epsilon^1)$ :

$$\partial_{\hat{t}}^2 x_1 + x_1 + \underbrace{2\partial_{\hat{t}} \partial_T x_0}_{2i \frac{dA}{dT} e^{i\hat{t}} + c.c.} = -\underbrace{x_0^3}_{A^3 e^{3i\hat{t}} + 3|A|^2 A e^{i\hat{t}} + 3|A|^2 A^* e^{-i\hat{t}} + A^{*3} e^{-3i\hat{t}}}$$

thus

$$\frac{\partial^2}{\partial \hat{t}^2} x_1 + x_1 = -\underbrace{e^{i\hat{t}}}_{\text{secular resonance term}} \left\{ 2i \frac{dA}{dT} + 3|A|^2 A \right\} - e^{3i\hat{t}} A^3 + c.c.$$

To avoid the secular term we require

$$\frac{dA}{dT} = +\frac{3}{2}i|A|^2A \quad (10)$$

There is no issue with the term  $A^3e^{i3\hat{T}}$ : use undetermined coefficient

$$x_1 = Be^{3i\hat{T}} + B^*e^{-3i\hat{T}}$$

and insert

$$-9Be^{3i\hat{T}} + Be^{3i\hat{T}} + c.c. = A^3e^{3i\hat{T}} + c.c.$$

to obtain

$$B = -\frac{1}{8}A^3$$

and

$$x_1 = -\frac{1}{8}A^3e^{3i\hat{T}} + c.c.$$

**Note:**

- The equation for  $A(T)$  is also nonlinear.
- It is a first-order equation. But it is complex, i.e. it is still effectively second order. So, what is gained?
- The equation has a special form that make the solution easier.

Separate into amplitude and phase

$$A(T) = R(T)e^{i\phi(T)}$$

$$\frac{d}{dT}R + iR\frac{d}{dT}\phi = \frac{3}{2}iR^3$$

Separating into real and imaginary part yields

$$\frac{dR}{dT} = 0 \quad \frac{d\phi}{dT} = \frac{3}{2}R^2.$$

Thus, the amplitude decouples from the phase

$$\phi = \frac{3}{2}R^2T$$

and

$$A = Re^{i\frac{3}{2}iR^2T}$$

Putting everything together we get

$$x = R e^{i(1+\frac{3}{2}\epsilon R^2)t} - \epsilon \frac{1}{8} \left( R e^{i(1+\frac{3}{2}\epsilon R^2)t} \right)^3 + c.c. + \mathcal{O}(\epsilon^2)$$

**Notes:**

- The nonlinearity induces a frequency shift:  $\omega = 1 + \frac{3}{2}\epsilon R^2$

→ soft and hard spring ( $\epsilon < 0$ )

$$\ddot{x} + (1 + \epsilon x^2)x = 0$$

- At order  $\mathcal{O}(\epsilon^2)$  additional frequency shifts arise from secular terms in  $x_0^2 x_1$   
⇒ approximate and exact solution get out of sync for  $t \sim \mathcal{O}(\epsilon^{-2})$ :

$$\cos((\omega + \epsilon\omega_1 + \underbrace{\epsilon^2\omega_2}_{\epsilon^2\omega_2 t \sim 2\pi} t) )$$

$$t = \mathcal{O}(\frac{1}{\epsilon^2})$$

⇒ introduce additional slow time  $\epsilon^2 t$

- To get a good solution at leading order ( $\mathcal{O}(\epsilon^0)$ ) we needed to make sure that the  $\mathcal{O}(\epsilon)$ -term does not grow forever. Beyond that one is often not very interested in the specific form of the  $\mathcal{O}(\epsilon)$ -term.
- Two-timing is also very useful near bifurcations, where one time scale becomes very slow.

### 3.5.3 Hopf Bifurcation<sup>41</sup>

For complex eigenvalues we get stable or unstable spiral points: what kind of bifurcation does the transition represent?

Consider the example

$$\dot{x} = \mu x - y - x^3 \tag{11}$$

$$\dot{y} = x + \mu y \tag{12}$$

Linear stability of the fixed point  $(0, 0)$  yields the Jacobian

$$\begin{pmatrix} \mu & -1 \\ 1 & \mu \end{pmatrix} \Rightarrow \lambda = \mu \pm i$$

The eigenvectors at the bifurcation point are given by

$$\begin{pmatrix} 0 & -1 \\ 1 & 0 \end{pmatrix} \begin{pmatrix} x_0 \\ y_0 \end{pmatrix} = \pm i \begin{pmatrix} x_0 \\ y_0 \end{pmatrix} \quad y_0 = \mp ix_0 \quad \mathbf{v} = \begin{pmatrix} 1 \\ \mp i \end{pmatrix}$$

In the Duffing oscillator we assumed the nonlinear term is small:  $\ddot{x} + x = -\epsilon x^3$  with  $\epsilon \ll 1$ . Here we assume the nonlinear term is small because  $|x|, |y| \ll 1$ . Under what conditions are  $x$  and  $y$  small?

At  $\mu = 0$  the stable spiral turns into an unstable spiral and for small  $\mu > 0$  the growth rate of the spiral is small: we may expect the spiral to saturate to a periodic orbit that has a

---

<sup>41</sup>Strogatz Ch. 8.2

small amplitude. We therefore want to determine an approximation for this periodic orbit near the bifurcation point where the stability of the fixed point changes, i.e. for  $|\mu| \ll 1$ , i.e. for small growth or decay rate.

We therefore write

$$\mu = \epsilon^2 \mu_2 \quad \epsilon \ll 1.$$

A small growth rate means growth on a slow time scale: therefore we introduce a slow time via

$$T = \epsilon^2 t.$$

Expand now

$$\begin{pmatrix} x \\ y \end{pmatrix} = \epsilon \begin{pmatrix} x_1(\hat{t}, T) \\ y_1(\hat{t}, T) \end{pmatrix} + \epsilon^2 \begin{pmatrix} x_2(\hat{t}, T) \\ y_2(\hat{t}, T) \end{pmatrix} + \epsilon^3 \begin{pmatrix} x_3(\hat{t}, T) \\ y_3(\hat{t}, T) \end{pmatrix} + c.c.$$

Again we have

$$\frac{d}{dt} x(\hat{t}, T) = \frac{\partial}{\partial \hat{t}} x(\hat{t}, T) + \epsilon^2 \frac{\partial}{\partial T} x(\hat{t}, T)$$

### Notes:

- At this point the scaling of  $x = \mathcal{O}(\epsilon)$  and  $y = \mathcal{O}(\epsilon)$  is a guess:
  - Since the periodic orbit just came into existence we may assume that it is small; but this does not have to be the case.
  - We do not know at this point how to scale  $x$  and  $y$  relative to  $\mu$ . In general:  $x = \epsilon^\alpha$  with  $\alpha$  not known yet. Therefore we are making a guess for  $\alpha$  right now. Once we understand the structure of the problem, we will know before hand how to choose  $\alpha$ . Often symmetries can be exploited.

Insert and collect powers of  $\epsilon$ :

$\mathcal{O}(\epsilon)$ :

$$\begin{aligned} \frac{\partial}{\partial \hat{t}} x_1 &= -y_1 \\ \frac{\partial}{\partial \hat{t}} y_1 &= x_1 \end{aligned}$$

This recovers the linearization at the bifurcation point  $\mu = 0$ . From the linearization we know

$$\begin{pmatrix} x_1 \\ y_1 \end{pmatrix} = A(T) e^{i\hat{t}} \underbrace{\begin{pmatrix} 1 \\ -i \end{pmatrix}}_{\text{eigenvector}} + \underbrace{A(T)^* e^{-i\hat{t}} \begin{pmatrix} 1 \\ +i \end{pmatrix}}_{\text{C.C.}}$$

with  $A(T)$  yet undetermined. Our main goal is to determine an equation for  $A(T)$ .

$\mathcal{O}(\epsilon^2)$ :

$$\begin{aligned}\frac{d}{dt}x_2 + y_2 &= 0 \\ \frac{d}{dt}y_2 - x_2 &= 0\end{aligned}$$

A solution at this order is

$$\begin{pmatrix} x_2 \\ y_2 \end{pmatrix} = \begin{pmatrix} 0 \\ 0 \end{pmatrix}$$

**Note:**

- one could keep a homogeneous solution

$$\begin{pmatrix} x_2(\hat{t}, T) \\ y_2(\hat{t}, T) \end{pmatrix} = A_1(T) e^{i\hat{t}} \begin{pmatrix} 1 \\ -i \end{pmatrix} + c.c.,$$

but this is not needed if we only want to determine the amplitude  $A(T)$ .

$\mathcal{O}(\epsilon^3)$ :

$$\begin{aligned}\partial_{\hat{t}}x_3 + y_3 &= -\partial_T x_1 + \mu_2 x_1 - x_1^3 \\ \partial_{\hat{t}}y_3 - x_3 &= -\partial_T y_1 + \mu_2 y_1\end{aligned}$$

With

$$x_1^3 = A^3 e^{3i\hat{t}} + 3|A|^2 A e^{i\hat{t}} + 3|A|^2 A^* e^{-i\hat{t}} + A^{*3} e^{-3i\hat{t}}$$

we can write this as

$$\partial_{\hat{t}}x_3 + y_3 = I_{11}e^{i\hat{t}} + I_{13}e^{3i\hat{t}} + c.c. \quad (13)$$

$$\partial_{\hat{t}}y_3 - x_3 = I_{21}e^{i\hat{t}} + I_{23}e^{3i\hat{t}} + c.c. \quad (14)$$

with

$$I_{11} = -\frac{dA}{dT} + \mu_2 A - 3|A|^2 A \quad I_{21} = -(-i)\frac{dA}{dT} + \mu_2(-i)A.$$

**Note:**

- Given our experience with secular terms arising from the inhomogeneities  $I_{11}e^{i\hat{t}}$  and  $I_{21}e^{i\hat{t}}$  we could be tempted to conclude now that we need to require that both  $I_{11}$  and  $I_{21}$  vanish. However, this would amount to two different differential equations for  $A$ , which cannot be satisfied at the same time. What is going on?

Ansatz with undetermined coefficients

$$\begin{pmatrix} x_3 \\ y_3 \end{pmatrix} = \begin{pmatrix} B_1 \\ B_2 \end{pmatrix} e^{i\hat{t}} + \begin{pmatrix} C_1 \\ C_2 \end{pmatrix} e^{3i\hat{t}} + c.c. \quad (15)$$

Since the different Fourier modes  $e^{i\hat{t}}$  and  $e^{3i\hat{t}}$  are linearly independent we can separate the equations into equations involving the terms  $\propto e^{i\hat{t}}$  and those involving  $e^{3i\hat{t}}$ .

The terms  $e^{it}$  lead to the matrix equation

$$\begin{pmatrix} i & 1 \\ -1 & i \end{pmatrix} \begin{pmatrix} B_1 \\ B_2 \end{pmatrix} = \begin{pmatrix} I_{11} \\ I_{21} \end{pmatrix}. \quad (16)$$

Try to solve for  $B_{1,2}$

$$iB_1 + B_2 = I_{11} \quad \Rightarrow \quad B_2 = I_{11} - iB_1$$

insert it into the second equation,

$$-B_1 + i(I_{11} - iB_1) = I_{21}$$

This equation has only a solution if

$$iI_{11} = I_{21}. \quad (17)$$

Thus, we find that a *single solvability condition* has to be satisfied to eliminate the secular growth.

If the solvability condition is satisfied, there are infinitely many solutions since  $B_1$  is arbitrary and  $B_2 = I_{11} - iB_1$ .

**Note:**

- Mathematically, this solvability condition is a consequence of the Fredholm Alternative Theorem of linear algebra (see below).

In our case the solvability condition (17) amounts to

$$i \left( -\frac{dA}{dT} + \mu_2 A - 3|A|^2 A \right) = -\frac{dA}{dT}(-i) + \mu_2 A(-i)$$

Thus

$$\frac{dA}{dT} = \mu_2 A - \frac{3}{2}|A|^2 A \quad (18)$$

Look for simple solutions: rewrite again using magnitude and phase

$$A(T) = R(T)e^{i\phi(T)}$$

$$\frac{dR}{dT} = \mu_2 R - \frac{3}{2}R^3 \quad (19)$$

$$\frac{d\phi}{dT} = 0 \quad (20)$$

Steady state,  $\frac{dR}{dT} = 0$ ,

$$R_0 = \sqrt{\frac{2\mu_2}{3}} \quad A = R_0 e^{i\phi_0} \quad \text{with } \phi_0 \text{ arbitrary}$$

Bifurcation diagrams:

**Notes:**

- Thus, we found a periodic orbit arising from the Hopf bifurcation, which amounts to an oscillation with an amplitude that goes to 0 at the bifurcation point.
- In this case the coefficients in (18) turned out to be real. In general they are complex: The **normal form** for the Hopf bifurcation and also for weakly nonlinear oscillators is given by

$$\frac{dA}{dT} = (\mu + i\Omega) A + (\gamma_r + i\gamma_i) |A|^2 A.$$

(cf. (10) for the Duffing oscillator, where  $\gamma_r = 0$  and  $\gamma_i = \frac{3}{2}$ .)

- Solutions exist for any phase  $\phi_0$ : there is a continuous family of solutions.
- The determinant of the linearization around the fixed point  $(0, 0)$  does not vanish  $\Rightarrow$  in agreement with the implicit function theorem the number of fixed points does not change in a Hopf bifurcation.
- At the Hopf bifurcation the fixed point is not hyperbolic: the real part of the eigenvalue vanishes. The Hartman-Grobman theorem does not apply: at  $\mu = 0$  the solution is not a center but a decaying spiral since  $R \rightarrow 0$  (cf. (19)).
- The equation (19) for the magnitude  $R$  looks like the equation for a pitchfork bifurcation. Why? Is there a reflection symmetry in  $R$ ? The phase  $\phi_0$  is arbitrary  $\Rightarrow$  if  $Re^{i\phi_0}$  is a solution then  $Re^{i\phi_0+i\pi}$  is also a solution. But  $Re^{i\phi_0+i\pi} = -Re^{i\phi_0}$ . Therefore  $-R$  must also be a solution of the equation for  $R$ , i.e. the equation for  $R$  must have the reflection symmetry  $R \rightarrow -R$ .

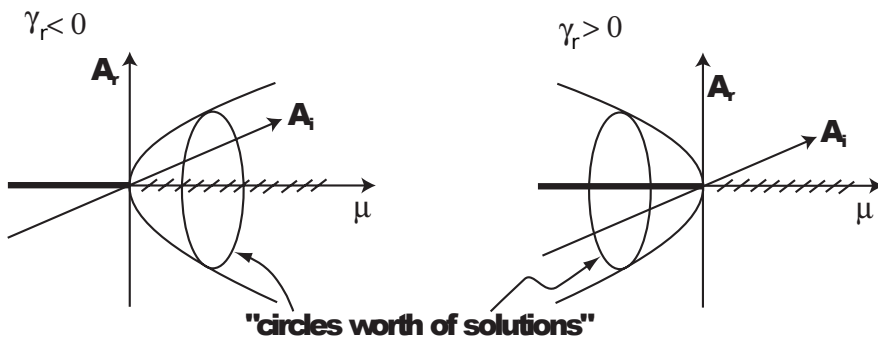


Figure 30: Supercritical (left) and subcritical (right) Hopf bifurcation leading to a stable/unstable periodic orbit.

Why is there only a single solvability condition although there are 2 equations and in each of the equations appear Fourier terms  $e^{it}$ , which can drive secular terms? This is best understood by looking at the problem as a linear algebra problem and recognizing that the condition we derived is a result of the Fredholm Alternative Theorem.

### Fredholm Alternative Theorem

Consider

$$\mathbf{Mx} = \mathbf{b}. \quad (21)$$

If  $\det \mathbf{M} = 0$  the matrix  $\mathbf{M}$  cannot be inverted and the equation may or not have a solution. Moreover,  $\mathbf{M}$  has a 0 eigenvalue with an associated eigenvector  $\mathbf{v}$ ,

$$\mathbf{M}\mathbf{v} = 0.$$

There is also a left (row) eigenvector  $\mathbf{v}_l^t$ ,

$$\mathbf{v}_l^t \mathbf{M} = 0.$$

Therefore, if we multiply the equation from the left with  $\mathbf{v}_l^t$  we get

$$\mathbf{v}_l^t \mathbf{M} \mathbf{x} = 0 = \mathbf{v}_l^t \mathbf{b}$$

and any  $\mathbf{b}$  that satisfies  $\mathbf{M}\mathbf{x} = \mathbf{b}$  has to satisfy

$$\mathbf{v}_l^t \mathbf{b} = 0.$$

Thus, the Fredholm Alternative Theorem states that if  $\det \mathbf{M} = 0$ , then either of the following statements hold

- $\mathbf{v}_l^t \mathbf{b} = 0$ . Then (21) has infinitely many solutions, corresponding to the arbitrariness of  $B_1$  in our calculation above.
- $\mathbf{v}_l^t \mathbf{b} \neq 0$ . Then (21) has no solution.

To make the connection with our case, consider again the matrix equation (16) for which we have

$$\mathbf{M} = \begin{pmatrix} i & 1 \\ -1 & i \end{pmatrix}$$

Calculate the eigenvalues of  $\mathbf{M}$

$$(i - \lambda)^2 + 1 = 0 \quad \Rightarrow \quad \lambda_1 = 0 \quad \lambda_2 = 2i$$

We need the left eigenvector for the eigenvalue  $\lambda_1$

$$(u^+, v^+) \begin{pmatrix} i & 1 \\ -1 & i \end{pmatrix} = (0, 0)$$

i.e.

$$u^+i - v^+ = 0 \quad v^+ = iu^+$$

In order to be able to solve equation (16) the condition

$$(u^+, v^+) \begin{pmatrix} I_{11} \\ I_{21} \end{pmatrix} = 0$$

has to be satisfied

$$u^+I_{11} + iu^+I_{21} = 0$$

which recovers the solvability condition (17) that we obtained earlier.

**Note:**

- The Fredholm Alternative Theorem shows that we get only a single solvability condition if  $M$  has only a single vanishing eigenvalue. This is the case even though (13,14) look as if one had to impose 2 conditions in order to avoid the secular terms.

Summarizing, to see the whole structure:

We started with

$$\begin{pmatrix} \frac{dx}{dt} \\ \frac{dy}{dt} \end{pmatrix} = \underbrace{\begin{pmatrix} \mu & -1 \\ 1 & \mu \end{pmatrix}}_{\text{linear term: matrix } L} \begin{pmatrix} x \\ y \end{pmatrix} + \underbrace{\begin{pmatrix} -x^3 \\ 0 \end{pmatrix}}_{\text{nonlinearity}}$$

We introduced a slow time  $T = \epsilon^2 t$  and expanded the bifurcation parameter  $\mu$  around the value at the Hopf bifurcation,  $\mu = \mu_{hopf} + \epsilon^2 \mu_2$ . In our example it turns out that  $\mu_{hopf} = 0$ .

Rearranging the terms we get

$$\begin{pmatrix} \frac{dx}{dt} \\ \frac{dy}{dt} \end{pmatrix} - \underbrace{\begin{pmatrix} \mu_{hopf} & -1 \\ 1 & \mu_{hopf} \end{pmatrix}}_{\text{matrix } L_0} \begin{pmatrix} x \\ y \end{pmatrix} = \epsilon^2 \underbrace{\begin{pmatrix} \mu_2 & 0 \\ 0 & \mu_2 \end{pmatrix}}_{\text{matrix } L_2} \begin{pmatrix} x \\ y \end{pmatrix} - \epsilon^2 \begin{pmatrix} \frac{dx}{dT} \\ \frac{dy}{dT} \end{pmatrix} + \begin{pmatrix} -x^3 \\ 0 \end{pmatrix} \quad (22)$$

We now expand  $x = \epsilon x_1 + \epsilon^2 x_2 \dots$  and  $y = \epsilon y_1 + \epsilon^2 y_2 \dots$ . All terms on the r.h.s. are then  $\mathcal{O}(\epsilon^3)$ .

Sorting by powers of  $\epsilon$  we get therefore 3 problems:

$\mathcal{O}(\epsilon)$ :

$$\begin{pmatrix} \frac{dx_1}{dt} \\ \frac{dy_1}{dt} \end{pmatrix} - L_0 \begin{pmatrix} x_1 \\ y_1 \end{pmatrix} = 0 \quad (23)$$

This equation is the same equation as that of the linear stability analysis. It yielded the eigenvalues  $\lambda_{1,2} = \pm i\omega$  (in our case  $\omega = 1$ ) and eigenvectors  $\begin{pmatrix} u \\ v \end{pmatrix}$  and  $\begin{pmatrix} u^* \\ v^* \end{pmatrix}$ . The homogeneous solution was then

$$\begin{pmatrix} x_1 \\ y_1 \end{pmatrix} = A(T) e^{it} \begin{pmatrix} u \\ v \end{pmatrix} + c.c.$$

$\mathcal{O}(\epsilon^2)$ :

$$\begin{pmatrix} \frac{dx_2}{dt} \\ \frac{dy_2}{dt} \end{pmatrix} - L_0 \begin{pmatrix} x_2 \\ y_2 \end{pmatrix} = 0.$$

**Note:**

- At order  $\epsilon^2$  the left-hand side has the same form as (23). This will be the case at all orders.

Since there are no inhomogeneous terms it has the solution

$$\begin{pmatrix} x_2 \\ y_2 \end{pmatrix} = \begin{pmatrix} 0 \\ 0 \end{pmatrix}.$$

$\mathcal{O}(\epsilon^3)$

$$\begin{pmatrix} \frac{dx_3}{dt} \\ \frac{dy_3}{dt} \end{pmatrix} - \mathbf{L}_0 \begin{pmatrix} x_3 \\ y_3 \end{pmatrix} = \mathbf{L}_2 \begin{pmatrix} x_1 \\ y_1 \end{pmatrix} - \begin{pmatrix} \frac{dx_1}{dT} \\ \frac{dy_1}{dT} \end{pmatrix} + \underbrace{\begin{pmatrix} -x_1^3 \\ 0 \end{pmatrix}}_{\dots e^{i\hat{t}} + \dots e^{3i\hat{t}} + \dots} = \begin{pmatrix} I_{11} \\ I_{21} \end{pmatrix} e^{i\hat{t}} + \begin{pmatrix} I_{13} \\ I_{23} \end{pmatrix} e^{3i\hat{t}} + c.c.$$

Using undetermined coefficients

$$\begin{pmatrix} x_3 \\ y_3 \end{pmatrix} = \begin{pmatrix} B_1 \\ B_2 \end{pmatrix} e^{i\hat{t}} + \begin{pmatrix} C_1 \\ C_2 \end{pmatrix} e^{3i\hat{t}} + c.c.$$

the terms containing  $e^{i\hat{t}}$  are then given by

$$\begin{pmatrix} iB_1 \\ iB_2 \end{pmatrix} - \mathbf{L}_0 \begin{pmatrix} B_1 \\ B_2 \end{pmatrix} = \underbrace{\left( \begin{pmatrix} i & 0 \\ 0 & i \end{pmatrix} - \mathbf{L}_0 \right)}_{\mathbf{M} \equiv \begin{pmatrix} i & 1 \\ -1 & i \end{pmatrix}} \begin{pmatrix} B_1 \\ B_2 \end{pmatrix} = \begin{pmatrix} I_{11} \\ I_{21} \end{pmatrix} \quad (24)$$

The resulting  $\mathbf{M}$  is exactly the same  $\mathbf{M}$  as that in the linear stability analysis and in (23). Therefore  $\mathbf{M}$  will always be singular<sup>42</sup> and satisfy  $\det \mathbf{M} = 0$ . Therefore it has a left (row) eigenvector with eigenvalue 0,

$$(u^+, v^+) \begin{pmatrix} i & 1 \\ -1 & i \end{pmatrix} = 0 \quad \Rightarrow \quad iu^+ = v^+,$$

and we get the solvability condition

$$(u^+, v^+) \begin{pmatrix} I_{11} \\ I_{21} \end{pmatrix} = 0.$$

**Note:**

- The same structure arises when considering other bifurcations in systems of equations, rather than single differential equations.

### 3.6 1d-Bifurcations in 2d: Reduction of Dynamics

Higher-dimensional systems can undergo the same bifurcations as 1-dimensional systems.

⇒ can reduce dynamics to 1 dimension near the bifurcation.

---

<sup>42</sup>This is the reason this kind of perturbation calculation is called singular.

### 3.6.1 Center-Manifold Theorem

Consider first a linear example: stable node

$$\begin{pmatrix} \dot{x} \\ \dot{y} \end{pmatrix} = \begin{pmatrix} \mu & 0 \\ 0 & -1 \end{pmatrix} \begin{pmatrix} x \\ y \end{pmatrix}$$

thus

$$\begin{aligned} \lambda_1 &= \mu & \mathbf{v}_1 &= \begin{pmatrix} 1 \\ 0 \end{pmatrix} \\ \lambda_2 &= -1 & \mathbf{v}_2 &= \begin{pmatrix} 0 \\ 1 \end{pmatrix} \end{aligned}$$

Obtain trajectories by eliminating time from the solution,

$$\begin{pmatrix} x(t) \\ y(t) \end{pmatrix} = x_0 \begin{pmatrix} 1 \\ 0 \end{pmatrix} e^{\mu t} + y_0 \begin{pmatrix} 0 \\ 1 \end{pmatrix} e^{-t} \quad \Rightarrow \quad y = y_0 \left( \frac{x}{x_0} \right)^{-\frac{1}{\mu}}.$$

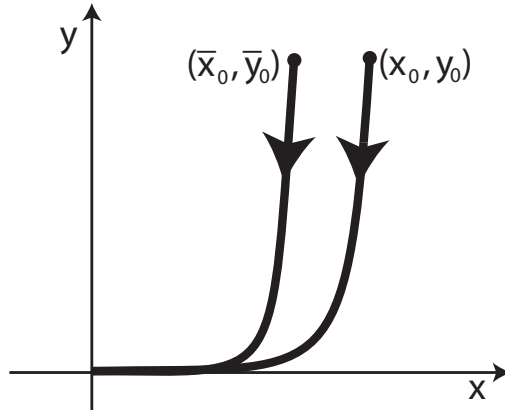


Figure 31: Phase plane for  $\mu < 0$  and  $|\mu| \ll 1$ .

For small  $|\mu|$

- for  $\mu < 0$ :  $y \rightarrow 0$  extremely rapidly as  $x \rightarrow 0$
- for  $\mu > 0$ :  $y \rightarrow 0$  extremely rapidly as  $x \rightarrow \infty$

**Thus:**

- After a short time *any* initial condition approaches the  $x$ -axis, which is in the direction of the eigenvector  $\mathbf{v}_1$  with  $|\lambda_1| \ll |\lambda_2|$ . Thereafter, the dynamics are essentially one-dimensional.

Can this also work for nonlinear systems? Add nonlinearities to our example<sup>43</sup>.

$$\dot{x} = \mu x + \alpha xy - \gamma x^3 \quad (25)$$

$$\dot{y} = -y + x^2 \quad (26)$$

If it was not for the term involving  $y$ , the equation for  $x$  would describe a supercritical pitch-fork bifurcation. What effect does  $y$  have?

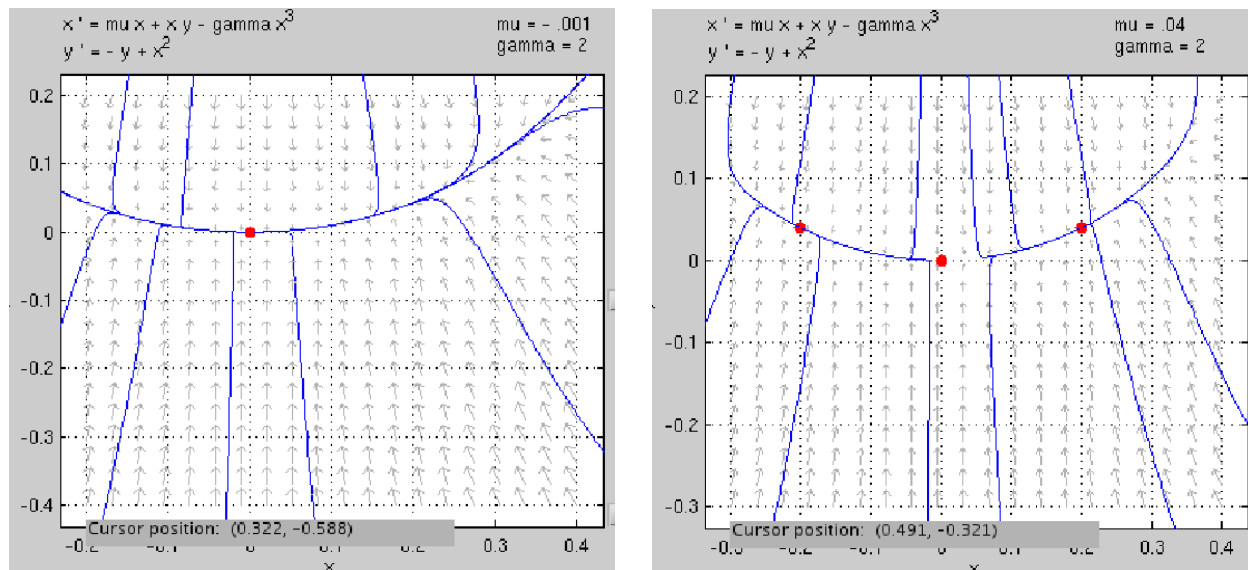


Figure 32: Phase plane for  $\mu = -0.001$  (single fixed point) and  $\mu = 0.04$  (3 fixed points) showing the slow manifold and the dynamics on it.

To discuss the dynamics we need to distinguish 3 types of eigenvectors and eigenspaces:

- the stable eigenspace, which is spanned by the eigenvectors with  $\text{Re}(\lambda_i^{(s)}) < 0$   
 $E^{(s)} = \{\underline{x} \mid \underline{x} = \sum \alpha_i \underline{v}_i^{(s)}, \text{Re}(\lambda_i^{(s)}) < 0\}$   
 that is the direction of rapid contraction
- center eigenspace:  $E^{(c)} = \{\underline{x} \mid \underline{x} = \sum \alpha_i \underline{v}_i^{(c)}\}, \text{Re}(\lambda_i^{(c)}) = 0\}$   
 slow dynamics
- unstable eigenspace:  $E^{(u)} = \{\underline{x} \mid \underline{x} = \sum \alpha_i \underline{v}_i^{(u)}, \text{Re}(\lambda_i^{(u)}) > 0\}$   
 rapid expansion

Eigenspaces of the linearization of  $(0, 0)$  in (25,26):

$\mu < 0 :$	$E^{(s)} = \mathbb{R}^2$	$E^{(c)}$ empty	$E^{(u)}$ empty
$\mu = 0 :$	$E^{(s)} = y\text{-axis}$	$E^{(c)} = x\text{-axis}$	$E^{(u)}$ empty
$\mu > 0 :$	$E^{(s)} = y\text{-axis}$	$E^{(c)}$ empty	$E^{(u)} = x\text{-axis}$

<sup>43</sup>Demo:  $\gamma = 2$ , window  $[-.4 .4 -.4 .4]$   $\mu = -0.1, -0.01, +0.1$ . find also unstable fixed point  $(0,0)$  and determine its stable/unstable manifold.

**Notes:**

- For small  $|\mu|$ :
  - rapid compression in the direction of the eigenvector corresponding to the stable eigenvalue: stable eigenspace.
  - all trajectories converge to a line ('manifold') that is **not** given by the eigenvector  $v_1$  corresponding to the small (vanishing) eigenvalue (center eigenspace), but that manifold is *tangent* to the center eigenspace.
  - a pitch-fork bifurcation occurs on the center manifold as  $\mu$  goes through 0.

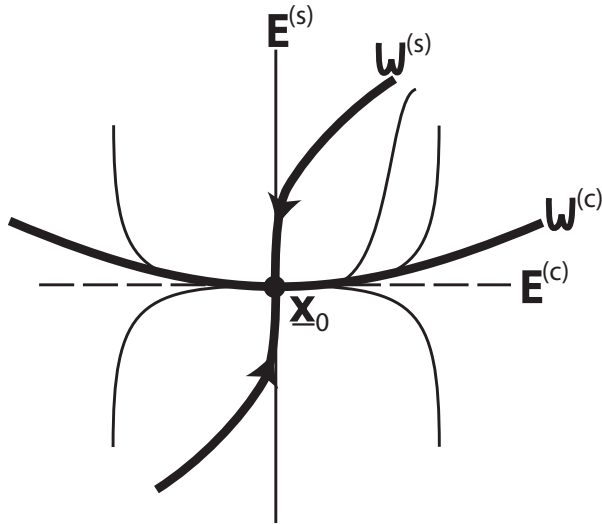
**Goal:**

- obtain a description of higher-dimensional system in terms of these *slow low-dimensional dynamics*

Extension to nonlinear systems:

**Center Manifold Theorem:**

- For a fixed point  $\underline{x}_0$  with eigenspaces  $E^{(s,u,c)}$  there exist stable, unstable, and center manifolds  $W^{(s,u,c)}$  such that  $W^{(s,u,c)}$  are tangent to  $E^{(s,u,c)}$  at  $\underline{x}_0$ , respectively.
- The manifolds  $W^{(s,u,c)}$  are invariant under the flow.  $W^{(s)}$  and  $W^{(u)}$  are unique.  $W^{(c)}$  need not be unique.

**Notes:**

- To get a mathematically justified separation of the fast decay of the initial transient and the slow evolution thereafter we need an *infinite* ratio between the respective time scales: we need a *center* manifold. On it the dynamics are *infinitely* slower than on the stable manifold.
- To have a center eigenspace and a center manifold we need to be at a bifurcation point.

### 3.6.2 Reduction to Dynamics on the Center Manifold

We exploit the separation of time scales between the stable manifold and the center manifold and use again multiple time scales.

We introduce a slow time  $T$ , which is associated with the slow evolution on the center manifold and which reflects the small growth rate stemming from the eigenvalue that has a vanishing real part at the bifurcation point.

**Example from before:**

$$\dot{x} = \mu x + xy - \gamma x^3 \quad (27)$$

$$\dot{y} = -y + \alpha x^2 \quad (28)$$

The eigenvalues of the linearization around the fixed point, which happens to be  $(0, 0)$ , are given by

$$\lambda_1 = \mu \quad \lambda_2 = -1.$$

The bifurcation occurs at  $\mu = 0$ . Near the bifurcation point  $\mu$  is small,

$$\mu = \epsilon^2 \mu_2 \quad T = \epsilon^2 t.$$

**Note:**

- The slow time scale is chosen to match the growth rate of the mode that destabilizes the fixed point,

$$e^{\lambda_1 t} = e^{\mu t} = e^{\mu_2 \epsilon^2 t} \xrightarrow[!]{\text{slow}} e^{\mu_2 T}.$$

Since the bifurcation is a steady bifurcation there is no fast time scale (which was associated with oscillations for the Hopf bifurcation):

$$x = x(T) \quad y = y(T) \quad \frac{d}{dt} = \epsilon^2 \frac{\partial}{\partial T}$$

Near the fixed point we can also expand  $x$  and  $y$

$$\begin{aligned} x &= \epsilon x_1 + \epsilon^2 x_2 + \epsilon^3 x_3 + \dots \\ y &= \epsilon y_1 + \epsilon^2 y_2 + \epsilon^3 y_3 + \dots \end{aligned}$$

**Note:**

- At this point the scaling of  $x$  and  $y$  is a guess based on previous experience.
- Without the  $y$  the system would undergo a pitchfork bifurcation, since the  $x$ -equation is odd in  $x$ . We would then expect an equation like

$$\dot{x} = \mu x - \gamma x^3 \quad \text{and} \quad x^2 \sim \mu$$

- Including also the  $y$ : Eqs.(27,28) are odd in  $x$  and even in  $y$ . Since the eigenvector associated with  $\lambda = \mu$  is in the  $x$ -direction one may expect a pitch-fork bifurcation due to the reflection symmetry. This provides guidance for the choice of the scaling of  $x, y$ .

Insert the expansion:

$\mathcal{O}(\epsilon)$ :

$$\begin{aligned} 0 &= 0 \\ 0 &= -y_1 \end{aligned}$$

thus:

$$y_1 = 0 \quad x_1 \text{ is still undetermined}$$

$\mathcal{O}(\epsilon^2)$ :

$$\begin{aligned} 0 &= x_1 y_1 \\ 0 &= -y_2 + \alpha x_1^2 \end{aligned}$$

thus:

$$y_2 = \alpha x_1^2$$

$\mathcal{O}(\epsilon^3)$ :

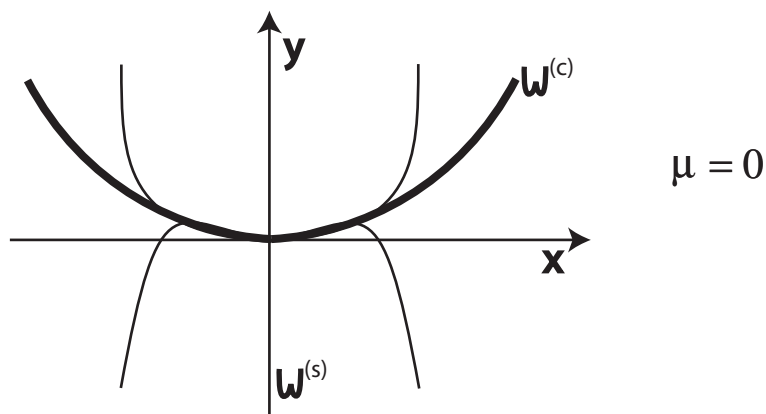
$$\begin{aligned} \frac{\partial x_1}{\partial T} &= \mu_2 x_1 + x_1 y_2 - \gamma x_1^3 \\ \frac{\partial y_1}{\partial T} &= -y_3 + 2\alpha x_1 x_2 \end{aligned}$$

Since  $y_1 = 0$ , we have

$$y_3 = 2\alpha x_1 x_2$$

and

$$\frac{\partial x_1}{\partial T} = \mu_2 x_1 + (\alpha - \gamma) x_1^3 \quad (29)$$



### Notes:

- The system undergoes a pitch-fork bifurcation at  $\mu = 0$ 
  - the bifurcation is supercritical for  $\alpha < \gamma$
  - the bifurcation is subcritical for  $\alpha > \gamma$

The  $y$ -variable can change the nonlinear dynamics qualitatively, although it is damped.

- The coefficient of the linear term  $\mu_2 x_1$  of the amplitude equation (29) is given by the growth rate  $\lambda_1$  of the relevant mode (to leading order)

$$x_1 \sim e^{\mu_2 T} = e^{\mu_2 \epsilon^2 t} = e^{\mu t} = e^{\lambda_1 t}$$

- The center manifold  $W^{(c)}$  is given to leading order in  $x$  by

$$\begin{aligned} y &= \epsilon y_1 + \epsilon^2 y_2 + \epsilon^3 y_3 + \dots \\ &= \epsilon^2 \alpha x_1^2 + 2\epsilon^3 \alpha x_1 x_2 + \dots \\ &= \alpha x^2 + \mathcal{O}(x^3). \end{aligned}$$

As expected, the center manifold is tangent to the center eigenspace spanned by  $\mathbf{v}_1 = (1, 0)$

In terms of the eigenvectors the solution can be written as

$$\begin{pmatrix} x \\ y \end{pmatrix} = \epsilon x_1(T) \underbrace{\begin{pmatrix} 1 \\ 0 \end{pmatrix}}_{\mathbf{v}_1} + \epsilon^2 \left\{ x_1^2(T) \underbrace{\begin{pmatrix} 0 \\ 1 \end{pmatrix}}_{\mathbf{v}_2} + x_2(T) \underbrace{\begin{pmatrix} 1 \\ 0 \end{pmatrix}}_{\mathbf{v}_1} \right\} + \mathcal{O}(\epsilon^3)$$

### Note:

- For a general problem

$$\dot{\mathbf{u}} = \mathbf{L}\mathbf{u} + \mathbf{N}(\mathbf{u}),$$

in which  $\mathbf{L}$  is a linear operator, i.e. a matrix, and  $\mathbf{N}$  contains all the nonlinear terms, one expands the solution efficiently as

$$\mathbf{u} = \epsilon A(T)\mathbf{v}_1 + \epsilon^2 \mathbf{u}_2(T) + \dots$$

where  $\mathbf{v}_1$  is the eigenvector for eigenvalue  $\lambda_1 = 0$  of  $\mathbf{L}$

$$\mathbf{L}\mathbf{v}_1 = 0.$$

### Example:

$$\begin{pmatrix} \dot{x} \\ \dot{y} \end{pmatrix} = \underbrace{\begin{pmatrix} 1 + \mu & -1 \\ 2 & -2 \end{pmatrix}}_{\mathbf{L}} \begin{pmatrix} x \\ y \end{pmatrix} + \begin{pmatrix} x^2 \\ 0 \end{pmatrix} \quad (30)$$

Linearization around the fixed point  $(0, 0)$ :

eigenvalues and eigenvectors of  $\mathbf{L}$

$$\text{trace}(\mathbf{L}) = -1 + \mu \quad \det(\mathbf{L}) = -2\mu$$

$$2\lambda_{1,2} = \text{trace}(\mathbf{L}) \pm \sqrt{\text{trace}(\mathbf{L})^2 - 4\det(\mathbf{L})}$$

Possible bifurcations:

- No Hopf bifurcation: it would require  $\mu = 1$  to make  $\text{trace}(\mathbf{L}) = 0$ , which makes  $\det(\mathbf{L})$  negative
- Steady bifurcation for  $\det(\mathbf{L}) = 0$ , i.e.  $\mu = 0$

$$\lambda_{1,2} = \frac{1}{2} \left( -1 + \mu \pm \sqrt{(-1 + \mu)^2 + 8\mu} \right) = \frac{1}{2} \left( -1 + \mu \pm \sqrt{1 + 6\mu + \mu^2} \right) = \begin{cases} 2\mu + \mathcal{O}(\mu^2) \\ -1 + \mathcal{O}(\mu) \end{cases}$$

Growth rate positive for  $\mu > 0$ .

Eigenvector  $\mathbf{v}_1$  at the bifurcation point  $\mu = 0$

$$\begin{pmatrix} 1 & -1 \\ 2 & -2 \end{pmatrix} \mathbf{v}_1 = 0 \quad \Rightarrow \quad \mathbf{v}_1 = \begin{pmatrix} 1 \\ 1 \end{pmatrix}$$

What kind of bifurcation should we expect?

- $(0, 0)$  is a fixed point for all values of  $\mu$
- no reflection symmetry due to the term  $x^2$

If this was a 1d-problem, we would therefore expect a transcritical bifurcation. It would be described by an equation of the form

$$\frac{dA}{dT} = a(\mu)A + bA^2$$

with  $a(\mu)$  corresponding to the growth rate of the relevant mode:  $a(\mu) \sim \lambda_1 \sim \mu$

For our expansion this suggests

$$A \sim a(\mu) \sim \mu$$

Expansion

$$\begin{pmatrix} x \\ y \end{pmatrix} = \epsilon A(T) \underbrace{\begin{pmatrix} 1 \\ 1 \end{pmatrix}}_{\mathbf{v}_1} + \epsilon^2 \begin{pmatrix} x_2 \\ y_2 \end{pmatrix} + \dots$$

with scaling

$$\mu = \epsilon \mu_1 \quad T = \epsilon t$$

Insert into (30)

$\mathcal{O}(\epsilon)$ :

$$\begin{pmatrix} 0 \\ 0 \end{pmatrix} = \underbrace{\begin{pmatrix} 1 & -1 \\ 2 & -2 \end{pmatrix}}_{\mathbf{L}_0} A(T) \mathbf{v}_1$$

At this order  $A(T)$  is still undetermined

$\mathcal{O}(\epsilon^2)$ :

$$\underbrace{-\begin{pmatrix} 1 & -1 \\ 2 & -2 \end{pmatrix}}_{\mathbf{L}_0} \begin{pmatrix} x_2 \\ y_2 \end{pmatrix} = -\frac{dA}{dT} \mathbf{v}_1 + \begin{pmatrix} \mu_1 x_1 \\ 0 \end{pmatrix} + \begin{pmatrix} x_1^2 \\ 0 \end{pmatrix}$$

We could now again start solving for  $x_2$  and  $y_2$ . We expect that a solvability condition will arise.

The solvability condition can be obtained more directly without solving for  $x_2$  and  $y_2$ . The matrix  $\mathbf{L}$  has also a left zero-eigenvector  $\mathbf{v}^+$  (row eigenvector rather than column eigenvector)

$$\left( \begin{array}{c} x_0^+, \quad y_0^+ \end{array} \right) \left( \begin{array}{cc} 1 & -1 \\ 2 & -2 \end{array} \right) = 0 \quad \Rightarrow \quad \mathbf{v}_1^+ = \left( \begin{array}{c} x_0^+, \quad y_0^+ \end{array} \right) = \left( \begin{array}{c} 2, \quad -1 \end{array} \right)$$

### Note:

- the left eigenvector  $\mathbf{v}_1^+$  is not the transpose of the right eigenvector  $\mathbf{v}_1^t$
- if the matrix is symmetric then  $\mathbf{v}^+ = \mathbf{v}^t$

Multiply the equation at  $\mathcal{O}(\epsilon^2)$  by  $\mathbf{v}_1^+ = \left( \begin{array}{c} x_0^+, \quad y_0^+ \end{array} \right)$

LHS:

$$-\left( \begin{array}{c} x_0^+, \quad y_0^+ \end{array} \right) \left( \begin{array}{cc} 1 & -1 \\ 2 & -2 \end{array} \right) \left( \begin{array}{c} x_2 \\ y_2 \end{array} \right) = 0$$

for any  $x_2$  and  $y_2$ .

Thus, RHS yields

$$\left( \begin{array}{c} x_0^+, \quad y_0^+ \end{array} \right) \left\{ -\frac{dA}{dT} \mathbf{v}_1 + \left( \begin{array}{c} \mu_1 x_1 \\ 0 \end{array} \right) + \left( \begin{array}{c} x_1^2 \\ 0 \end{array} \right) \right\} = 0 \quad (31)$$

$$-\frac{dA}{dT} \left( \begin{array}{c} 2, \quad -1 \end{array} \right) \left( \begin{array}{c} 1 \\ 1 \end{array} \right) + 2 [\mu_1 x_1 + x_1^2] = 0$$

with  $x_1 = A$

$$\frac{dA}{dT} = 2\mu_1 A + 2A^2$$

### Note:

- This reduction to the center manifold works for systems of arbitrary dimension.
- If the linearization has multiple 0 eigenvalues the center manifold has as many dimensions as there are vanishing eigenvalues and one obtains as many solvability conditions.

### Formally:

Consider the system

$$\dot{\mathbf{u}} = \mathbf{L}\mathbf{u} + \mathbf{N}(\mathbf{u})$$

where  $\mathbf{L}$  is a linear operator, i.e. a matrix, and  $\mathbf{N}$  contains all the nonlinear terms.

Analogous to Hopf: expand for small amplitudes  $A$  in the ‘direction’ of the critical eigenvector  $\mathbf{v}_1$  of the linearized operator  $\mathbf{L}_0$

$$\mathbf{L}_0 \mathbf{v}_1 = 0$$

Expand the  $\mathbf{u}$

$$\mathbf{u} = \epsilon^\beta A(T) \mathbf{v}_1 + \epsilon^{2\beta} \mathbf{u}_2(T) + \dots$$

Introduce a slow time

$$T = \epsilon^\alpha t$$

and expand the control parameter

$$\mu = \mu_0 + \epsilon^\gamma \mu_\gamma$$

Since the control parameter variation should appear at the same order as the solvability condition, which in turn should include the slow time derivative one typically has  $\gamma = \alpha$ .

Since  $\mathbf{L}$  is singular, i.e. the homogeneous linear equation has a non-trivial solution, the higher-order equations can only be solved if a solvability condition is satisfied. This solvability condition can be seen to arise since  $\mathbf{L}$  also has a left-eigenvector with vanishing eigenvalue

$$\mathbf{v}^+ \mathbf{L} = 0$$

Thus at higher orders one has

$$\mathcal{O}(\epsilon^{2\beta}) :$$

$$-\mathbf{L}_0 \mathbf{u}_2 = \mathbf{L}_1 \mathbf{u}_1 + \mathbf{N}_2(\mathbf{u}_1)$$

where  $\mathbf{L}_1 \mathbf{u}_1$  contains terms from expanding the control parameter in  $\epsilon$  and also from the slow time derivative. Multiply this equation from the left with  $\mathbf{v}^+$  to obtain the condition

$$0 = -\mathbf{v}^+ \mathbf{L}_0 \mathbf{u}_2 = \mathbf{v}^+ \{\mathbf{L}_1 \mathbf{u}_1 + \mathbf{N}_2(\mathbf{u}_1)\}$$

### 3.6.3 Reduction to Center Manifold without Multiple Scales

Revisit (27,28)

$$\begin{aligned} \dot{x} &= \mu x + xy - \gamma x^3 \\ \dot{y} &= -y + \alpha x^2. \end{aligned}$$

Using multiple time-scales we reduced the dynamics to that on a slow manifold that corresponds to the center manifold  $W^{(c)}$  at the bifurcation point, i.e. for  $\mu = 0$ . On the center manifold we can derive these dynamics without introducing a slow time scale. For  $W^{(c)}$  to exist need to be at the bifurcation point:  $\mu = 0$

$$E^{(c)} = \{(x, 0)\}, \quad E^{(s)} = \{(0, y)\}$$

$\Rightarrow$  on the center manifold  $y$  is directly given by  $x$ ,

$$y = h(x).$$

Insert this relation into the differential equations

$$\dot{y} = \frac{dh}{dx}\dot{x} = \frac{dh}{dx}(xy - \gamma x^3) \xrightarrow{!} -y + x^2 = -h(x) + x^2.$$

**Thus:**

- This defines a nonlinear differential equation for  $h(x)$ .
- From the center manifold theorem we know  $W^{(c)}$  is *tangent* to  $E^{(c)}$   $\Rightarrow h(x)$  is strictly nonlinear.
- We are aiming for a local analysis  $\Rightarrow$  expand  $h(x)$  for small  $x$

Expansion

$$h = h_2 x^2 + h_3 x^3 + h_4 x^4 + \dots \quad |x| \ll 1.$$

Inserted

$$(2h_2 x + 3h_3 x^2 + \dots) \{x(h_2 x^2 + h_3 x^3) - \gamma x^3\} = \\ \xrightarrow{!} -h_2 x^2 - h_3 x^3 - h_4 x^4 + x^2$$

collect different orders in  $x$ :

$$\begin{aligned} \mathcal{O}(x^2) &: 0 = -h_2 + 1 \Rightarrow h_2 = 1 \\ \mathcal{O}(x^3) &: 0 = h_3 \Rightarrow h_3 = 0 \\ \mathcal{O}(x^4) &: 2h_2(h_2 - \gamma) = -h_4 \\ &\quad h_4 = 2(\gamma - 1) \end{aligned}$$

**Thus:**

$$y = h(x) = x^2 + 2(\gamma - 1)x^4 + \mathcal{O}(x^5)$$

and

$$\dot{x} = x(x^2 + 2(\gamma - 1)x^4 + \dots) - \gamma x^3$$

Evolution equation on center manifold:

$$\dot{x} = (1 - \gamma)x^3 + 2(\gamma - 1)x^5 + \dots$$

**More generally:** we want also description for  $0 \neq |\mu| \ll 1$

To use center manifold theorem consider **suspended system**

$$\begin{aligned} \dot{\mu} &= 0 \\ \dot{x} &= \mu x + xy - \gamma x^3 \\ \dot{y} &= -y + x^2 \end{aligned}$$

**Thus:**

- $\mu x$  is now a nonlinear term
- dynamics in  $\mu$ -direction is trivial:  
value of  $\mu$  is simply given by initial condition

**Now:**

$$E^{(c)} = \{(\mu, x, 0)\} \quad E^{(s)} = \{(0, 0, y)\}$$

$$\Rightarrow y = h(\mu, x) \quad \text{for} \quad (\mu, x, y) \in W^{(c)}$$

Expand  $h(\mu, x)$  in  $\mu$  and  $x$ :to keep relevant terms in expansion guess relationship  $x \Leftrightarrow \mu$  from expected equation on  $W^{(c)}$ **Symmetries:**Reflections:  $(\mu, x, y) \rightarrow (\mu, -x, y)$  $\Rightarrow$  expect

$$\begin{aligned} m\dot{x} &= f(\mu, x) \quad \text{with } f \text{ odd in } x \\ &= a\mu x + bx^3 + \dots \end{aligned}$$

 $\Rightarrow$  expect  $\mu \sim \mathcal{O}(x^2)$ ,  $h$  even in  $x$ 

$$\text{Expand } h(\mu, x) = \underbrace{h_{20}\mu^2}_{\text{higher order}} + \underbrace{h_{11}\mu x}_{\text{wrong symmetry}} + h_{02}x^2 + [h_{12}\mu x^2 + h_{04}x^4] + \dots$$

Inserted:

$$\begin{aligned} \dot{y} = \frac{dh}{dx}\dot{x} + \frac{dh}{d\mu} \underbrace{\dot{\mu}}_0 &= (h_{11}\mu + 2h_{02}x + 2h_{12}\mu x + 4h_{04}x^3 + \dots)(\mu x + x(h_{02}x^2 + \dots) - \gamma x^3) \\ &= -(h_{20}\mu^2 + h_{11}\mu x + h_{02}x^2 + h_{12}\mu x^2 + \dots) + x^2 \end{aligned}$$

$$\begin{aligned} \mathcal{O}(\mu^2 x^0) : \quad -h_{20} &= 0 \\ \mathcal{O}(\mu^1 x^1) : \quad -h_{11} &= 0 \\ \mathcal{O}(\mu^0 x^2) : \quad 0 &= -h_{02} + 1 \Rightarrow h_{02} = 1 \\ \mathcal{O}(\mu^1 x^2) : \quad 2h_{02}(1 + h_{10}) &= -h_{12} \\ &\Rightarrow h_{12} = -2 \\ \mathcal{O}(x^4) : \quad -2h_{02}\gamma + 2h_{02}^2 &= -h_{04} \\ &\quad h_{04} = 2(1 - \gamma) \end{aligned}$$

$$\begin{aligned} my &= x^2 - 2\mu x^2 + 2(1 - \gamma)x^4 \\ \dot{x} &= \mu x + x(x^2 - 2\mu x^2 + 2(1 - \gamma)x^4) - \gamma x^3 \end{aligned}$$

Evolution on center manifold

$$\dot{x} = \mu x - (\gamma - 1 + 2\mu)x^3 + [2(1 - \gamma)x^5 + \dots]$$

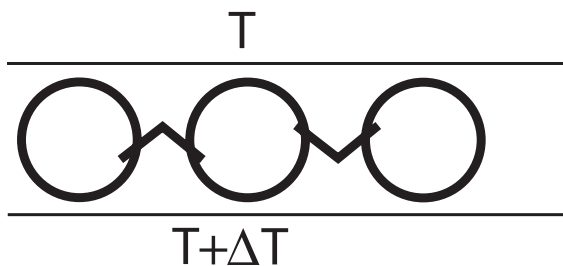
**Thus:**

- For  $\gamma > 1$  supercritical pitchfork bifurcation
- For  $\gamma < 1$  subcritical pitchfork bifurcation

## 4 Chaos

### 4.1 Lorenz Model<sup>44</sup>

Lorenz considered a minimal model for thermal convection



In two dimensions the fluid velocity  $\mathbf{v}$  of an incompressible fluid can be expressed in terms of a stream function  $(v_x, v_z) = (-\partial_z \psi, \partial_x \psi)$ .

The stream function  $\psi$  and the temperature  $T$  satisfy the coupled Navier-Stokes equation and the heat equation.

The stream function was approximated as

$$\psi = 2\sqrt{6} X(t) \cos \pi z \sin \left( \frac{\pi}{\sqrt{2}} x \right)$$

The temperature profile of the layer was approximated as

$$T(x, z, t) = \underbrace{-rz}_{\text{basic profile}} + \underbrace{9\pi^3 \sqrt{3} Y(t) \cos \pi z \cos \left( \frac{\pi}{\sqrt{2}} x \right)}_{\text{critical mode}} + \underbrace{\frac{27\pi^3}{4} Z(t) \sin 2\pi z}_{\text{harmonic mode}}$$

The Rayleigh number  $r$  characterizes the temperature difference across the layer.

To obtain differential equations for the three amplitude  $X(t)$ ,  $Y(T)$ ,  $Z(t)$  this ansatz was inserted into the Navier-Stokes equations. Keeping only terms of the form used in the ansatz yields then

$$\begin{aligned}\dot{X} &= -\sigma(X - Y) \\ \dot{Y} &= rX - Y - XZ \\ \dot{Z} &= XY - bZ\end{aligned}$$

#### Notes:

---

<sup>44</sup>Strogatz Ch. 9.2, 9.3, 9.4

- The model constitutes a severe truncation of a Galerkin expansion for free-slip boundary conditions. It may be expected to give reasonable results for weak convection. But, in contrast to the center-manifold reduction, this procedure does not represent a systematic expansion.
- The Prandtl number  $\sigma$  is given by the ratio of viscosity to thermal diffusivity.
- The parameter  $b$  is related to the wavenumber of the convection pattern.

## Demo: Lorenz Attractor<sup>45</sup>

<sup>46</sup>

For  $r > r_H$  one gets an attractor that looks very different than the attractors we had before (fixed points and periodic orbits): it is a *strange attractor*.

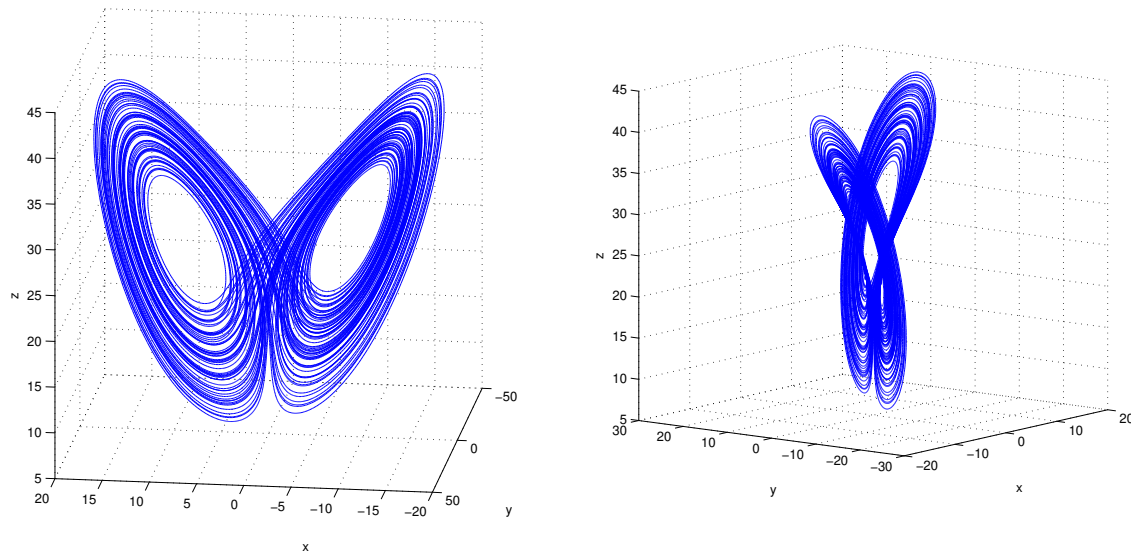
---

<sup>45</sup>Very nice Java programs by M. Cross (Caltech) at  
[http://www.cmp.caltech.edu/%7emcc/Chaos\\_Course/Lesson1/Demos.html](http://www.cmp.caltech.edu/%7emcc/Chaos_Course/Lesson1/Demos.html)  
 However, Java is not allowed in the most browsers any more. Only Internet Explorer under Windows seems to work these days.

<sup>46</sup>go to list of topics first; (if program does not plot right away: make sure speed is below 500. may have to reload java program or click at Lorenz.

Use  $X - Z$  projection. Increase  $r$  ( $= a$  in Cross program;  $\sigma = c$ ):

- 0.5 origin is stable fixed point (use initial condition  $X_0 = 4.85$ ,  $Y_0 = 5$ ,  $Z_0 = 23.5$  and set  $trans = 0$  (i.e. plot all transients, plot  $X$  and  $Z$ )
- 1.2 origin is unstable, new fixed point (symmetry-related fixed points, in fact)
- 4 this initial condition goes to the other fixed point
- 10 fixed point is clearly a stable spiral point.
- 24 the fixed point is still linearly stable spiral point
- 24.4 still attracting for this initial condition. with  $z_0 = 20$  the spiral grows  $\Rightarrow$  there must be an unstable periodic orbit in between.
- 24.8 fixed point unstable spiraling outward, but growth still slow. Hopf bifurcation
- 25 transition to strange attractor.  
 transitions occur at:  $r = 1$  ,  $r_H = 24.739$
- 3d plot of attractor
- $X(t)$  (choose variable =0 in  $x - ax$ )

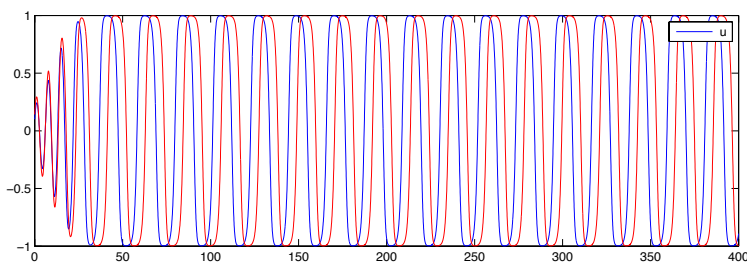


### Demo: Sensitive dependence on initial conditions

first simulation of Hopf oscillator from the homework: tb\_multi.

For stable periodic orbit:

- different initial conditions evolve to periodic orbits that are shifted with respect to each other in time
- the phase shift reaches a constant after a transient: the distance between the two oscillations does not grow or shrink  
⇒ small perturbations in the initial conditions lead only to small changes in the solution at any later time.



For Lorenz attractor simulation with  $x_0 = 2$   $y_0 = 5$   $z_0 = 20$  and  $z_0 = 20 + \Delta z$

$$r (= a) = 28 \quad \sigma (= c) = 10 \quad b = 8/3 \quad \Delta z = 10^{-3} \quad 10^{-5} \quad 10^{-7}$$

$x - z$  plot: the two trajectories separate ever further as time progresses.

count the number of periods over which the two trajectories are sort of in sync

- $\Delta z = 10^{-3}$  ca 15
- $\Delta z = 10^{-5}$  ca 22
- $\Delta z = 10^{-7}$  ca. 26

- $\Delta z = 10^{-9}$  ca 35
- $\Delta z = 10^{-11}$  ca 44

looks logarithmic in the initial difference: ca 4 periods per decade

**Note:**

- even extremely small perturbations in the initial conditions can lead to large changes in the solution after some time, which is not even very long

#### 4.1.1 Simple Properties of the Lorenz Model

i) Reflection symmetry:

The equations are *equivariant* under

$$(X, Y, Z) \rightarrow (-X, -Y, Z)$$

i.e. the left- and right-hand sides of the equations are transformed in the same way under this operation: the equations for  $\dot{X}$  and  $\dot{Y}$  change sign, while that for  $\dot{Z}$  stays the same. This symmetry is reflected in the appearance of two symmetrically related fixed points near  $r = 1$ .

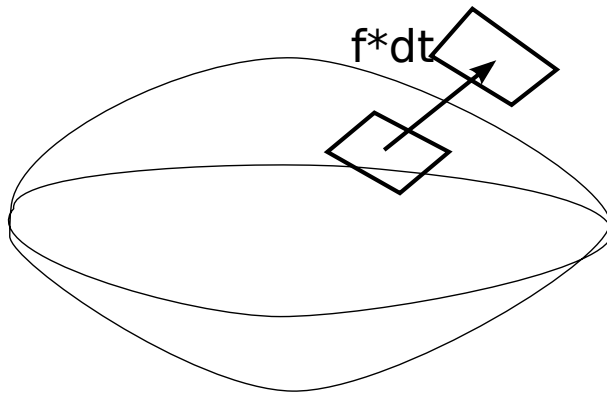
ii) Volume contraction

The Lorenz system is *dissipative*, i.e. volumes in phase space shrink under the evolution of the system.

Consider general dynamical system in 3 dimensions

$$\dot{\mathbf{x}} = \mathbf{f}(\mathbf{x}) .$$

Consider a volume  $V(t)$  in phase space with the closed surface  $S(t)$



During a time interval  $dt$

- each point  $\mathbf{x}$  on the surface moves from  $\mathbf{x}(t)$  to  $\mathbf{x}(t + dt) = \mathbf{x}(t) + \mathbf{f}(\mathbf{x}(t))dt$

- any patch  $dS$  of the surface sweeps out a volume  $dS \mathbf{n} \cdot \mathbf{f} dt$

The volume  $V(t)$  changes therefore by

$$dV = dt \int_S \mathbf{n} \cdot \mathbf{f} dS.$$

Using the divergence theorem

$$\frac{dV}{dt} = \int_S \mathbf{n} \cdot \mathbf{f} dS = \int_V \nabla \cdot \mathbf{f} dV.$$

**Note:**

- This expression holds in arbitrary dimensions.

For the Lorenz equations we have

$$\begin{aligned} \nabla \cdot \mathbf{f} &= \frac{\partial}{\partial X} \{-\sigma(X - Y)\} + \frac{\partial}{\partial Y} \{rX - Y - ZX\} + \frac{\partial}{\partial Z} \{b(XY - Z)\} \\ &= -\sigma - 1 - b < 0 \end{aligned}$$

Thus:

- all volumes in phase space shrink under the evolution of the Lorenz equations
- since  $\nabla \cdot \mathbf{f}$  is constant for the Lorenz equations all volumes decrease exponentially and with the same rate

**Note:**

- since  $\frac{dV}{dt} < 0$  everywhere there can be no fixed points with only unstable directions: all unstable fixed points have to have at least one stable direction (saddles)

### iii) Fixed Points and Bifurcations

The origin  $(0, 0, 0)$  is a fixed point.

Linear stability

$$\begin{pmatrix} \dot{X} \\ \dot{Y} \\ \dot{Z} \end{pmatrix} = \begin{pmatrix} -\sigma(X - Y) \\ rX - Y - ZX \\ -bZ \end{pmatrix} = \begin{pmatrix} -\sigma & +\sigma & 0 \\ r & -1 & 0 \\ 0 & 0 & -b \end{pmatrix} \begin{pmatrix} X \\ Y \\ Z \end{pmatrix}$$

Eigenvalues

$$\lambda_3 = -b$$

For  $\lambda_{1,2}$

$$\text{trace} = -(\sigma + 1) \quad \det = \sigma(1 - r)$$

- Since  $\text{trace} < 0$  this fixed point cannot undergo a Hopf bifurcation

- Real eigenvalue goes through 0 for  $r = 1$ : steady bifurcation

A  $r = 1$

$$\lambda_1 = 0 \quad \mathbf{v}_1 = \begin{pmatrix} 1 \\ 1 \\ 0 \end{pmatrix}$$

The center eigenspace is spanned by  $\mathbf{v}_1$ . The combined reflection  $x \rightarrow -x$  and  $y \rightarrow -y$  flips also the sign of  $\mathbf{v}_1$ . This symmetry suggests that the bifurcation is a pitch-fork bifurcation. It creates the fixed points  $(\pm X_0, \pm Y_0, Z_0)$  with

$$Y_0 = X_0 \quad Z_0 = \frac{1}{b} X_0^2 = r - 1$$

One can show that this fixed point is stable for

$$1 < r < r_H = \frac{\sigma(\sigma + b + 3)}{\sigma - b - 1} \quad \text{for } \sigma - b - 1 > 0$$

and undergoes a Hopf bifurcation at  $r = r_H$ .

### Notes:

- Consider the function  $V(X, Y, Z) = \frac{1}{\sigma} X^2 + Y^2 + Z^2$

$$\begin{aligned} \frac{dV}{dt} &= -X(X - Y) + Y(rX - Y - XZ) + Z(XY - bZ) \\ &= \underbrace{-X^2 + (1+r)XY - Y^2}_{f(X,Y)} - bZ^2. \end{aligned}$$

We have  $f(0, Y) < 0$  and  $f(X, 0) < 0$ . In order for  $f(X, Y)$  to become positive, it has to become 0 first. For what values of  $r$  is this not possible? Solve for  $X$  given  $Y$

$$X_{1,2} = \frac{1}{2} \left( -(1+r)Y \pm \sqrt{(1+r)^2 Y^2 - 4Y^2} \right) = \frac{Y}{2} \left( -(1+r) \pm \sqrt{(1+r)^2 - 4} \right).$$

Thus, for  $r < 1$  the square root is imaginary and no such  $X$  exists, implying  $\frac{dV}{dt} < 0$  if  $(X, Y, Z) \neq (0, 0, 0)$ . Therefore  $(0, 0, 0)$  is globally attractive for  $r < 1$ .

- For the standard parameter set the Hopf bifurcation occurs at  $r_H = 24.737$ .
- The numerical simulations indicate that the Hopf bifurcation is subcritical.
- The three fixed points  $(0, 0, 0)$  and  $(\pm X_0, \pm Y_0, Z_0)$  are the only fixed points of the Lorenz equations.

For  $r > r_H$  we have so far

- no stable fixed points
- no stable small-amplitude periodic orbit
- trajectories remain confined to some region

- phase space volume decreases monotonically
- trajectories are pushed down along  $z$ -axis.
- instability of the origin pushes trajectories apart along the diagonal in the  $xy$ -plane. Even close trajectories can be separated, if they are on opposite sides of the  $z$ -axis (in quadrants 1 and 3, that is).

#### 4.1.2 Lyapunov Exponents

Characterize the sensitive dependence on initial conditions.

Consider the dynamical system

$$\dot{\mathbf{x}} = \mathbf{f}(\mathbf{x})$$

and two trajectories that start very close to each other at  $t = 0$

$$\mathbf{x}(t; \mathbf{x}_0) \quad \mathbf{x}(t; \mathbf{x}_0 + \delta\mathbf{x}_0),$$

with the second argument indicating the initial condition.

At later times the two trajectories are separated by  $\Delta\mathbf{x}(t)$ ,

$$\Delta\mathbf{x}(t) = \mathbf{x}(t; \mathbf{x}_0 + \delta\mathbf{x}_0) - \mathbf{x}(t; \mathbf{x}_0).$$

Measure the distance between these trajectories

$$\|\Delta\mathbf{x}(t)\| = \|\mathbf{x}(t; \mathbf{x}_0 + \delta\mathbf{x}_0) - \mathbf{x}(t; \mathbf{x}_0)\|.$$

If  $\Delta\mathbf{x}(t)$  is very small one can linearize the differential equation around  $\mathbf{x}(t; \mathbf{x}_0, t_0)$  at the time  $t$

$$\begin{aligned} \frac{d}{dt}\Delta\mathbf{x}(t) &= \mathbf{f}(\mathbf{x}(t; \mathbf{x}_0 + \delta\mathbf{x}_0)) - \mathbf{f}(\mathbf{x}(t; \mathbf{x}_0)) \\ &= \mathbf{f}(\mathbf{x}(t; \mathbf{x}_0) + \Delta\mathbf{x}(t)) - \mathbf{f}(\mathbf{x}(t; \mathbf{x}_0)) \\ &\approx \mathbf{J}(\mathbf{x}(t; \mathbf{x}_0)) \Delta\mathbf{x}(t), \end{aligned}$$

where  $\mathbf{J}(\mathbf{x}(t; \mathbf{x}_0))$  is the Jacobian of  $\mathbf{f}(\mathbf{x})$  at time  $t$  and position  $\mathbf{x}(t)$ .

**Notes:**

- If the Jacobian was constant in time, we could determine its eigenvalues. The solution  $\Delta\mathbf{x}(t)$  would then grow or decay exponentially depending on the eigenvalues.
- However, in general the Jacobian depends on time through the position  $\mathbf{x}(t)$  on the attractor.
- Over long times  $\mathbf{x}(t)$  explores the whole attractor and one could imagine that the growth and decay of  $\Delta\mathbf{x}$  is determined by something like an ‘average Jacobian’.

Numerically one finds in the limit of long times and small initial distance

$$\|\Delta\mathbf{x}(t)\| \sim \|\Delta\mathbf{x}(0)\| e^{\lambda t}.$$

Motivated by this observation one defines

$$\lambda \equiv \lim_{t \rightarrow \infty} \lim_{\|\Delta\mathbf{x}(0)\| \rightarrow 0} \frac{1}{t} \ln \left( \frac{\|\Delta\mathbf{x}(t)\|}{\|\Delta\mathbf{x}(0)\|} \right).$$

### Notes:

- For the linearization that leads to the Jacobian to be valid one has to consider first the limit of an infinitesimal perturbation,  $\Delta\mathbf{x}(0) \rightarrow 0$ , and only then the limit of large times.
- $\lambda$  is a Lyapunov exponent of the system
  - more precisely, this  $\lambda$  is the largest Lyapunov exponent, which dominates  $\|\Delta\mathbf{x}(t)\|$  for large  $t$
  - in an  $N$ -dimensional system there are  $N$  Lyapunov exponents, corresponding to the  $N$  dimensions of  $\Delta\mathbf{x}(0)$ .
- In principle,  $\lambda$  depends on the specific trajectory  $\mathbf{x}(t; \mathbf{x}_0)$  and one needs to average over multiple trajectories on the attractor.
- Systems with time-independent coefficient have time translation symmetry
  - if  $\mathbf{x}(t)$  is a solution, then  $\mathbf{x}(t + \Delta t)$  is also a solution for any  $\Delta t$ .
  - therefore perturbations along the attractor do not grow or shrink, which implies that one Lyapunov exponent has to vanish,  $\lambda = 0$  (cf. evolution of perturbations for stable periodic orbits).
- The Lorenz system has 3 Lyapunov exponents. For the strange attractor one has

$$\lambda_1 > 0 \quad \lambda_2 = 0 \quad \lambda_3 < 0.$$

If none of the Lyapunov exponents is positive, the system is not chaotic.

The volume contraction is determined by the sum of the three Lyapunov exponents. Therefore  $\lambda_1 + \lambda_2 + \lambda_3 < 0$  for all  $r$ .

### Time Horizon:

A key feature of chaotic systems is that the exponential growth of the difference between nearby trajectories limits predictions severely.

Assume we can measure the initial condition with a precision  $\delta_0 = \|\Delta\mathbf{x}(0)\|$ . If we need to make a prediction with an accuracy  $\delta_{max}$ , i.e. we require  $\|\Delta\mathbf{x}(t)\| < \delta_{max}$ , then we can predict the system up to a time  $t_h$  determined by

$$\delta_{max} = \|\Delta\mathbf{x}(t_h)\| = \|\Delta\mathbf{x}(0)\| e^{\lambda t_h}$$

i.e.

$$t_h(\delta_0) = \frac{1}{\lambda} \ln \left( \frac{\delta_{max}}{\delta_0} \right).$$

### Note:

- Thus, the time horizon  $t_h$  grows *only logarithmically* with the precision  $\delta_0$  of our knowledge of the initial condition. This matches our simulations where we found that each increase in the precision by a factor of 10 increased the time over which the two trajectories stayed close to each other only by roughly 4 periods.

To increase the prediction time from 22 periods to 44 periods we had to increase the precision by a factor of  $10^6$ .

### Characterization of Chaos:

Chaos is aperiodic, long-term behavior in a deterministic system that exhibits sensitive dependence on initial conditions.

- Aperiodic: trajectories do not settle down to a fixed point, periodic orbit, or quasi-periodic orbit.
- Sensitive dependence: distances between trajectories grow exponentially fast: positive Lyapunov exponent.

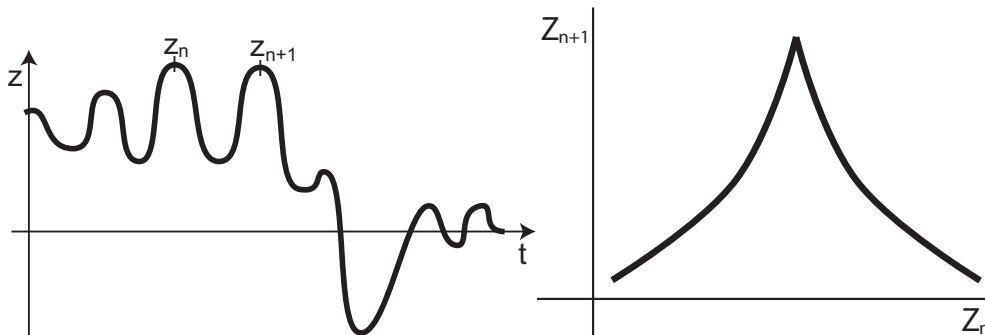
### Quasi-periodic motion:

Consider two uncoupled harmonic oscillators, e.g. mass-spring system in the  $x$ -direction to which a pendulum is attached that swings only in the  $y - z$ -plane.

- if both have the same frequency the pendulum tip traces out a circle
- if the frequencies are different the trace is a Lissajous figure
  - for rational ratios of the two frequencies the traces close on themselves: periodic motion
  - for irrational frequency ratios the figures never close: quasi-periodic motion

**Question:** How can one understand the complex dynamics of the Lorenz equations and of other systems like that? How can one characterize the behavior in simpler models yet?

Lorenz reduced the three-dimensional flow to a one-dimensional iterated map by asking: can we predict the next maximum of the variable  $z$ ,  $z_{n+1}$ , if we only know the previous maximum  $z_n$ . He therefore plotted  $z_{n+1}$  vs.  $z_n$  and obtained a map.



### Demo:

- $Z(t)$  ( $x\text{-ax} = 0$   $y\text{-ax} = 3$ )
- keep only maxima of  $Z$  and plot  $Z_{n+1}$  vs  $Z_n$ . (demo max map)

**Notes:**

- The line in that map is actually not a line, but has finite thickness  
For the Lorenz model the line thickness is, however, very small  $\Rightarrow$  the knowledge of  $Z_n$  is sufficient to predict  $Z_{n+1}$  quite reliably.
- The reduction to this map must be an approximation:
  - The original ode's can also be solved backward.
  - The map can, however, not be iterated backward since  $f^{-1}(z)$  is multi-valued.

## 4.2 One-Dimensional Maps<sup>47</sup>

Consider maps as dynamical systems

$$x_{n+1} = f(x_n)$$

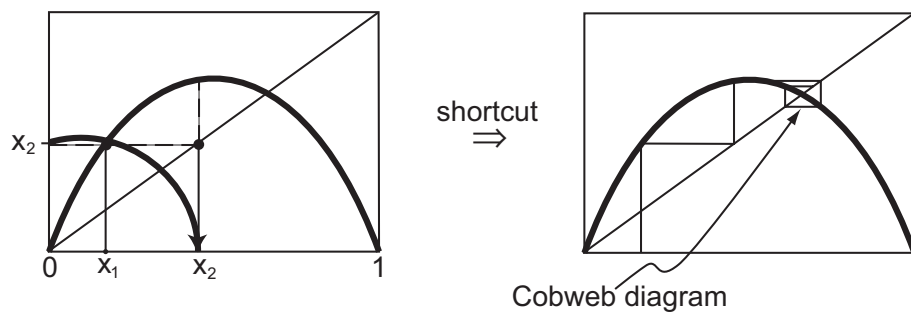
Classic example: logistic map

$$x_{n+1} = ax_n(1 - x_n) \quad 0 \leq x_n \leq 1$$

**Notes:**

- This map could be thought of as a (very poor) numerical solution of the logistic differential equation (using forward Euler with large time step).
- The logistic map has a maximum at  $x = \frac{1}{2}$ . It maps  $[0, 1]$  onto  $[0, \frac{1}{4}a]$ . For  $0 \leq a \leq 4$  the  $x_n$  remain in the interval  $[0, 1]$ .
- The parameter  $a$  gives the slope of  $f(x)$  at the origin.

Graphical iteration via the cobweb diagram:

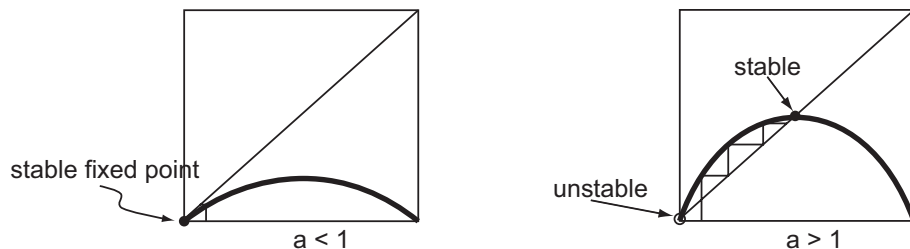


<sup>47</sup>Strogatz Ch. 10

Consider the transitions as  $a$  is varied.

For all values of  $a$  the point  $x^{(0)} = 0$  is a fixed point.

Increase  $a$ :

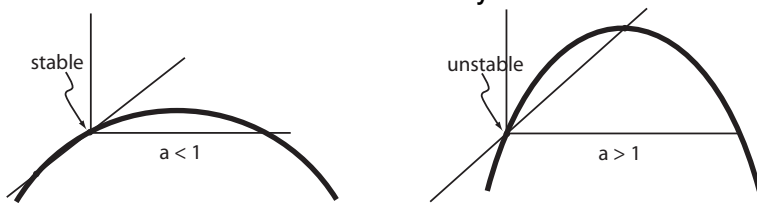


For  $a = 1$  an additional fixed point appears

$$\begin{aligned} x = ax - ax^2 &\Rightarrow 0 = x(a - 1 - ax) \\ x^{(1)} &= \frac{a-1}{a} \end{aligned}$$

**Note:**

- This fixed point arises in a transcritical bifurcation. For  $a < 1$  the second fixed point  $x^{(1)} < 0$  and not relevant for this system.



### Linear stability analysis for maps:

Linearize around a fixed point  $x_f$

$$\begin{aligned} x_n &= x_f + \epsilon \Delta x_n \\ x_f + \epsilon \Delta x_{n+1} &= f(x_f + \epsilon \Delta x_n) = f(x_f) + \epsilon \Delta x_n f'(x_f) \\ \Rightarrow \Delta x_{n+1} &= \Delta x_n f'(x_f) \end{aligned}$$

$\Rightarrow |\Delta x_n|$  grows for  $|f'(x_f)| > 1$  and  $|\Delta x_n|$  decays for  $|f'(x_f)| < 1$ .

**Thus:**

- The stability limits for maps are given by  $|f'(x_f)| = 1$ .
- Comparison: for one-dimensional *flows* the stability limit is given by  $f'(x_f) = 0$ .
- In the maxima map of the Lorenz model  $|f'(z)| > 1$  for all  $z$ : the fixed point of the maxima map, which corresponds to a periodic orbit in the full Lorenz system, is unstable.

As expected from the graph: at  $a = 1$  the fixed point  $x^{(0)}$  becomes linearly unstable.

Stability of the fixed point  $x^{(1)} = \frac{a-1}{a}$ :

$$f'(x^{(1)}) = a - 2ax^{(1)} = a - 2(a - 1) = 2 - a.$$

Thus,

$$|f'(x_1)| < 1 \quad \text{for} \quad 1 < a < 3.$$

**Note:**

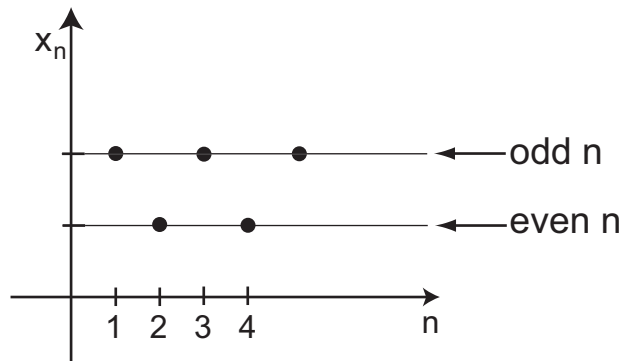
- At  $a = 1$  the stability limit corresponds to the transcritical bifurcation identified above. It has  $f'(x^{(1)}) = +1$ .
- At  $a = 3$  one has  $f'(x^{(1)}) = -1$ ,

$$\Delta x_{n+1} = -\Delta x_n,$$

which suggests that the solution jumps back and forth.

Demo: what happens at the bifurcation at  $a = 3$ ?

⇒ converges to period-2 solution.



Determine period-2 solution:

Period 2: fixed point under second iterate of  $f(x)$

$$\begin{aligned} x_{n+2} &= f(x_{n+1}) = f(f(x_n)) \equiv f^{(2)}(x_n) \\ &= ax_{n+1}(1 - x_{n+1}) = a(a x_n(1 - x_n))(1 - a x_n(1 - x_n)) \end{aligned}$$

Fixed point of  $f^{(2)}$ :  $x_{n+2} = x_n$

$$x^{(2)} = f^{(2)}(x^{(2)})$$

Fixed points of the first iterate  $f(x)$  itself are also fixed points of the second iterate. Therefore the fixed point condition can be factored as

$$\underbrace{-x(xa + 1 - a)}_{\text{known fixed points}} (a^2x^2 - a(1 + a)x + 1 + a) = 0$$

Thus one gets two new fixed points of the second iterate  $f^{(2)}$

$$x_{1,2}^{(2)} = \frac{1}{2a} \left\{ 1 + a \pm \sqrt{a^2 - 2a - 3} \right\}$$

They arise in a pitch-fork bifurcation and exist for  $a > 3$ .

The fixed points of  $f^{(2)}$  correspond to a period-2 orbit alternating  $x_1^{(2)} \leftrightarrow x_2^{(2)}$ .

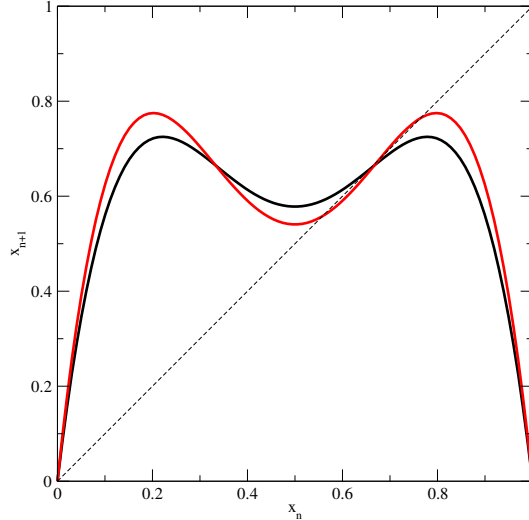


Figure 33: The creation of a period-2 orbit is a pitchfork bifurcation in the second iterate  $f^{(2)}$ .

Stability of the period-2 orbit  $x_{1,2}^{(2)}$ : consider the stability of the fixed points of the second iterate

$$\begin{aligned} x_{1,2}^{(2)} + \Delta x_{n+2} &= f \left( f(x_{1,2}^{(2)} + \Delta x_n) \right) \\ \Delta x_{n+2} &= \underbrace{\frac{d}{dx} (f(f(x)))}_{\lambda} \Big|_{x_{1,2}^{(2)}} \Delta x_n \\ \lambda &= f' \left( f(x_{1,2}^{(2)}) \right) f'(x_{1,2}^{(2)}) \end{aligned}$$

With

$$f(x_{1,2}^{(2)}) = x_{2,1}^{(2)}$$

we get

$$\begin{aligned} \lambda &= f' \left( x_1^{(2)} \right) f' \left( x_2^{(2)} \right) = a^2 \left( 1 - 2x_1^{(2)} \right) \left( 1 - 2x_2^{(2)} \right) \\ &= a^2 \left( 1 - 2 \left( x_1^{(2)} + x_2^{(2)} \right) + 4x_1^{(2)}x_2^{(2)} \right) \\ &= a^2 - 2a(1+a) + (1+a)^2 - (a^2 - 2a - 3) \\ &= -a^2 + 2a + 4 \end{aligned}$$

The stability limits are given by

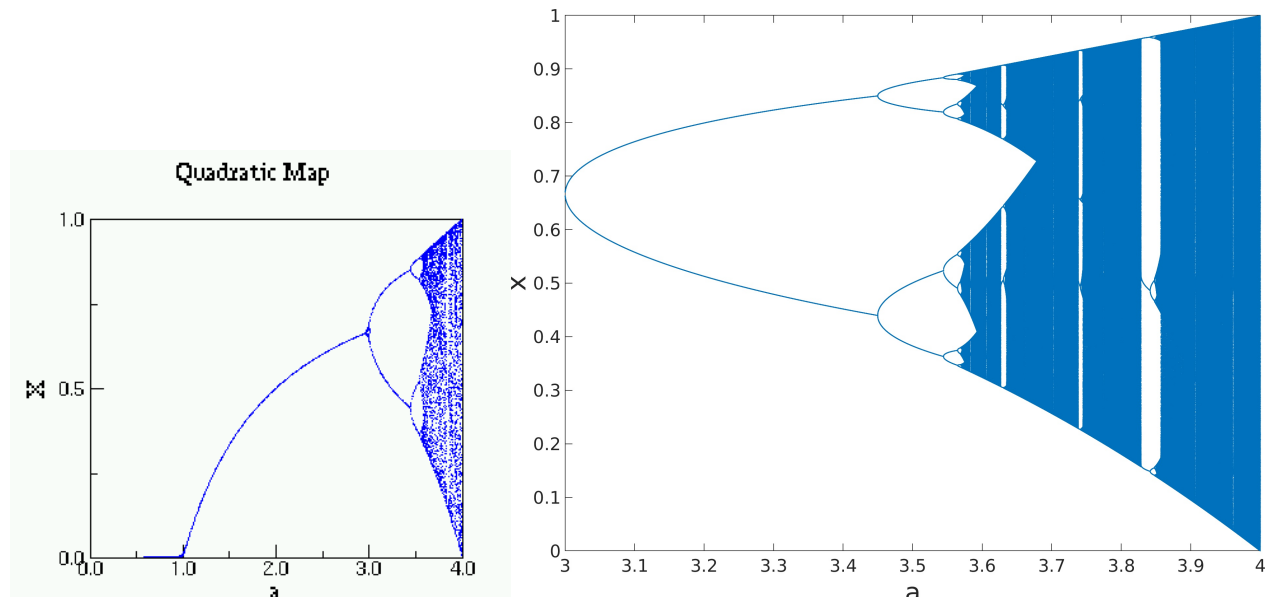
$$\begin{aligned}\lambda_1 &= +1 \quad \Rightarrow \quad a = 3 \\ \lambda_2 &= -1 \quad \Rightarrow \quad a = 1 + \sqrt{6} \approx 3.4495\end{aligned}$$

### Notes:

- At  $a = 3$  the fixed point of  $f^{(1)}(x)$  undergoes a period-doubling bifurcation and the eigenvalue of its linearization is  $\lambda^{(1)} = -1$ . The eigenvalue of the linearization of  $f^{(2)}(x)$  at  $a = 3$  is

$$\lambda^{(2)} = 1 = f' \left( \underbrace{f(x^{(1)})}_{x^{(1)}} \right) f'(x^{(1)}) = \lambda^{(1)} \lambda^{(1)} = +1$$

- For  $a = 1 + \sqrt{6}$  the fixed point of  $f^{(2)}$  becomes unstable in a period-doubling bifurcation: birth of a period-4 orbit.



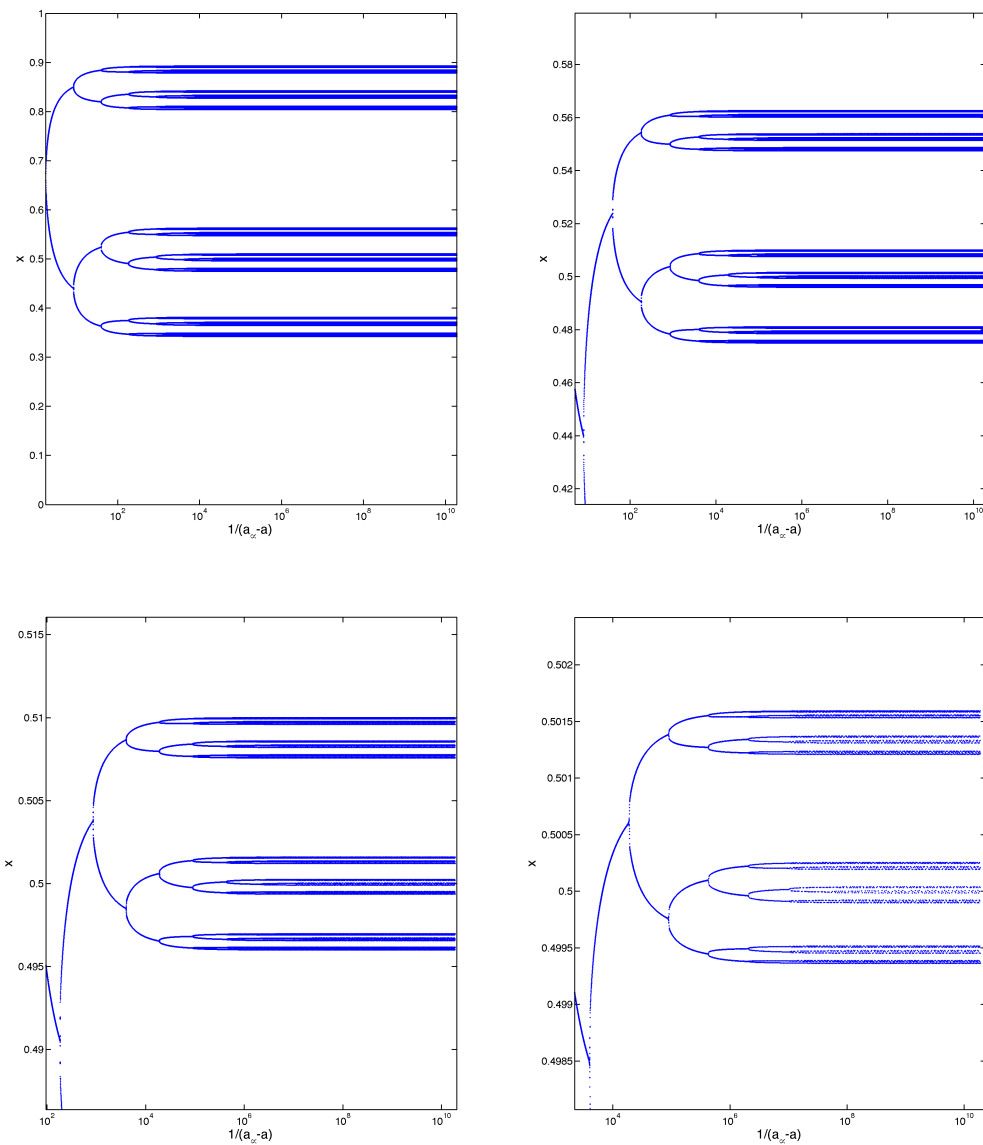


Figure 34: The cascade of period-doublings is self-similar: note the zoomed in scales (logarithmic on the  $x$ -axis).

### Period-Doubling Cascade:

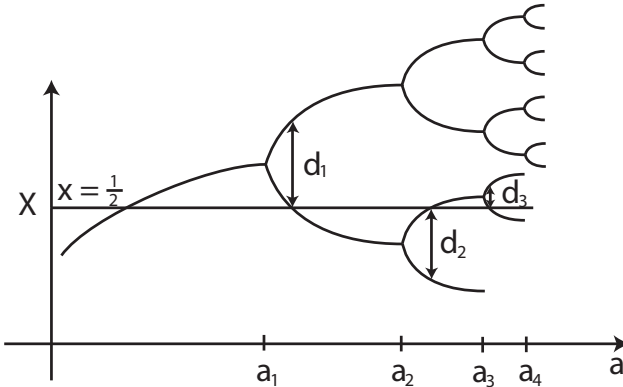
- There is an infinite number of period-doubling bifurcations, which accumulate at

$$a_\infty = 3.569945672\dots$$

- With each bifurcation the period doubles: at  $a_\infty$  the period is infinite and dynamics are not periodic any more.

- The distance between successive bifurcations becomes smaller with each bifurcation. Their ratio approaches a fixed value

$$\lim_{n \rightarrow \infty} \frac{a_n - a_{n-1}}{a_{n+1} - a_n} = \delta = 4.6692016091029909\dots$$



The constant  $\delta$  is called the Feigenbaum constant, after M. Feigenbaum who discovered the scaling and showed that it is *universal for all maps with a single quadratic maximum*.

In terms of  $a_\infty$  this scaling can be written as

$$a_n = a_\infty - Ae^{-\delta'n}$$

with

$$\delta = \frac{1 - e^{\delta'}}{e^{-\delta'} - 1} = e^{\delta'} \quad \delta' = 1.54098809542.$$

- The width of the bifurcation also gets smaller in each bifurcation. The ratio of the widths, measured when one branch intersects  $x_m = \frac{1}{2}$ , also approaches a fixed value

$$\lim_{n \rightarrow \infty} \frac{d_n}{d_{n+1}} = \alpha = -2.5029\dots$$

The minus sign indicates that successive bifurcations are on opposite sides of the mid point  $x_m = \frac{1}{2}$ .

- The approach to fixed fixed ratios suggests self-similarity as  $a_\infty$  is approached: zooming in yields a picture that looks essentially the same again, the same structures repeat on smaller scales
- The self-similarity can be described with a *renormalization theory*. It shows that period-doubling cascades in *all* maps with a quadratic maximum have the same *universal behavior*. i.e. they all have the same values of the Feigenbaum constant  $\delta$  and of  $\alpha$ .

Among the early experimental observations of the period-doubling cascade to chaos and the measurement of the Feigenbaum constant were experiments on Rayleigh-Benard convection of mercury (Fauve and Libchaber, 1983):

$$\delta = 4.4 \pm 0.1$$

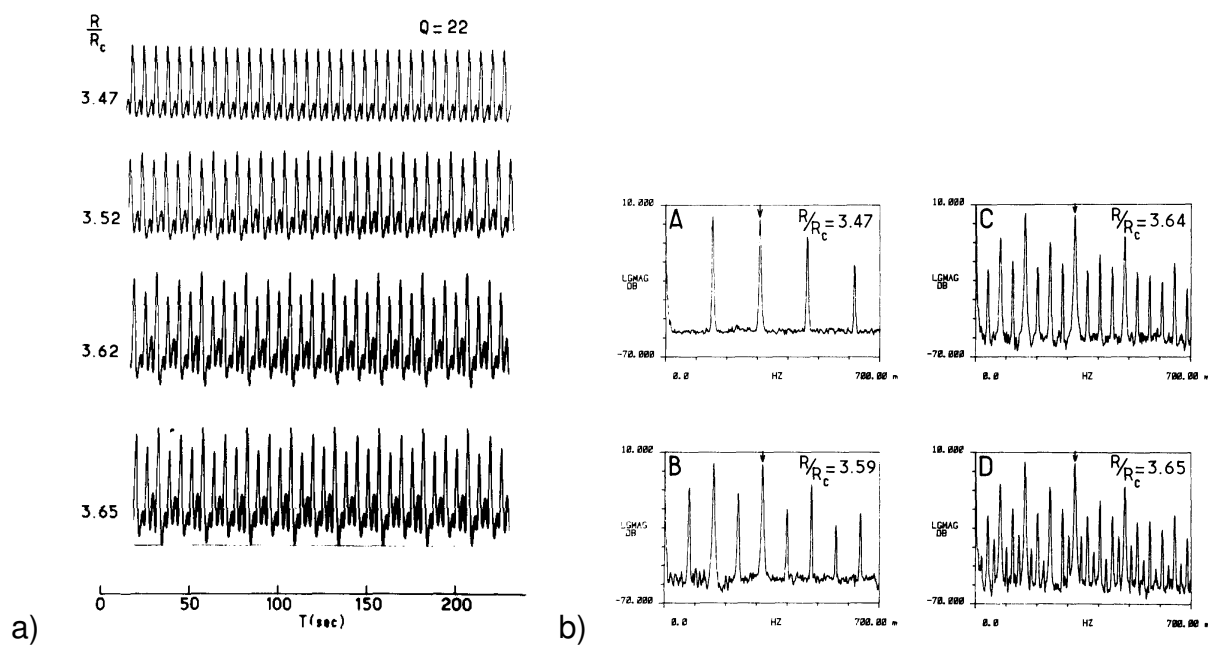


Figure 35: Period doubling cascade observed in convection of mercury with a horizontal magnetic field. a) Temporal evolutions. b) Power spectra. The arrow marks the fundamental frequency. (Libchaber et al., 1983; Fauve and Libchaber, 1983)

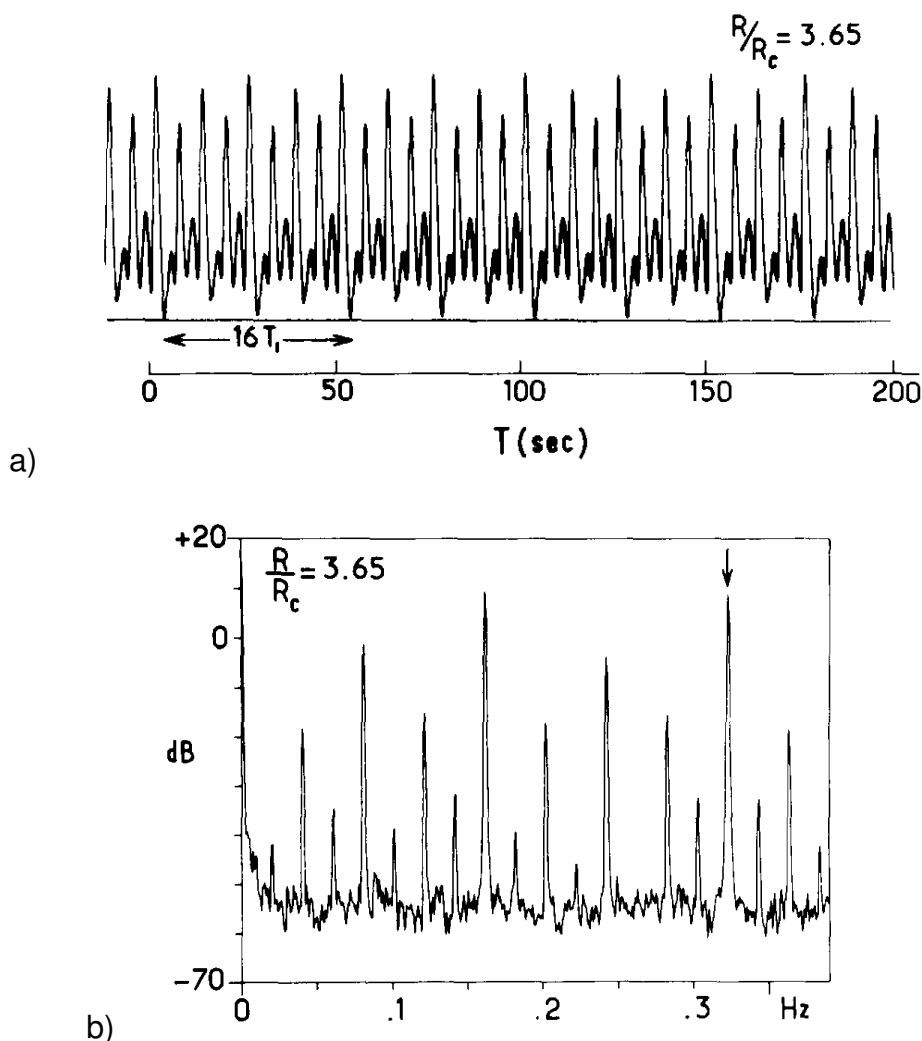


Figure 36: Period doubling cascade observed in convection of mercury with a horizontal magnetic field. a) Period 16. b) Power spectrum of a). The arrow marks the fundamental frequency in the power spectrum. (Libchaber et al., 1983; Fauve and Libchaber, 1983)

### Chaotic Dynamics:

For  $a > a_\infty$  the dynamics are chaotic and exhibit sensitive dependence on initial conditions.

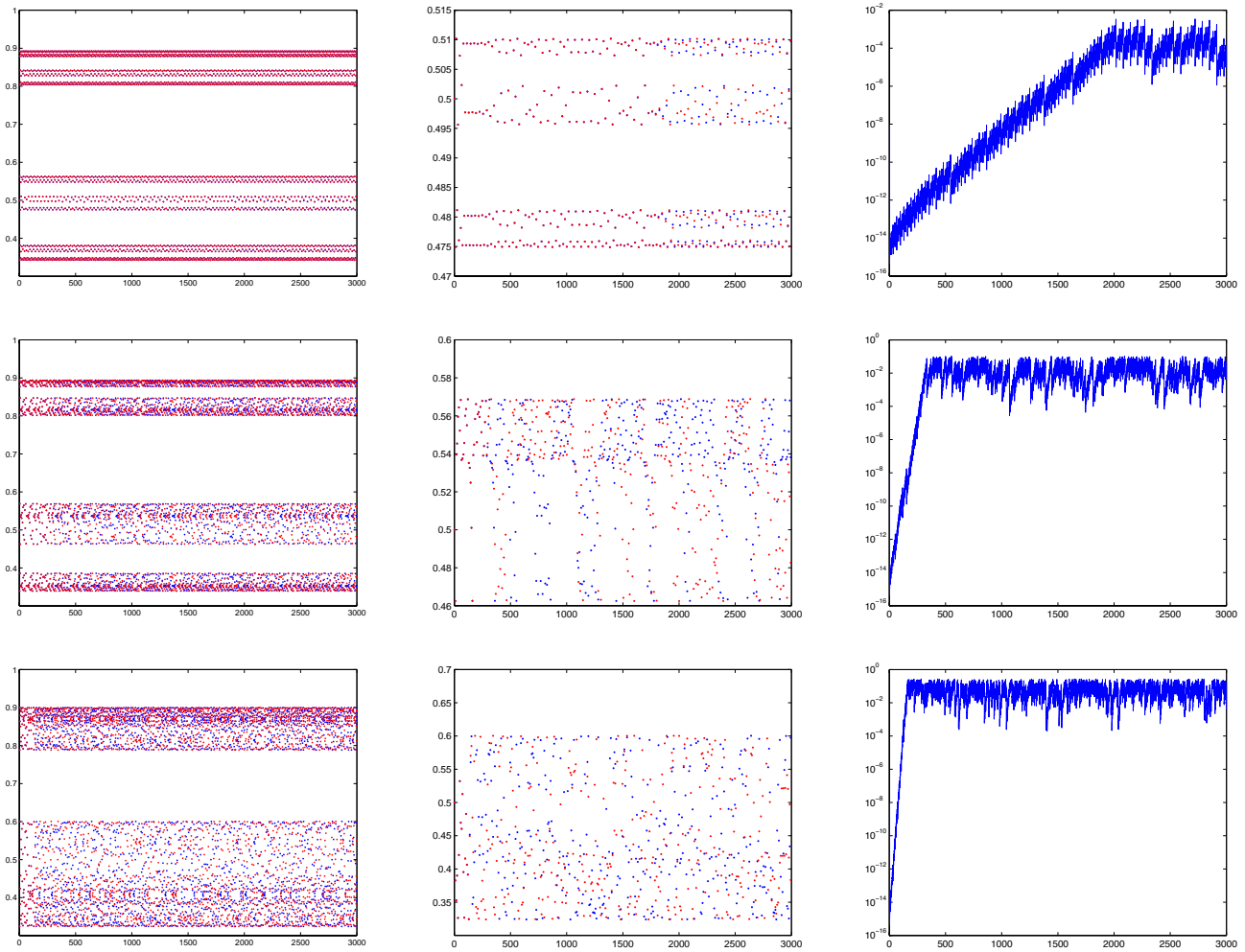


Figure 37: Sensitive dependence on initial conditions. Left panel: orbit for two slightly different initial conditions,  $x_0 = 0.5$  (red) and  $x_0 = 0.5 + 10^{-8}$  (blue). Middle panel: zoomed in showing the orbits for every 8th iteration. Right panel: growth of the difference between orbits. a)  $a = 3.569994$ : chaotic period-32 band with the period 32 still clearly visible. b)  $a = 3.5753$ : close to the merging of the period-8 and period-4 band. c)  $a = 3.6$ : chaotic period-2 band.

In analogy to the Lyapunov exponents for flows introduce Lyapunov exponents for maps

$$\lambda = \lim_{n \rightarrow \infty} \lim_{\Delta x_0 \rightarrow 0} \frac{1}{n} \ln \left| \frac{\Delta x_n}{\Delta x_0} \right|$$

Use

$$\begin{aligned} \Delta x_n &= f^{(n)}(x_0 + \Delta x_0) - f^{(n)}(x_0) \\ &= \left. \frac{df^{(n)}}{dx} \right|_{x_0} \Delta x_0 = \prod_{j=1}^n f'(x_j) \Delta x_0 \end{aligned}$$

with

$$x_j = f^{(j)}(x_0)$$

Thus

$$\lambda = \lim_{n \rightarrow \infty} \frac{1}{n} \ln \left| \prod_{j=1}^n f'(x_j) \right| = \lim_{n \rightarrow \infty} \frac{1}{n} \sum_{j=1}^n \ln |f'(x_j)|$$

For a periodic orbit with period  $p$  we get

$$\lambda = \frac{1}{p} \ln \left| \prod_{j=1}^p f'(x_j) \right| = \frac{1}{p} \ln \left| \frac{df^{(n)}}{dx} \Big|_{x_0} \right|$$

### Superstable orbits:

If  $\frac{df^{(n)}(x)}{dx} = 0$  then  $\lambda \rightarrow -\infty$ : small perturbations of such orbits decay extremely fast.

Consider for simplicity a superstable fixed point  $x_{ss}$

$$\begin{aligned} \Delta x_n &= \underbrace{f'(x_{ss})}_0 \Delta x_{n-1} + \frac{1}{2} f''(x_{ss}) \Delta x_{n-1}^2 + \mathcal{O}(\Delta x_n^3) \\ &= \frac{1}{2} f''(x_{ss}) \left( \frac{1}{2} f''(x_{ss}) \Delta x_{n-2}^2 \right)^2 = \frac{1}{2} f'(x_{ss}) \left[ \frac{1}{2} f''(x_{ss}) \left( \frac{1}{2} f''(x_{ss}) \Delta x_{n-3}^2 \right)^2 \right]^2 \\ &= \left( \frac{1}{2} f''(x_{ss}) \right)^{\sum_{j=0}^{n-1} 2^j} (\Delta x_0)^{(2^n)} = \left( \frac{1}{2} f''(x_{ss}) \right)^{2^n-1} (\Delta x_0)^{(2^n)} \\ &= \left( \frac{1}{2} f''(x_{ss}) \right)^{-1} \left( \frac{1}{2} f''(x_{ss}) \Delta x_0 \right)^{(2^n)} \end{aligned}$$

This decay is much faster than exponential. For comparison

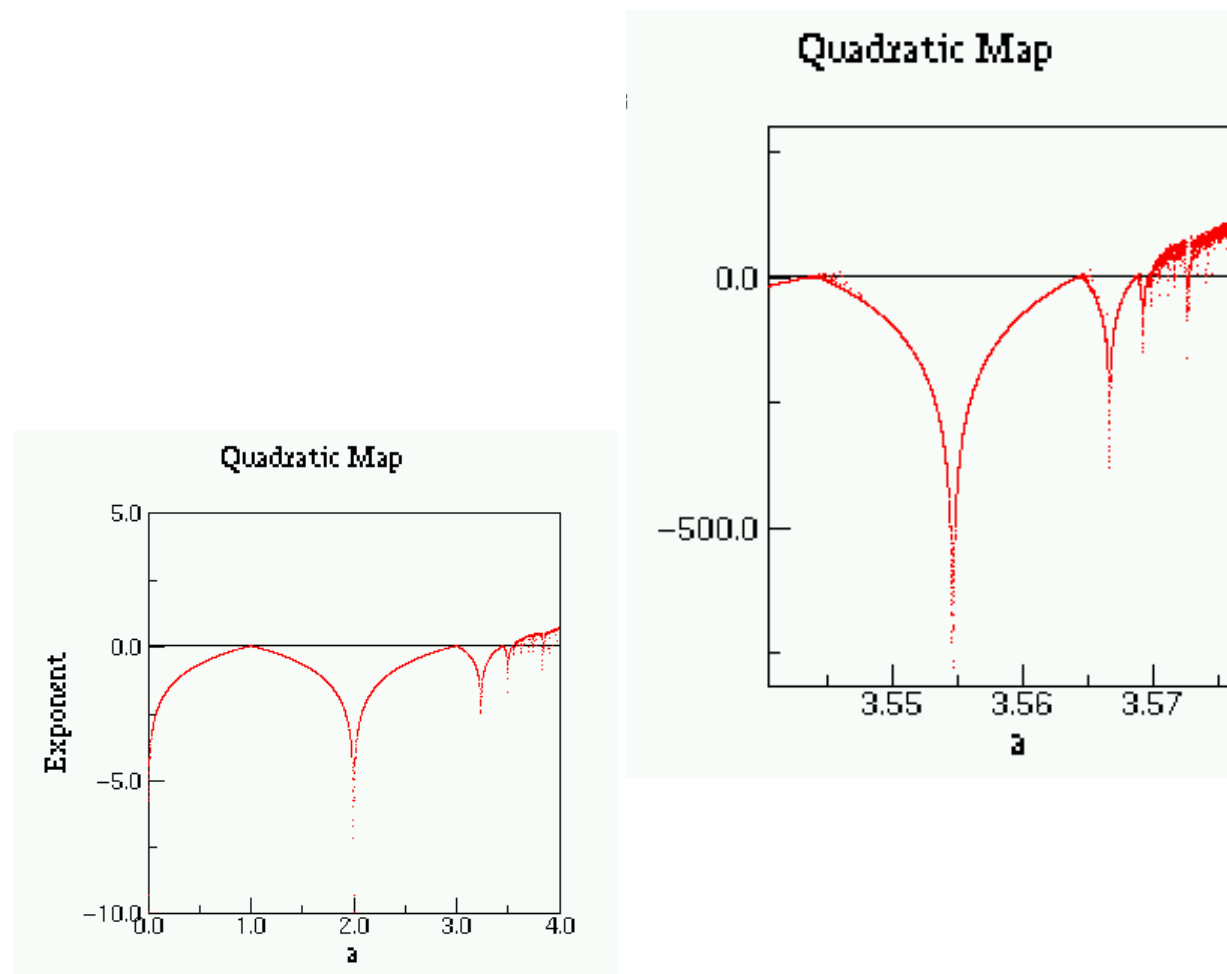
$$\frac{\Delta x_{n+1}}{\Delta x_n} = \begin{cases} c & \text{for exponential decay to stable fixed point} \\ \propto \Delta x_n & \text{for convergence to superstable fixed point} \end{cases}$$

e.g.

$$\begin{array}{ccccccc} 10^{-1} & 10^{-2} & 10^{-3} & 10^{-4} & 10^{-5} & 10^{-6} & \text{for exponential decay} \\ 10^{-1} & 10^{-2} & 10^{-4} & 10^{-8} & 10^{-16} & 10^{-32} & \text{decay at superstable fixed point} \end{array}$$

### Note:

- when a periodic orbit first arises its Lyapunov exponent is  $f'(x) = +1$
- when a periodic orbit undergoes a period-doubling bifurcation  $f'(x) = -1$
- between these two bifurcations  $f'(x)$  has to go through 0,  $\lambda \rightarrow -\infty$ : the periodic orbit is superstable
- At the period-doubling bifurcations perturbations grow or decay very slowly  $\rightarrow$  it takes a long time for the orbit to approach the attractor. Measuring the bifurcation points precisely is therefore computationally quite expensive. To characterize the period-doubling cascade it is computationally more efficient to mark the superstable points rather than the bifurcation points (cf. homework)



Origin of the sensitive dependence on initial conditions:

Consider  $a = 4$ :

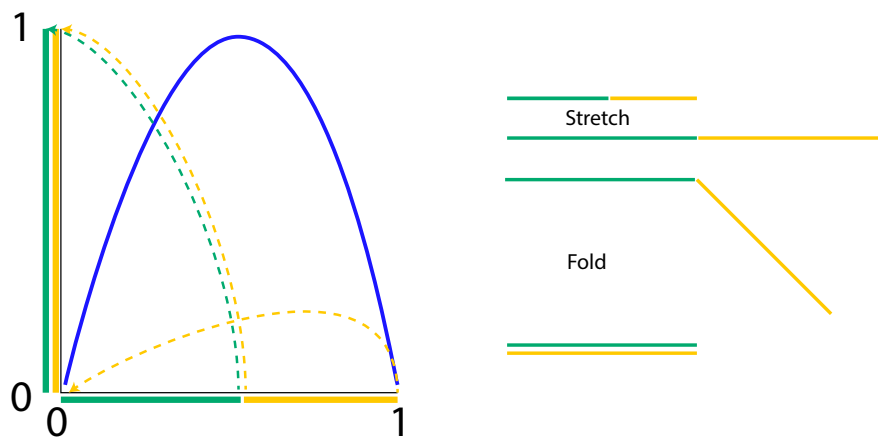


Figure 38: Chaotic dynamics are characterized by *stretching* and *folding*.

### Notes:

- The interval  $[0, \frac{1}{2}]$  is *stretched* all the way to  $[0, 1]$
- The interval  $[\frac{1}{2}, 1]$  is also stretched in length to  $[0, 1]$ , but it is at the same time *folded* back
- The separation of trajectories requires stretching and folding because the trajectories are stretched, but at the same time they confined to a finite interval.

The stretching suggests a positive Lyapunov exponent. A very rough hand-waving guess gives

$$\Delta x_{n+1} \sim 2\Delta x_n \sim 2^{n+1}\Delta x_0$$

leading to

$$\lambda \sim \lim_{n \rightarrow \infty} \frac{1}{n} \ln 2^{n+1} \rightarrow \ln 2.$$

For  $a = 4$  one can actually give an explicit exact solution of the iteration for any initial condition. Rewrite the iteration

$$x_{n+1} = 4x_n(1 - x_n)$$

in terms of a new variable  $\theta_n$  defined via

$$x_n = \sin^2 \theta_n \quad x_{n+1} = \sin^2 \theta_{n+1}.$$

Then

$$\begin{aligned} \sin^2 \theta_{n+1} &= 4 \sin^2 \theta_n \underbrace{(1 - \sin^2 \theta_n)}_{\cos^2 \theta_n} = \\ &= (2 \sin \theta_n \cos \theta_n)^2 = \sin^2(2\theta_n) \end{aligned}$$

Thus, in terms of the variable  $\theta$  the dynamics are simple

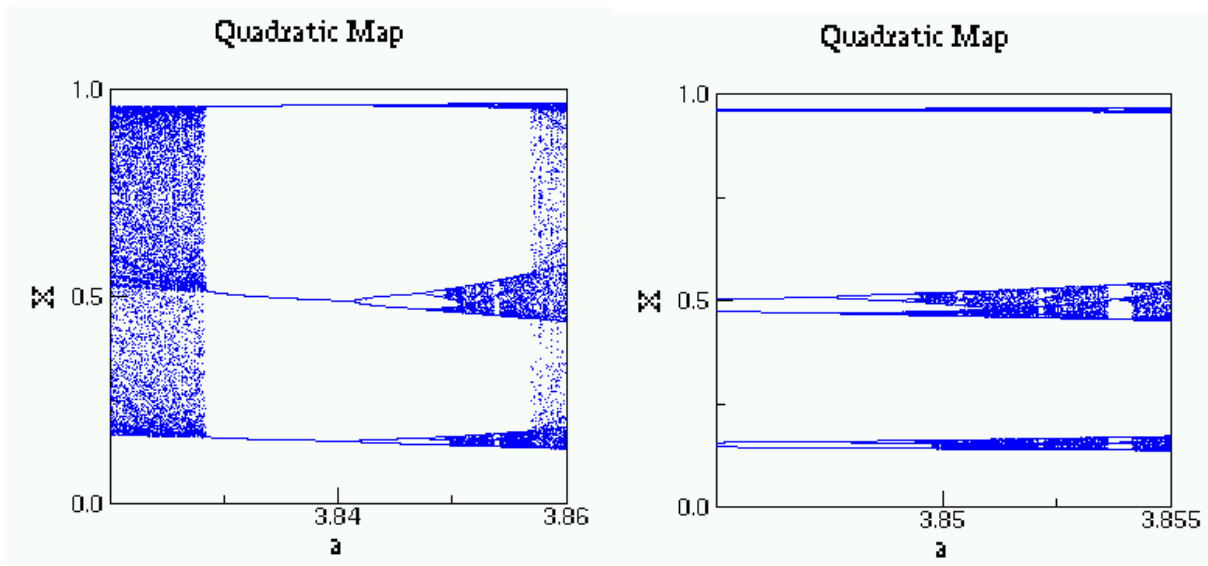
$$\begin{aligned} \theta_{n+1} &= 2\theta_n \\ \Rightarrow \theta_n &= 2^n \theta_0 \\ x_n &= \sin^2(2^n \theta_0) = \sin^2(2^n \arcsin \sqrt{x_0}) \end{aligned}$$

The analytical solution allows to compute the Lyapunov exponent exactly as well

$$\begin{aligned}\lambda &= \lim_{n \rightarrow \infty} \frac{1}{n} \ln \left| \frac{df^{(n)}(x)}{dx} \Big|_{x_0} \right| \\ &= \lim_{n \rightarrow \infty} \frac{1}{n} \ln \left| 2 \sin(2^n \theta_0) \cos(2^n \theta_0) 2^n \frac{d}{dx} \arcsin \sqrt{x} \Big|_{x_0} \right| \\ &= \ln 2 + \lim_{n \rightarrow \infty} \left( \frac{1}{n} \mathcal{O}(1) \right) = \ln 2\end{aligned}$$

'Chaotic' regime, periodic windows:

$$\begin{aligned}a &= 3.825 \rightarrow 3.85 \rightarrow 3.86 \\ a &= 3.83 \rightarrow 3.82\end{aligned}$$



### Periodic windows in the chaotic regime

- Tangent bifurcation (saddle-node bifurcation) of  $f^{(3)}(x)$  at  $1 + \sqrt{8} = 3.8284\dots$ . A stable and an unstable fixed point of  $f^{(3)}(x)$  are created, corresponding to a stable and an unstable period-3 orbit.
- Just before the saddle-node bifurcation the 'ghost' of the period-3 orbit traps the orbit for a long time  $\Rightarrow$  intermittent behavior: long durations of near period-3 behavior, which are interrupted by chaotic excursions. Their duration scales like

$$T \propto \epsilon^{-\frac{1}{2}} \quad \text{with } \epsilon = 1 + \sqrt{8} - a \ll 1.$$

Thus, when decreasing  $a$  from values inside the periodic window the transition to chaos occurs via the intermittent occurrence of chaotic bursts rather than by period-doubling.

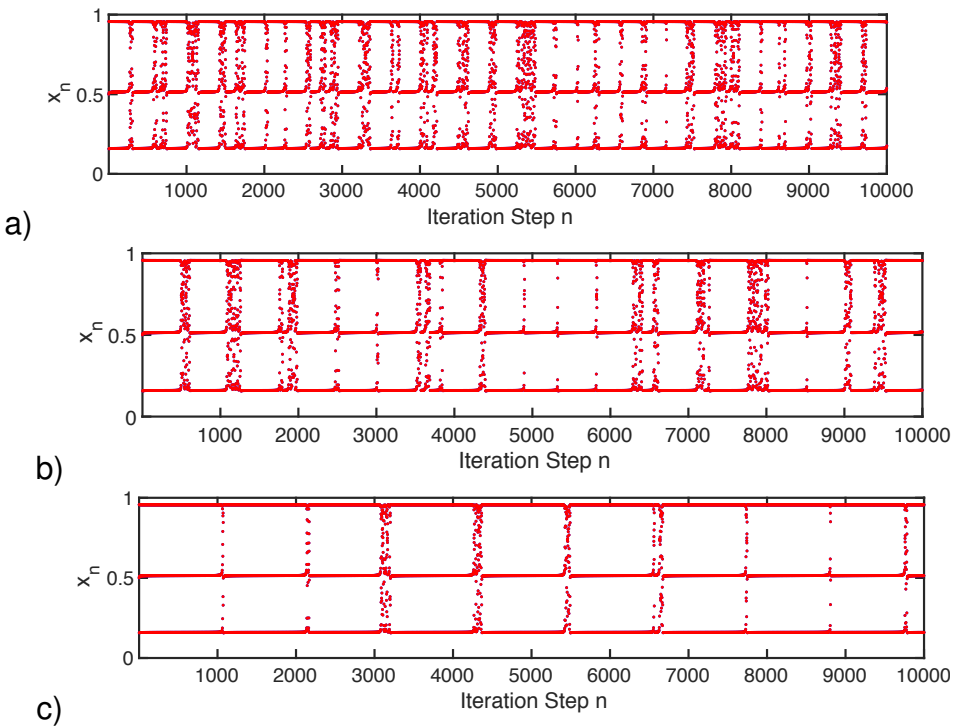


Figure 39: Intermittency at the transition to the period-3 window. a)  $a = 3.82841$  b)  $a = 3.828422$ . c)  $a = 3.828426$ . The intermittency reflects the ‘ghost’ of the period-3 orbit that is created via a saddle-node bifurcation (tangent bifurcation) at slightly larger  $a$ .

- The period-3 orbit also undergoes a period-doubling cascade.
- There are also windows with period 5, 7, 9, 11, etc. and each window has its own period-doubling cascade.

### 4.3 Self-Similarity: Renormalization<sup>48</sup>

To understand and quantify the essence of the self-similarity seen in the simulations implement the rescaling explicitly in a simple version.

Consider a quadratic approximation of a map in the vicinity of a period-doubling bifurcation. Shift the coordinate  $x$  and the control parameter  $\mu$  such that the fixed point is at  $x = 0$ ,

$$x_{n+1} = -(1 + \mu)x_n + ax_n^2 + \dots$$

and the period doubling occurs at  $\mu = 0$ .

Procedure: Identify the two fixed points of the iterated map  $f^{(2)}$  and find its period-doubling point. Near that bifurcation  $f^{(2)}$  can be written to quadratic order in the same form as  $f$ , just with different coefficients. Comparing the two maps gives then a mapping between the coefficients in which the coefficients are ‘renormalized’. This renormalization can then

<sup>48</sup>Strogatz Ch 10.7

be repeated for the period-doubling of  $f^{(4)}$  and so on. The numerical simulations suggest that the process converges and then yields the universal constants  $\delta$  and  $\alpha$ .

Simplify the start by rescaling  $x_n$  to set  $a = 1$ ,

$$x_{n+1} = -(1 + \mu)x_n + x_n^2 + \dots \equiv f(x_n). \quad (32)$$

The period-2 orbit is given by  $x_{2n} = q$  and  $x_{2n+1} = p$ , i.e.

$$p = -(1 + \mu)q + q^2 \quad q = -(1 + \mu)p + p^2.$$

Subtracting the two equations yields

$$p - q = -(1 + \mu)(q - p) + (q - p)(q + p).$$

The period-2 orbit has  $p \neq q$  yielding

$$q + p = \mu.$$

Multiplying the two equations together gives

$$\begin{aligned} pq &= (-(1 + \mu)q + q^2)(-(1 + \mu)p + p^2) \\ &= (1 + \mu)^2 pq - (1 + \mu) \underbrace{(qp^2 + q^2p)}_{qp(p+q)=qp\mu} + q^2 p^2 \\ &= pq \left\{ \underbrace{(1 + \mu)^2 - (1 + \mu)\mu}_{1+\mu} + pq \right\} \end{aligned}$$

yielding

$$pq = -\mu.$$

Thus

$$(\mu - q)q + \mu = 0 \quad q, p = \frac{1}{2} \left( -\mu \pm \sqrt{\mu^2 + 4\mu} \right).$$

Both,  $q$  and  $p$ , are fixed points of the second iterate  $f^{(2)}$ .

As  $\mu$  is increased this period-2 orbit undergoes another period-doubling bifurcation to a period-4 solution, i.e. the fixed point  $p$  of  $f^{(2)}$  undergoes a period doubling. Aiming for an equation analogous to (32), rewrite  $x_n$  in terms of the deviation from that fixed point,  $x_n = p + \eta_n$ ,

$$p + \eta_{n+1} = f^{(2)}(p + \eta_n).$$

Near the period-doubling bifurcation of  $f^{(2)}$  the iteration will again be (approximately) described by a quadratic map, this time in  $\eta_n$ . Explicitly evaluating

$$p + \eta_{n+1} = f(-(1 + \mu)(p + \eta_n) + (p + \eta_n)^2)$$

to quadratic order in  $\eta_n$ , yields after some algebra

$$\eta_{n+1} = (1 - 4\mu - \mu^2)\eta_n + C\eta_n^2 + \dots \quad \text{with} \quad C = 4\mu + \mu^2 - 3\sqrt{\mu^2 + 4\mu}.$$

We can get this into the same form as (32) by rescaling  $\eta_n$  to absorb the coefficient  $C$  and by introducing a new bifurcation parameter  $\mu^{(1)}$ ,

$$x_n^{(1)} = C\eta_n \quad - (1 + \mu^{(1)}) = 1 - 4\mu - \mu^2 \quad \text{i.e.} \quad \mu^{(1)} = \mu^2 + 4\mu - 2,$$

i.e. in terms of the new variables we have then

$$x_{n+1}^{(1)} = - (1 + \mu^{(1)}) x_n^{(1)} + (x_n^{(1)})^2 + \dots$$

The period doubling of the period-2 orbit occurs at  $\mu^{(1)} = 0$  and generates a period-4 orbit, which is a fixed point of  $f^{(4)}$ . We can investigate when this fixed point of  $f^{(4)}$  (i.e. the period-4 orbit of  $f$ ) undergoes a period-doubling and repeat the analogous rescaling. Repeating this leads in general to equations for the deviations of  $x$  from the fixed point of  $f^{(2^k)}$

$$x_{n+1}^{(k)} = - (1 + \mu^{(k)}) x_n^{(k)} + (x_n^{(k)})^2 + \dots \quad \text{with} \quad \mu^{(k)} = (\mu^{(k-1)})^2 + 4\mu^{(k-1)} - 2 \equiv h(\mu^{(k-1)})$$

and

$$\mu^{(0)} \equiv \mu.$$

### Note:

- The different ‘generations’ of  $\mu^{(k)}$  constitute different coordinates of  $\mu$ , which are transformed into each other with the function  $h$ .

$$\mu^{(k)} = h(\mu^{(k-1)}) = h(h(\mu^{(k-2)})) = h^{(2)}(\mu^{(k-2)}) = h^{(k)}(\mu^{(0)}) = h^{(k)}(\mu).$$

We are interested in the values of  $\mu$  at the various bifurcations. Call  $\mu_k^{(l)}$  the value of  $\mu^{(l)}$  at the  $k^{\text{th}}$ -period doubling. We then have by construction

$$\mu_k^{(k)} = 0.$$

Thus, transforming back from the coordinate  $\mu^{(k)}$  to the original control parameter  $\mu$  we have for the parameter values at the  $k^{\text{th}}$  and the  $(k-1)^{\text{th}}$  period-doubling bifurcation,

$$\mu_k^{(k)} = h^{(k)}(\mu_k) = 0 \quad \mu_{k-1}^{(k-1)} = h^{(k-1)}(\mu_{k-1}) = 0$$

i.e.

$$h^{(k)}(\mu_k) = h^{(k-1)}(\mu_{k-1})$$

Applying the inverse of  $h$   $k-1$  times yields then<sup>49</sup>

$$h(\mu_k) = \mu_{k-1} \quad \text{i.e.} \quad \mu_{k-1} = \mu_k^2 + 4\mu_k - 2. \quad (33)$$

In terms of a forward iteration this gives

$$\mu_k = -2 \pm \frac{1}{2} \sqrt{16 + 4(2 + \mu_{k-1})} = -2 + \sqrt{6 + \mu_{k-1}}. \quad (34)$$

---

<sup>49</sup>The inverse has two solutions; one has to take the correct branch.

The transition to chaos at  $\mu^*$  occurs in the limit  $k \rightarrow \infty$ . Therefore  $\mu^*$  must be a fixed point of the iteration (34),

$$\mu^* = -2 + \sqrt{6 + \mu^*}$$

or more easily of (33)

$$\mu^{*2} + 3\mu^* - 2 = 0 \quad \mu^* = \frac{1}{2}(-3 + \sqrt{17}) \approx 0.56.$$

Recalling that  $\mu$  was shifted to as to have the first period-doubling bifurcation at  $\mu = 0$ , whereas in terms of the original parameters it occurs at  $a = 3$ , we get as approximation

$$a_\infty \approx 3.56$$

to be compared with the correct value  $a_\infty = 3.569945672\dots$

The amplitude rescaling by  $C$  corresponds to the constant

$$\alpha = \lim_{n \rightarrow \infty} \frac{d_n}{d_{n+1}}.$$

We have

$$C = 4\mu + \mu^2 - 3\sqrt{\mu^2 + 4\mu},$$

which needs to be evaluated at  $\mu^* = \frac{1}{2}(= 3 + \sqrt{17})$ ,

$$C = \frac{1 + \sqrt{17}}{2} - 3\sqrt{\frac{1 + \sqrt{17}}{2}} \approx -2.24$$

to be compared to the correct value  $\alpha = 2.5029\dots$

Finally, regarding the accumulation of the bifurcations at  $a_\infty$ ,

$$a_n = a_\infty - Ae^{-\delta'n} \quad \text{for } n \rightarrow \infty,$$

i.e.

$$\lim_{n \rightarrow \infty} \frac{a_n - a_\infty}{a_{n+1} - a_\infty} = e^{\delta'} = \delta$$

Thus, consider

$$\delta = \lim_{k \rightarrow \infty} \frac{\mu_k - \mu^*}{\mu_{k+1} - \mu^*}$$

Since  $\mu_k \rightarrow \mu^*$  for  $k \rightarrow \infty$  the limit amounts to 0/0. Use l'Hopital, considering  $k$  a continuous variable

$$\begin{aligned} \delta &= \lim_{n \rightarrow \infty} \frac{\frac{d\mu_k}{dk}}{\frac{d\mu_{k+1}}{dk}} = \lim_{k \rightarrow \infty} \frac{\frac{d\mu_k}{d\mu_{k+1}} \frac{d\mu_{k+1}}{dk}}{\frac{d\mu_{k+1}}{dk}} = \lim_{k \rightarrow \infty} \frac{d\mu_{k-1}}{d\mu_k} \\ &= \lim_{k \rightarrow \infty} \frac{d}{d\mu_k} (\mu_k^2 + 4\mu_k - 2) = \lim_{k \rightarrow \infty} 2\mu_k + 4 = 2\mu^* + 4 = 1 + \sqrt{17} \approx 5.12, \end{aligned}$$

which is to be compared with  $\delta = 4.6692\dots$

## 4.4 Strange Attractors and Fractal Dimensions<sup>50</sup>

In the Lorenz system and the logistic map we saw that in the chaotic regime the trajectories converged onto a complicated set, a *strange attractor*.

We still need to define an attractor more precisely:

A set  $A$  is called an attractor if

1.  $A$  is an invariant set: any trajectory that starts in  $A$  remains in  $A$  for all times.
2.  $A$  attracts an open set of initial conditions: there exists an open set  $U$  containing  $A$  such that any trajectory starting in  $U$  converges to  $A$  for  $t \rightarrow \infty$ .
3.  $A$  is minimal, i.e. there is no proper subset of  $A$  that satisfies conditions 1 and 2.

**Note:**

- The largest open set  $U$  satisfying condition 2 is the basin of attraction of the attractor  $A$ .

The attractors of the Lorenz system and the logistic map give the impression of a complex geometry: they are *strange* attractors. How can we characterize their geometry?<sup>51</sup>

Consider yet another system since both the Lorenz system and the logistic map have draw-backs

- Lorenz system is complicated since it is three-dimensional: for chaotic flows this is the minimal dimension, however.
- The logistic map is not invertible, i.e. the dynamics cannot be run backwards in time. Chaotic one-dimensional maps have to be non-invertible, since they need to include stretching and folding. The folding introduces the non-invertibility.

Two-dimensional, invertible map: Hénon map

$$\begin{aligned}x_{n+1} &= y_n + 1 - ax_n^2 \\y_{n+1} &= bx_n\end{aligned}$$

The map can be thought of as composed of the following steps

1. stretch and fold a rectangle into a parabolic shape

$$x \rightarrow x \quad y \rightarrow y + 1 - ax^2$$

2. compress in the  $x$ -direction

$$x \rightarrow bx \quad y \rightarrow y$$

---

<sup>50</sup>Strogatz Ch. 11, 12

<sup>51</sup>Despite their striking geometric properties strange attractors are often defined via the property of sensitive dependence on initial conditions.

3. reflection about the diagonal to orient the object again along the original rectangle

$$x \rightarrow y \quad y \rightarrow x$$

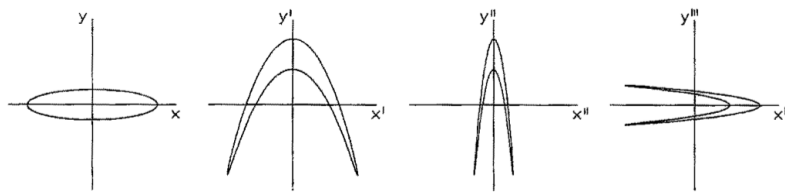


Figure 40: Hénon map decomposed

### Notes:

- The Hénon map is indeed invertible

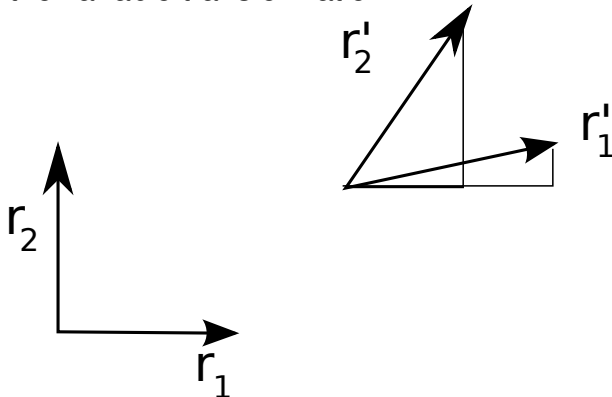
$$\begin{aligned} x_n &= \frac{1}{b}y_{n+1} \\ y_n &= x_{n+1} - 1 + ax_n^2 = x_{n+1} - 1 + \frac{a}{b}y_{n+1}^2 \end{aligned}$$

- The Hénon map is dissipative

Consider infinitesimal area  $dx dy$  and its mapping under a variable transformation

$$(x, y) \rightarrow (u(x, y), v(x, y))$$

from multi-variable integration we know that the rectangle with area  $dx dy$  is transformed into a parallelogram with area  $|\det \mathbf{J}| dx dy$  where  $\mathbf{J}(x, y)$  is the Jacobian of the variable transformation.



The area of the parallelogram generated by  $\mathbf{r}'_1$  and  $\mathbf{r}'_2$  is given by

$$|\mathbf{r}'_1 \times \mathbf{r}'_2| = |r_{1x}r_{2y} - r_{1y}r_{2x}| = \left| \frac{\partial u}{\partial x} \Delta x \frac{\partial v}{\partial y} \Delta y - \frac{\partial u}{\partial y} \Delta y \frac{\partial v}{\partial x} \Delta x \right| = |\det \mathbf{J}| \Delta x \Delta y$$

An iteration of the Hénon map can be thought of as a variable transformation  $\Rightarrow$  the change in area in the phase plane is determined by  $|\det \mathbf{J}|$

$$\det \mathbf{J} = \begin{vmatrix} -2ax_n & 1 \\ b & 0 \end{vmatrix} = -b$$

Thus: for  $|b| < 1$  the Hénon map is dissipative everywhere in the phase plane.

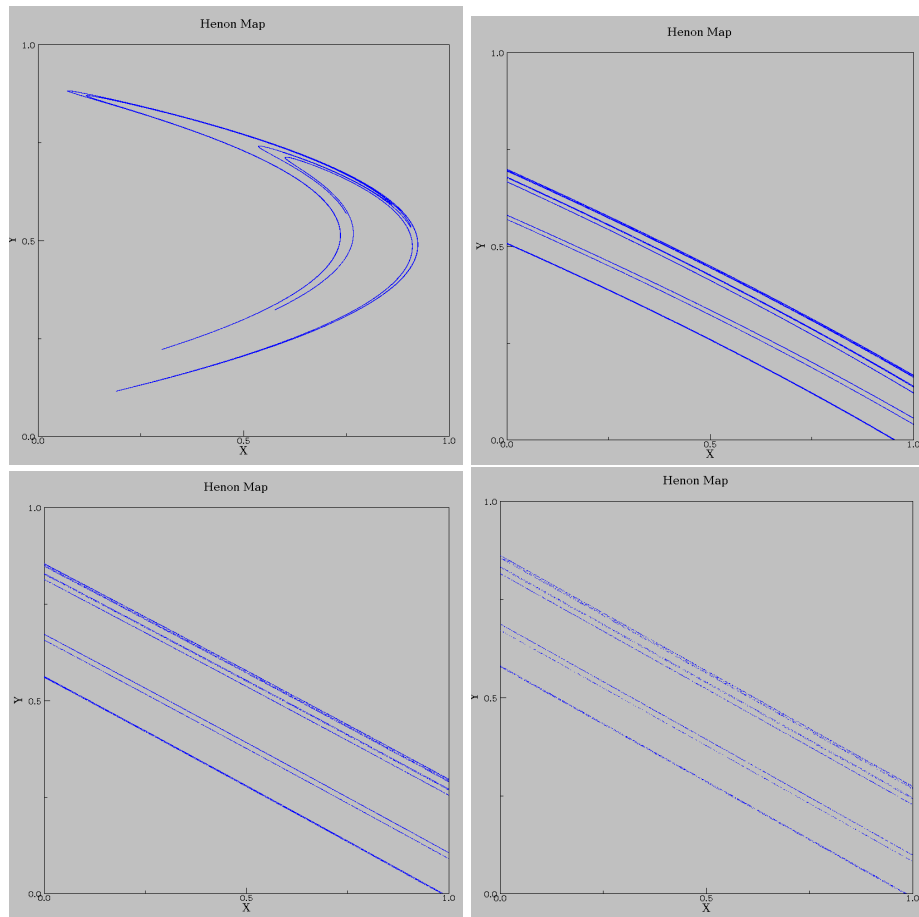


Figure 41: Self-similarity in the Henon map for  $a = 1.4$  and  $b = 0.3$ . Axes  $[xmin, xmax, ymin, ymax]$  are  $[0,1,0,1]$ ,  $[0.69,0.91,0.13,0.2]$ ,  $[0.77,0.80,0.16,0.17]$ , and  $[0.7829,0.7875,0.1629,0.1643]$ .

The Henon attractor exhibits self-similarity: zooming into the upper three-layered sheet of the three sheets reveals again three sheets comprised of 1, 2, and 3 sheets each. How do we characterize such structures?

Consider the following construction of a set  $\mathcal{S}$  that is somewhat similar to the cross section of the Henon attractor

1. Take the interval  $[0,1]$
2. cut out the middle third
3. from each remaining subinterval cut out the middle third
4. repeat step 3 ad infinitum

**Note:**

- the resulting set  $\mathcal{S}$  is called the Cantor set after Georg Cantor, the developer of set theory

Question:

- how many pieces make up the set  $\mathcal{S}$ ?
- can one count them?
- what is its cardinality?

### Countable and uncountable sets:

- a set is countable if there is a 1-to-1 correspondence between each of its elements and the natural numbers

### Examples

1. The rational numbers are countable

each rational number  $\frac{p}{q}$  can be represented as an element in a matrix  $Q$

$$\left( \begin{array}{c|cccccc} q \setminus p & 1 & 2 & 3 & 4 & 5 & 6 \\ \hline 1 & \frac{1}{1} & \frac{2}{1} & \dots & & & \\ 2 & \frac{1}{2} & \frac{2}{2} & \frac{3}{2} & \dots & & \\ 3 & \frac{1}{3} & \dots & & & & \\ 4 & \frac{1}{4} & \dots & & & & \\ 5 & \frac{1}{5} & \frac{2}{5} & & & & \end{array} \right)$$

then count  $Q_{11} \rightarrow Q_{21} \rightarrow Q_{12} \rightarrow Q_{31} \rightarrow Q_{22} \rightarrow Q_{13} \rightarrow Q_{41} \rightarrow \dots$

2. The real numbers in  $[0, 1]$  are not countable

Cantor showed this by contradiction using his ‘diagonal argument’:

Assume the real numbers were countable. Then they could be listed in sequence

$$\begin{aligned} 0.x_{11} x_{12} x_{13} \dots \\ 0.x_{21} x_{22} x_{23} \dots \\ 0.x_{31} x_{32} x_{33} \dots \\ 0.x_{41} x_{42} x_{43} \dots \\ \dots \\ \dots \end{aligned}$$

with  $x_{ij} \in \mathbb{N}$ .

Consider now the number

$$0.\bar{x}_{11} \bar{x}_{22} \bar{x}_{33} \dots$$

where  $\bar{x}_{jj}$  is arbitrary as long as  $\bar{x}_{jj} \neq x_{jj}$  for each  $j$ . This number is clearly a real number but it is not in the list because it differs from each number in the list by at least one digit. The enumerated list of numbers is therefore not complete.

3. What is the cardinality of the Cantor set?

Use again Cantor’s diagonal argument as in the case of the real numbers: each piece can be labeled by a number  $q \in \{0, 1, 2\}$  whose digit at the  $l^{th}$  position states whether at the  $l^{th}$  level of the Cantor construction this piece ends up in the left, middle

or right third subdivision of the interval

All points in  $\mathcal{S}$  are then given by a number whose digits are taken from  $\{0, 2\}$ , since the middle piece is always taken out<sup>52</sup>.

If the Cantor set is countable then the elements can be listed,

$$\begin{aligned}x_1 &= x_{11} x_{12} x_{13} \dots \\x_2 &= x_{21} x_{22} x_{23} \dots \\x_3 &= x_{31} x_{32} x_{33} \dots\end{aligned}$$

Again, the number  $\bar{x}_{11} \bar{x}_{22} \bar{x}_{33} \dots$  is not contained in the list, but it is in  $\mathcal{S}$ . Therefore  $\mathcal{S}$  is not countable.<sup>53</sup>

What is the total length ('measure') of the Cantor set  $\mathcal{S}$ ?

In each step a third of the remaining length is removed:

$$L_j = \frac{2}{3} L_{j-1} = \left(\frac{2}{3}\right)^j \quad \Rightarrow \quad \lim_{j \rightarrow \infty} L_j = \lim_{j \rightarrow \infty} \left(\frac{2}{3}\right)^j = 0$$

Thus, the Cantor set

- has zero measure (like the rational numbers, but unlike the real numbers)
- is uncountable (like the real numbers, but unlike the rationals)

#### 4.4.1 Dimensions

As one goes down the levels, the number of pieces in the Cantor set increases and diverges: the number of pieces diverges as one increases the spatial resolution. How fast does it diverge?

Define the dimension of an object in general by covering it with smaller pieces

Square:

- covering squares with smaller squares: if we reduce the linear size of the smaller squares by a factor of 2 we need  $4 = 2^2$  more squares to do so.

Cube:

- covering cubes with smaller cubes: if we reduce the linear size of the smaller cubes by a factor of 2 we need  $8 = 2^3$  more cubes to do so.

Thus define the dimension  $d$  of the object

---

<sup>52</sup>It is like a binary representation.

<sup>53</sup>The same argument can be applied to the Feigenbaum attractor.

- when we reduce the linear size of the covering pieces by a factor of  $r$  the number  $m$  needed goes up by a factor of  $r$

$$m = r^d \quad \text{defining} \quad d = \frac{\ln m}{\ln r},$$

i.e. in each dimension the number of pieces needed goes up by a factor of  $r$ .

Apply this approach to the Cantor set:

- in each step the linear dimension of the pieces decreases by a factor of 3
- in each step the number of pieces needed goes up by a factor of 2

$$d_{Cantor}^{(sim)} = \frac{\ln 2}{\ln 3} \approx 0.63.$$

### Notes:

- this definition of the dimension relies on the self-similarity of the structure: *similarity dimension*.

### Example:

von Koch<sup>54</sup> curve:

Recursive construction:

- replace each straight line segment of length  $l$  by 4 segments of length  $l/3$

Similarity dimension:

- in each step linear dimension of the pieces decreases by a factor of 3
- in each step the number of pieces increases by a factor of 4

$$d_{Koch}^{(sim)} = \frac{\ln 4}{\ln 3} \approx 1.26$$

For sets that are not self-similar we need to generalize the procedure: cover the set with elements of linear size  $\epsilon$  where  $\epsilon \rightarrow 0$ , i.e. reduce the linear dimension by a factor of  $r = \frac{1}{\epsilon}$ ,

$$d^{(box)} = \lim_{\epsilon \rightarrow 0} \frac{\ln N(\epsilon)}{\ln \left(\frac{1}{\epsilon}\right)}$$

### Note:

- This defines the *box counting dimension*.

---

<sup>54</sup>von Koch (1870–1924)

Apply this to the Cantor set:

At each level we choose  $\epsilon = \left(\frac{1}{3}\right)^n$ , then we need  $2^n$  ‘boxes’ to cover the Cantor set

$$d^{(box)} = \lim_{n \rightarrow \infty} \frac{\ln 2^n}{\ln \frac{1}{\left(\frac{1}{3}\right)^n}} = \lim_{n \rightarrow \infty} \frac{n \ln 2}{n \ln 3} = \frac{\ln 2}{\ln 3}$$

**Example:** Attractor of the Henon map

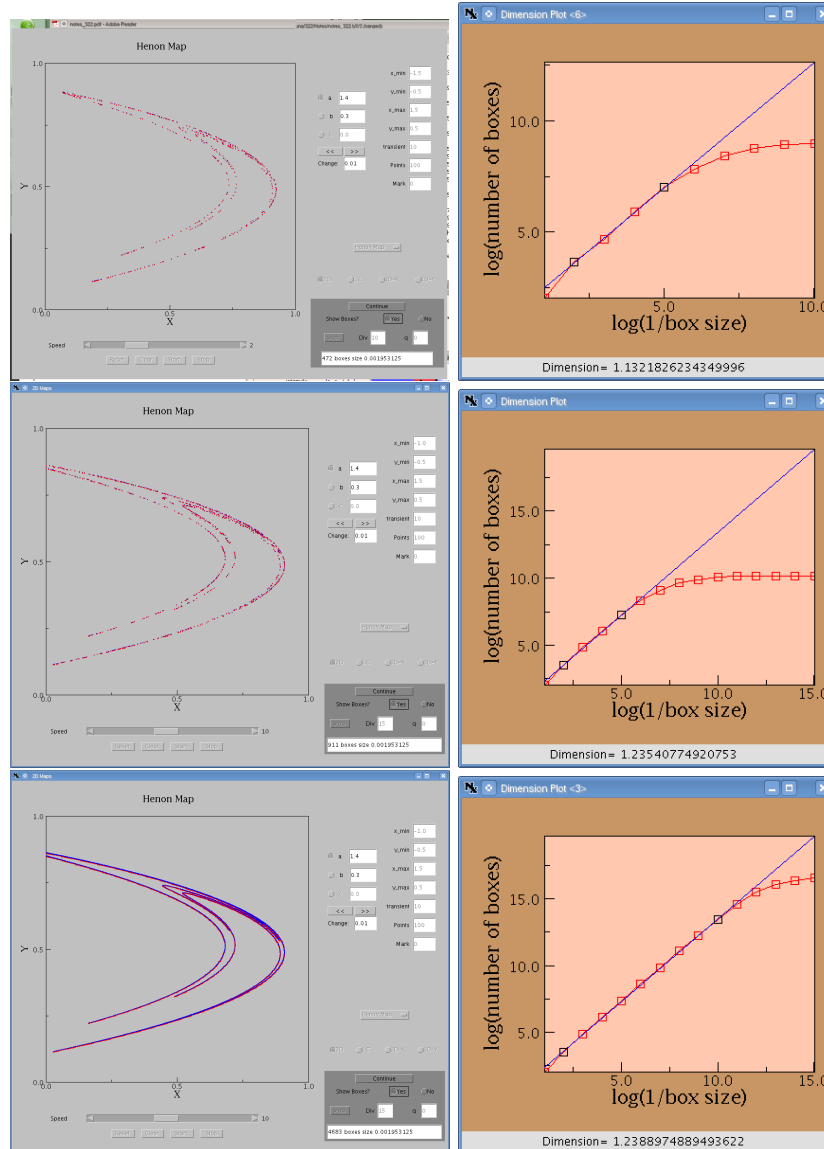


Figure 42: Box dimension of Henon attractor for 500, 1,000, and 100,000 points. Left panels: attractor with boxes; right panels: scaling of the number of boxes with the box size. At very small box sizes the number of boxes saturates at the total number of data points in the set.

### Notes:

- The box dimension does not depend on how many points of the trajectory are inside a given box as long as there is at least one point. It does not capture if some region

of the attractor is visited much more often than another. It therefore does not reflect the dynamics on the attractor, only its geometry.

- The box dimension is computationally very inefficient; a very large number of data points is needed to obtain a converged result.

### Correlation Dimension:

For a given point  $r$  on the attractor determine the number of other points on the attractor that fall within a ball of size  $\epsilon$  of  $r$

$$N_r(\epsilon) \propto \epsilon^{d_r}$$

$d_r$  is the *pointwise dimension* of  $r$ .

The correlation dimension is obtained by averaging  $N_r(\epsilon)$  over all (sufficiently many)  $r$  of the attractor

$$C(\epsilon) = \frac{1}{\mathcal{N}} \sum_{i=1}^{\mathcal{N}} N_{r_i}(\epsilon)$$

with  $\mathcal{N}$  the number of attractor points  $r$  included in the average.

Expecting

$$C(\epsilon) \propto \epsilon^{d_c}$$

define

$$d_c = \frac{d \ln C(\epsilon)}{d \ln (\epsilon)}.$$

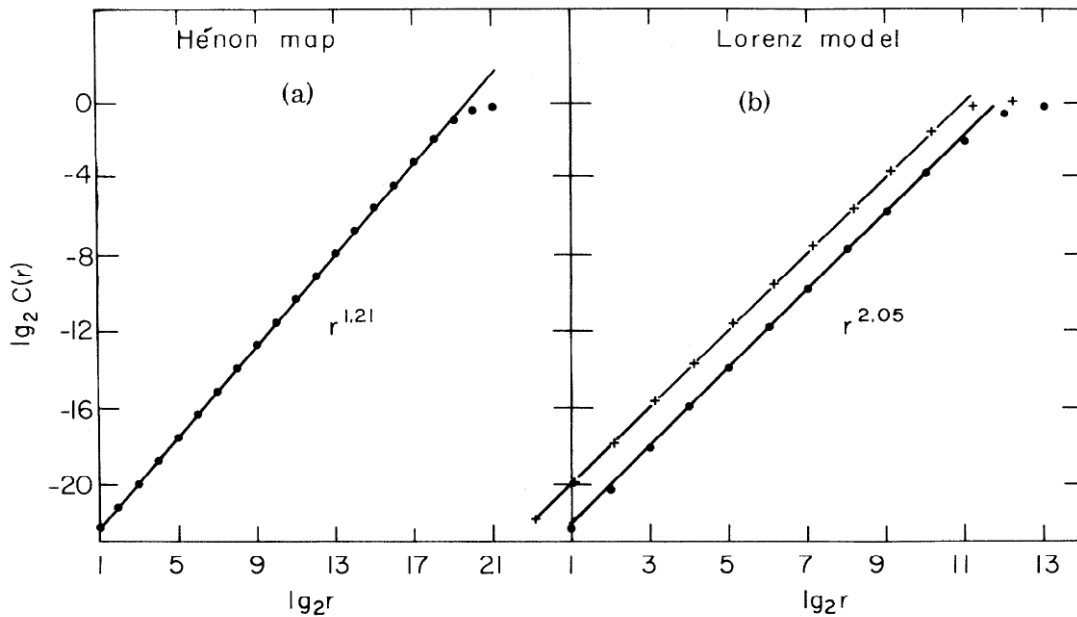


Figure 43: Correlation dimension for Henon map and Lorenz equations (Grassberger and Procaccia, 1983).

### Note:

- Dynamics do enter correlation dimension:  
due to the averaging over the points on the attractor, regions that are visited more often are weighted more heavily in the correlation dimension.
- One can show  $d_c \leq d_b$ , but usually  $d_c \sim d_b$ .

**Note:**

- there are further dimensions along these lines:  
whole spectrum of dimensions generated by weighing the probability of finding points in a small ball with different powers

**Lyapunov Dimension:**

Include dynamics explicitly in the definition of the dimension and aim for a quantity that indicates how many degrees of freedom are ‘active’.

Consider dimension of a volume that neither grows nor shrinks under the dynamics.

Fixed point attractor:

any volume shrinks to a point (the fixed point): the dimension of that volume is  $d_L = 0$ .

Periodic orbit:

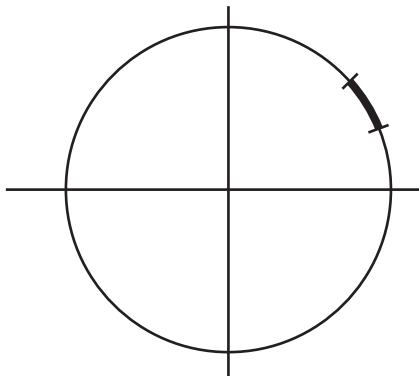


Figure 44: Line segments along a periodic attractor do not grow or shrink.

Line segments along the attractor are transported along the orbit without volume change (on average), but higher-dimensional sets covering the width of the attractor shrink to a line:  $d_L = 1$ .

The growth of a  $\nu$ -dimensional volume in phase space is given by the expansions in the  $\nu$  directions

$$V(t) = L_1 e^{\lambda_1 t} L_2 e^{\lambda_2 t} L_3 e^{\lambda_3 t} \dots L_\nu e^{\lambda_\nu t}$$

for  $V = \text{const.}$  we need

$$\sum_{i=1}^{\nu} \lambda_i = 0$$

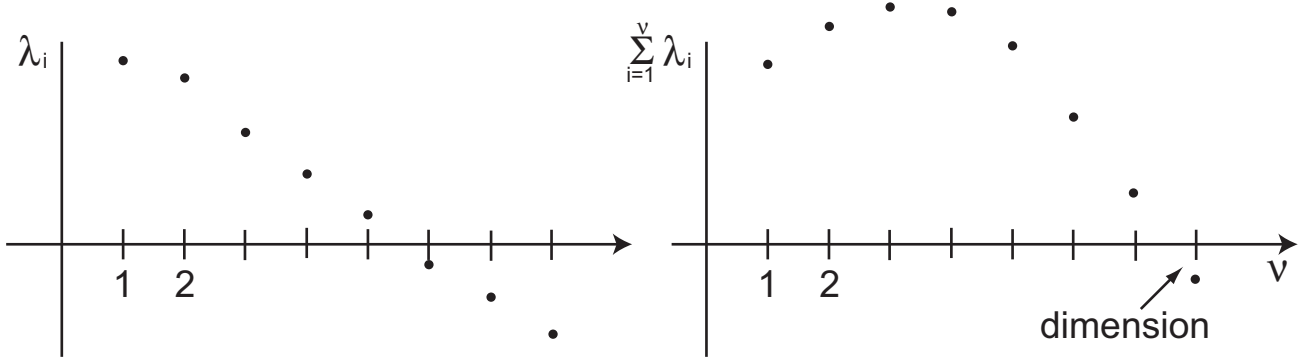


Figure 45: The Lyapunov dimension includes a few degrees of freedom with negative Lyapunov exponent.

Arrange the eigenvalues in decreasing order:  $\lambda_i \geq \lambda_{i+1}$

Consider

$$f(n) = \sum_{i=1}^n \lambda_i .$$

Use linear interpolation to find the zero of  $f(n)$  (taking  $n$  to be a continuous variable):

$$f(d_L) \approx f(\nu) + \frac{f(\nu+1) - f(\nu)}{\nu+1 - \nu} (d_L - \nu) \stackrel{!}{=} 0 \quad \Rightarrow \quad d_L = \nu - \frac{f(\nu)}{f(\nu+1) - f(\nu)}$$

Thus, choose  $\nu$  to satisfy  $\sum_{i=1}^{\nu} \lambda_i > 0$  but  $\sum_{i=1}^{\nu+1} \lambda_i < 0$ . Then the Lyapunov dimension is defined by

$$d_L = \nu + \frac{1}{|\lambda_{\nu+1}|} \sum_{i=1}^{\nu} \lambda_i .$$

**Note:**

- The Lyapunov dimension  $d_L$  gives a measure of how many degrees of freedom are "active" in the sense that some of these directions are actually expanding and compensating for the shrinking in the other directions (up to  $\nu$ ), driving other degrees of freedom.
- In spatially extended chaotic systems (e.g. fluid systems) it has been found that the Lyapunov dimension grows linearly with the system size. In these systems the chaos is *extensive*.

## 4.5 Experimental Data: Attractor Reconstruction and Poincaré Section

Experimentally, one typically cannot monitor all or even a large fraction of the relevant dynamical variables. How can one obtain relevant information about the attractor?

Given only the time series for a single dynamical variable  $x(t)$  one can reconstruct a representation of the attractor using *time-delayed coordinates*:

- plot  $x(t)$  vs  $x(t - \tau), x(t - 2\tau), \dots, x(-N\tau)$  etc.

How do we know how many delay coordinates we need to use? The Takens Embedding Theorem shows that for a  $d$ -dimensional attractor one needs *at most*  $N = 2d + 1$  coordinates.

In practice:

- Estimate the dimension (e.g. correlation dimension) of the resulting attractor as a function of the number  $N$  of delays.

\

- If the correlation dimension saturates above some value of  $N_s$ , one has found a sufficient embedding dimension for the attractor.

Example: Lorenz system

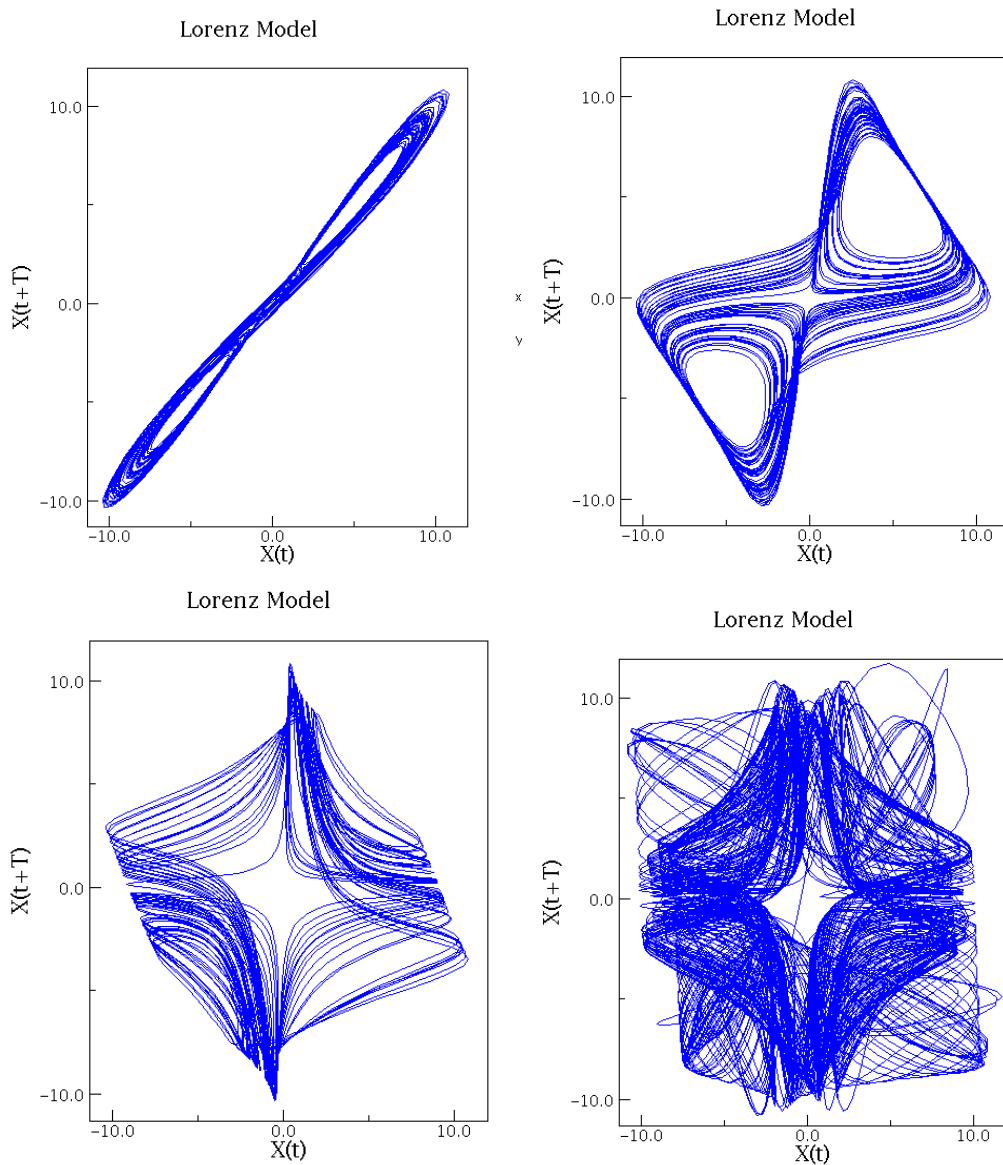


Figure 46: Reconstruction of the Lorenz attractor using delayed coordinates. a)  $\tau = 1$ , b)  $\tau = 10$ , c)  $\tau = 20$ , d)  $\tau = 100$ .

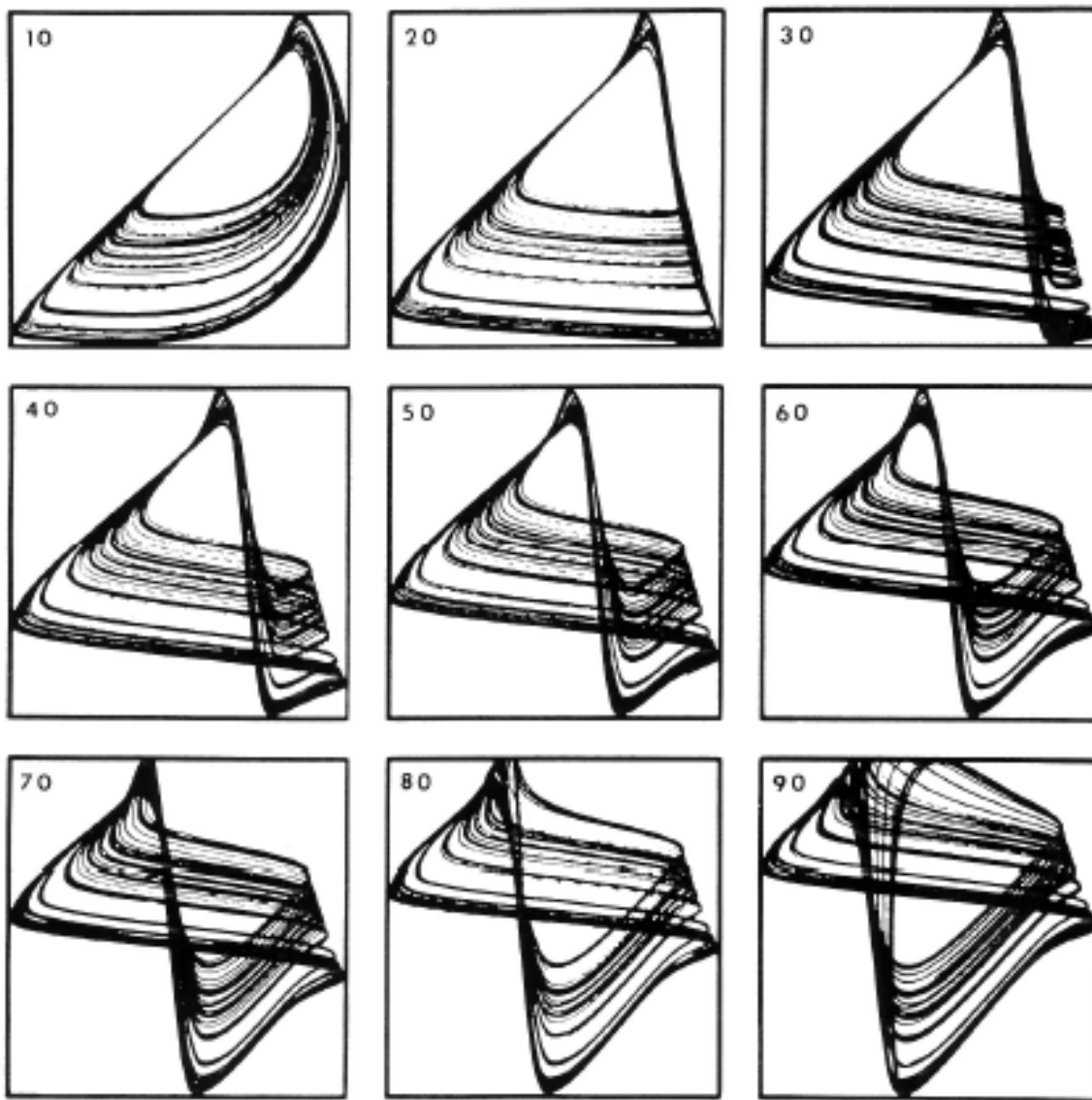


Figure 47: Attractor reconstruction for the Belousov-Zhabotinsky reaction. The delay used is indicated in each panel Roux et al. (1983).

### Note:

- The geometric shape of the attractor reconstruction depends on the delay  $\tau$ . its dimension dimension does not.
- For very small  $\tau$  the delayed variable  $x(t - \tau)$  is strongly correlated with  $x(t)$   $\Rightarrow$  they do not provide independent information about the attractor.
- For very large  $\tau$  the two variables are completely uncorrelated: they do not provide insight into the attractor
- Optimal delay at intermediate values: first minimum of the mutual information between the two variables is much better than the first 0 of the autocorrelation function Fraser and Swinney (1986).

From the attractor one may be able to obtain a description in terms of a map on the Poincare section, which generates a cross-section of the attractor:

For an attractor embedded in 3 dimensions mark all locations where the trajectory crosses a two-dimensional manifold in one direction. If that cross-section can be parameterized sufficiently well by a single variable one may obtain an iterated map for the dynamics.

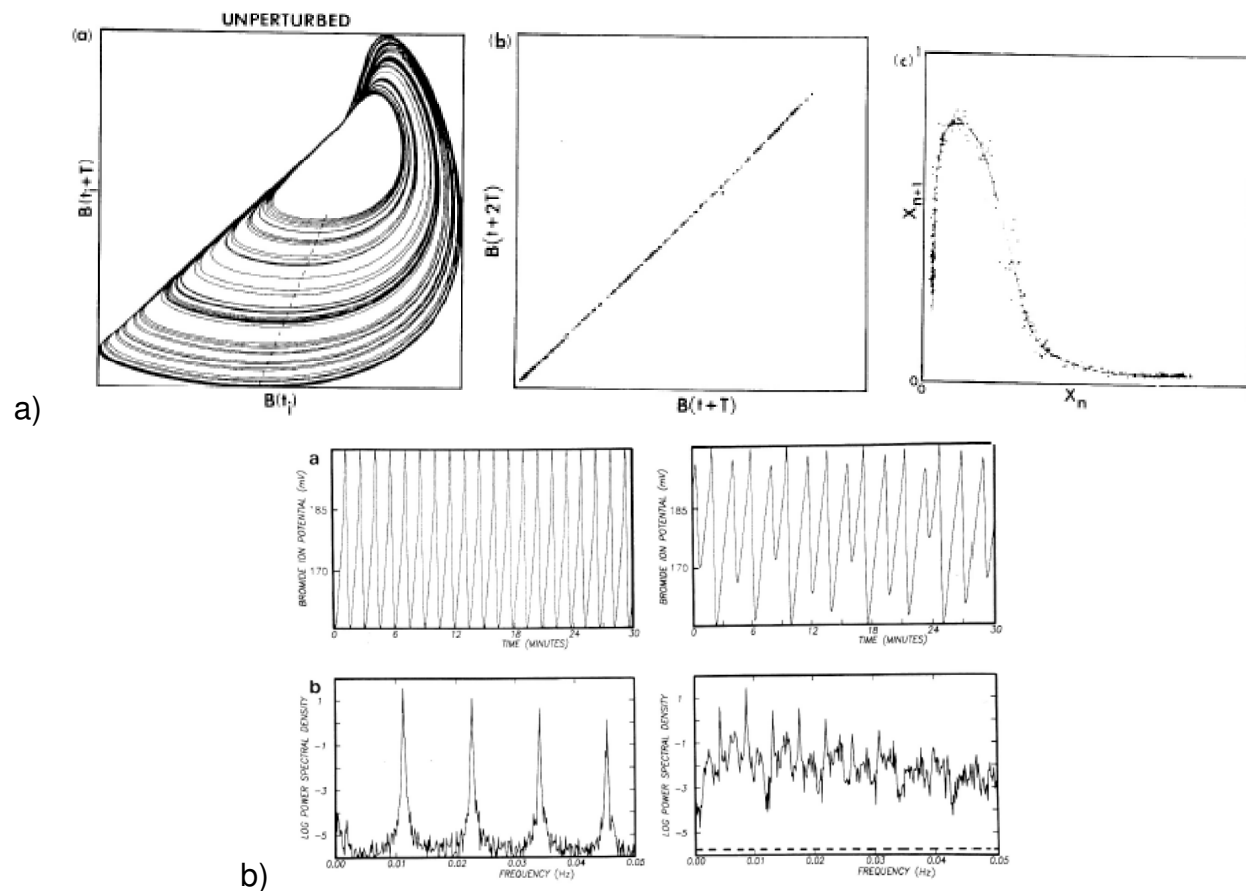


Figure 48: Belousov-Zhabotinsky reaction. a) Poincare section (dashed line in upper panel) yields a thin line (middle panel). The dynamics on that Poincare section is well captured by an (almost) one-dimensional iterated map on that Poincare section. The unimodal map suggests the appearance of a period-doubling cascade. The spectrum (b) shows a periodic oscillation and a chaotic oscillation that still reflects an approximate period 4 Roux et al. (1983).